Battery – Supercapacitor Hybrid Energy Storage System

A Practical Approach to Improve Lifecycle Performance of Seagoing Vessels

Georgios L. Karras, 4515250 , SDPO.19.040.m.

Master of Science Thesis

TU Delft Delft University of Technology

Challenge the future

(this page was intentionally left blank)

Battery – Supercapacitor Hybrid Energy Storage System

A Practical Approach to Improve Lifecycle Performance of Seagoing Vessels

In partial fulfilment of the requirements for the degree of
Master of Science
in Marine Technology with specialization in Marine Engineering

By:

Georgios-Logothetis Karras,

4515250 ,SDPO.19.040.m.

Performed at:

Wärtsilä Netherlands B.V.

Faculty of Mechanical, Maritime and Materials Engineering (3mE),
Delft University of Technology (Technische Universiteit Delft),
Delft, The Netherlands

University supervisor:
Dr. Ir. Peter de Vos

Company supervisor:
Ir. Teus van Beek

Thesis exam committee:

Prof. Ir. Klaas Visser	Delft University of Technology
Dr. Ir. Peter de Vos	Delft University of Technology
Ir. Teus van Beek	Wärtsilä Netherlands B.V.
Dr. Ir. M. Godjevac	Delft University of Technology
Dr. Ir. Y. Pang	Delft University of Technology

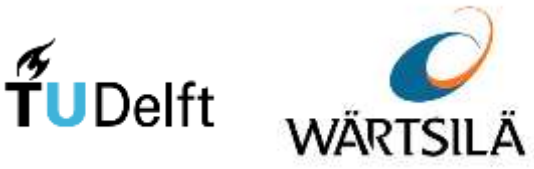

Keywords: Marine Energy Storage, Energy Storage Devices (ESDs), Hybrid Energy Storage System (HESS), Supercapacitor (SC), Li-Ion Batteries, Shipboard Applications, Sizing, Energy Management Strategy, Power Allocation, Life cycle performance.

ISBN 000-00-0000-000-0

An electronic version of this dissertation is available at
http://repository.tudelft.nl/.

Acknowledgements

First of all, I would like to thank Wärtsilä Netherlands B.V. for sponsoring this MSc thesis and for kindly providing operating data from real ship applications.

I would like to express my deepest appreciation to Mr. Ir. Teus van Beek of Wärtsilä Netherlands B.V, for his mentorship and contribution to this project. Teus has helped me considerably to develop as a professional and practise my project and time management skills (still some work to do!). He also encouraged me to become professionally outgoing and to actively seek for synergies where possible. Additionally, his honest vision for a more sustainable future within the maritime industry, has been a great inspiration during this early part of my professional career.

Following, I wish to express my sincere appreciation to my university supervisors; Dr. Milinko Godjevac for his supervision during the preliminary stages of the thesis. His justified scepticism early in the definition of the thesis topic, helped me build the project on solid academic foundations.

I would also like to specially acknowledge Dr. Peter de Vos for his invaluable guidance during the later and most critical parts of this thesis. Besides the very productive progress meetings, Dr. de Vos convincingly guided me and kept me motivated at moments where the goal seemed far. Without his persistent help, the goal of this project would not have been realized.

From TU Delft I also wish to thank Prof. Ir. Klaas Visser for his constructive feedback during group progress meetings and Dr. Ir. Y. Pang from Transport Engineering for being a part of the graduation committee.

In a personal level, I am indebted to all my friends from Delft who stood by me during this challenging period of my life. Special thanks to Nikolas B., Nikos M., Alexandros K. and Chris C.

Finally, I wish to dedicate this thesis to my family; my brothers Pavlos and Dimitris and my parents Venetia and Mihalis for always having faith in me and for enabling me to pursue this master's degree.

Georgios-Logothetis Karras
Delft, January 2020

(this page was intentionally left blank)

Abstract

For many maritime applications Li-Ion batteries are foreseen as energy storage units that can improve the performance of the on-board power system in terms of continuity of service, fuel consumption, emissions and running hours of main engines.

However, one of main limitations of battery application in on-board power systems is the aging of batteries. Applications of instantaneous power input/output such as propulsion dynamic assistance and heavy seas operation of ships, have an adverse effect on battery lifetime meaning that degradation of energy capacity over time is accelerated. Additionally, limited by their maximum current rating, batteries cannot deliver effectively high C-rates and therefore are not able to fully absorb the engine fluctuations.

A typical solution for this problem is to over-size the battery system. By paralleling more batteries, the max. C-rate is lowered, and battery lifetime can be extended. On the other hand, an over-sized battery system will result in additional capital cost and weight. Therefore, it is evident that in conventional approaches there is an undesirable trade-off between battery aging and battery size.

As an alternative practical approach into this problem, this thesis proposes an on-board hybrid energy storage system (HESS) that comprises of a battery and a supercapacitor component. By placing the supercapacitor in parallel to the battery and by using it for high peak currents, it is possible to reduce the stress on the battery and thus extend battery lifetime while improving the availability and the reliability of the power system. In addition, by taking advantage of the high specific power of the supercapacitor and the high specific energy of the battery it is possible to optimize sizing of the energy storage system for high power applications.

In this thesis, a parametric approach of combined sizing and energy management for hybrid energy storage system is developed and integrated into a typical DC shipboard power system . Based on a case load profile, the HESS operation is simulated and benchmarked to battery-only installations. The static outputs of the sizing process and the dynamic outputs of the simulation are extracted in the form of design exploration maps and arrays that are used to correlate them to the key design variables.

Finally, through this work, it is demonstrated that for high power applications with significant fluctuations, the proposed battery-supercapacitor HESS, can lead into smaller and more cost-effective installations, without compromising battery lifetime and while maintaining same levels of reliability performance.

(this page was intentionally left blank)

Table of Contents

List of Abbreviations

AC	Alternating Current
AES	All-Electric Ship
CAES	Compressed Air Energy Storage
CAPEX	Capital Expenses (Cost)
Csr	Capacity Split Ratio
DAB	Dual Active Bridge
DC	Direct Current
DG	Diesel Generator
DOD	Depth of Discharge
EDLC	Electric Double Layer Capacitor
EEDI	Energy Efficiency Design Index
EEOI	Energy Efficiency Operational Indicator
EMS	Energy Management Strategy
EOL	End of Lifetime
ESD	Energy Storage Device
EV	Electric Vehicle
FC	Fuel Consumption
HEES	Hybrid Electric Energy Storage
HESS	Hybrid Energy Storage Systems
IMO	International Maritime Organization
LCO	Lithium Cobalt Oxide Battery
LFP	Lithium Iron Phosphate Battery
Li-Ion	Lithium-Ion Battery
LLI	Loss of Load Instance
LLP	Loss of Load Probability
LMO	Lithium Manganese Oxide Battery
LNG	Liquefied Natural Gas
LTO	Lithium Titanate Battery
MARPOL	International Convention for the Prevention of Pollution from Ships
MCR	Maximum continuous rating of engine
MEPC	IMO Marine Environment Protection Committee
MSC	IMO Marine Safety Committee
MVDC	Medium Voltage DC
NCA	Lithium Nickel Cobalt Aluminium Oxide Battery
NMC	Lithium Nickel Manganese Cobalt Oxide Battery
OSV	Offshore Supply Vessel
PEMFC	Proton Exchange Membrane Fuel Cell
PHES	Pumped Hydroelectric Energy Storage
PM	Palmgren Miner Rule
PMS	Power Management System
psr	Power Split Ratio
PTO/PTI	Power Take-off/ Power Take-In
Ro-Pax	Roll-On/Roll-Off Passenger Ship
SC	Supercapacitor
SEEMP	Ship Energy Efficiency Management Plan
SFC	Specific Fuel Oil Consumption
SOC	State of Charge
Wh	Watt-hour

Roman Symbols

I	Current	[A]
R	Resistance	[Ω]
V	Voltage	[V]
C	Capacitance	[F]
E	Capacity	[Ah]
P	Power	[W]
t	Time	[s]

Subscripts

bat	Battery
convert	DC/DC Converter
eng	Diesel Generator
hess	Hybrid Energy Storage System (battery and sc)
load	Vessel Power Load Profile
sc	Supercapacitor
val	Validation
fuel	Marine Diesel Oil
ch	Charging Operation
dis	Discharging Operation

List of Figures

List of Tables

1 Introduction & Motivation

1.1 Background

In today's globalized economy, waterborne shipping is the predominant way of transporting goods between ports and countries. The effect of International Shipping in global greenhouse gas emissions is important, as about 1000 million tonnes of CO_2 gasses are emitted every year by ships worldwide [1]. In terms of percentages, shipping GHGs account for 2.8% of global greenhouse gasses while there is a clear upward trend, per which, total GHG emissions of shipping industry will increase between 50% and 250% by 2050, depending on future economic and energy developments [1]. This projection is not compatible with the internationally agreed goal of keeping global temperature increase to below 2°C compared to pre-industrial levels, which requires worldwide emissions to be at least halved from 1990 levels by 2050.

Based on these data, the International Maritime Organization (IMO) has introduced stricter regulations such as Emission Controlled Areas (ECAs), Energy Efficiency Design Index (EEDI) and Ship Energy Efficiency Management Plan (SEEMP) as a part of the international effort for the protection of the environment [1].

1.2 Marine Energy Storage Installations Trends

Following the introduction of stricter environmental regulations for shipping and the developments in lithium-ion batteries over the past few years, marine industry stakeholders such as ship owners, charterers, technology providers and classification societies have revitalized their interest in adapting electrical energy storage systems on-board ships.

The use of energy storage (ES), (i.e. the storage of energy that can be drawn upon later and usefully re-applied in another operation) has already been successfully incorporated to maritime applications as an enabling technology with significant potential. Because of their ability to accommodate intermittency and balance energy supply and demand, Energy Storage Devices (ESD) can either be coupled with conventional power sources such as diesel engines to improve their performance or be used as stand-alone power systems.

Environmental Restriction	Issuing Authority	Electrical ES Benefits
EEDI, SEEMP, EEOI	IMO MEPC	Reducing CO_2 emissions (fuel saving)
ECA	IMO MEPC	Reducing NO_x, SO_x and PM emissions (fuel saving)
Noise Code	IMO MSC	Reducing mechanical noise
Safe Return to Port	IMO MSC	Redundancy design for human safety
Green Port Program	Local / Port State	Zero-emissions at port

Table 1 Electrical Energy Storage benefits for environmental restrictions. Adopted by [2]

Between 2009 and 2018, more than 79 Electrical Energy Storage (EES) installations on-board commercial ships have been showcased, while there is a clear upward trend, according to which the number of battery ships being built/retrofitted per year has increased by a factor of 7 within less than a decade [Fig.1][1]. Back in 2009, there were only two new battery installations; one hybrid tugboat and the canal boat ‘’FCS Alsterwasser’’[3], that was utilizing batteries as a back-up to the primary fuel cells plant. By 2015, the number of installations was boomed to 14 per year including new vessel types such as Ro-Pax, Mega yacht, and OSVs.

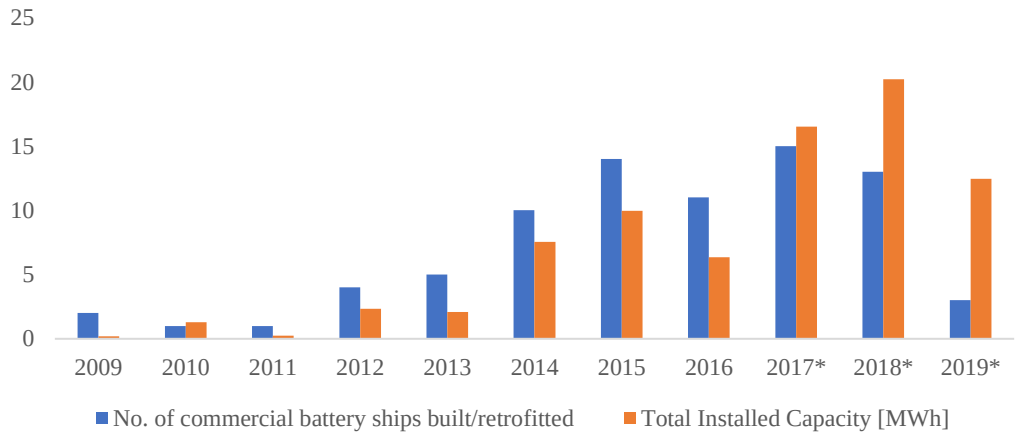

Figure 1 Commercial Battery Ships Built/Retrofitted

Another interesting point that can be derived from Fig.1, is the steep increase in total battery capacity for new installations. According to commercial sources, 2017 and 2018 set new records for newly installed capacity within a year with 16.5 and 20.2 MWh respectively. This means that marine energy storage system providers have responded to the growing demand of battery systems by the ship owners. From further analysis of the installations data [Fig. 2], it is derived that it is not only the application number that is growing strong but also the average capacity of each installation. Additionally, Fig. 2 shows that there is another growing trend concerning the size of the largest installation per year.

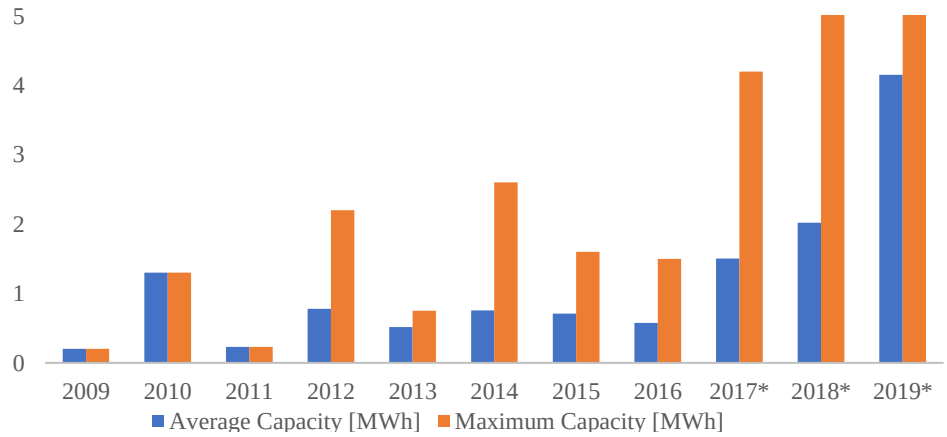

Figure 2 Installed battery capacity milestones on-board ships

[1] All data have been collected by publicly available sources. The entire ES installation database can be found in the Appendix A.

As of 2010, MS Tûranor PlanetSolar [4], a research solar boat, had the largest floating battery system in the world with 1.3 MWh of energy capacity. By 2012, Mitsui OSK Lines announced the completion of the hybrid car carrier Emerald Ace, designed to generate zero emissions while berthed. The Emerald Ace was built as world's first hybrid car carrier, and it combined a 160kW solar generation system with lithium-ion batteries that can store 2.2MWh of electricity [5]. In 2014, Scandlines's M/V Prins Richard raised the bar to 2.6MWh, while the same company is in await of the delivery of two full battery car ferries of 4.16 MWh each, within the year [6]. However, this record could soon be surpassed, as cruise operator Hurtigruten has an option for expansion of its two recently launched hybrid cruise ships "MS Roald Amundsen" and "MS Fridtjof Nansen" to capacities of up to 6 MWh each [7].

Having these trends in mind, the logical aftermath is to wonder why the propulsion plants are being hybridized with the addition of Li-Ion batteries and why these trends keep growing strong. To answer those questions the driving factors should be understood first. Additionally, in order to understand better the potential of electrical energy storage in maritime applications, the limitations and the challenges of battery technology should also be addressed.

1.3 Marine Energy Storage Applications

Electrical energy storage applications in ships can be divided into purely stored power supplied all-electric and hybrid depending on whether they are used stand-alone or in combination with other prime movers (i.e. diesel engines) [8].

On the first type (Fig.5c), all the power, for both propulsion and auxiliaries, is supplied by batteries or another electrical storage medium. The ship is sailing in zero emission mode. In this mode, the ESDs are getting charged from the shore as the ship has no (or limited) own capability to charge the electrical storage system. So far, the concept of all-electric ships has only been successfully demonstrated for short-sea vessels of medium power range with frequent port calls[9]. Hybrid propulsion systems can either be electrical-hybrid (Fig. 5a) or mechanical-hybrid with Power Take Off/Power Take In (PTO/PTI) (Fig. 5b) depending on the transmission system.

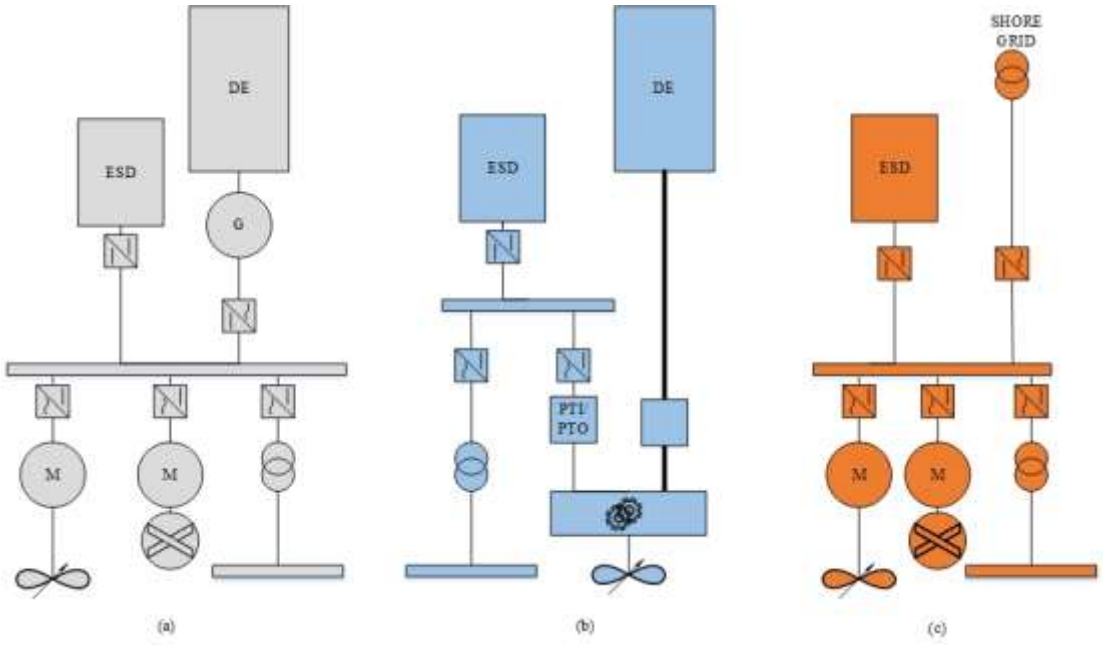

Figure 3 Block diagram for (a) Electrical-Hybrid (b) Mechanical-Hybrid with PTO/PTI (c) All-electric

Hybrid propulsion energy storage systems can further be analysed based on their operating function to plug-in hybrid, peak shaving of prime mover and integration of on-board renewable

generation systems. In plug-in hybrid system, the ship can operate solely on energy storage for parts of its operation. The most common, is for the ESDs to be charged while in port (preferably from a zero-carbon renewable source such as hydropower) and being used as a spinning reserve to reduce emissions at berthing or during manoeuvring.

Energy Storage Function	Examples
Renewables Integration	Texelstroom, Emerald Ace, Planet Solar
Peak Shaving	Viking Queen, HNLMS Noordze and Viking Lady
All-Electric	Ar Vag Tredan, Ampere and E-ferry
Plug-in	Viking Lady, Emerald Ace, Seaspan Reliant

Table 2 Categorization of ES Applications based on function

In peak shaving applications, secondary (rechargeable) batteries are used to effectively handle load fluctuations experienced by the diesel engine in applications such as manoeuvering or in heavy seas condition [10]. Specifically, for highly supercharged diesel engines, the turbocharger needs time to accelerate before it can deliver the required amount of air [11]. This requires that the engines are protected from load steps exceeding their maximum load acceptance capability. The propulsion control must include automatic limitation of the load increase rate such that the normal operation loading curve is not exceeded (Fig.4) [12]. Smooth load variations must be achieved whenever possible, therefore large load reductions from high load should also be performed gradually. A slower loading ramp than the maximum capability of the engine permits a more even temperature distribution in engine components during transients but on the other hand it is limiting the ability of the engine to absorb the load fluctuations.

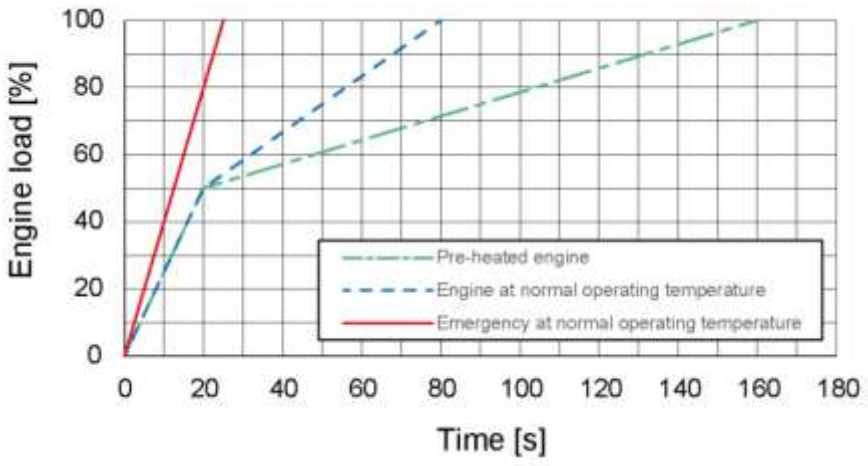

Figure 4 Max. recommended load ramp rates for Wartsila 31 diesel generator in emergency and normal operation modes [12].

It should be mentioned that modern diesel engines have also “Emergency” load curves that are closer to their maximum load capability, but it shall not be used as the normal limit[12]. In these instances, it might be preferable add batteries in a peak shaving arrangement to improve the vessel responsiveness and thereby system’s performance and reliability.

Another reason for hybridizing a marine propulsion plant is related to potential fuel savings. The specific fuel consumption (SFC) and the emissions of an internal combustion engine are function of the engine load. Typically, marine engines are selected for optimum performance

at high loads. In fluctuating profiles, the engine is often operated away of this optimum point. By effectively reducing the time in which the engine operates in non-optimum conditions, fuel savings can be achieved because of the higher engine thermal efficiency [13]. In other words, less fuel is required to produce the same amount of mechanical or electrical work. For ship types that experience large load variations and/or prolonged periods of low power demand, smaller engines can be installed with boost power provided by the batteries when required.

Lastly, hybrid energy storage integration is being used to deal with the intermittency of renewables (i.e. solar panels) that might be fitted to the ship. It should however be mentioned that these purposes are not mutually exclusive. Depending on the operational profile and the design philosophy, one ES application might fulfil more than one function.

1.4 Li-Ion Battery Driving Factors

Besides the outlined benefits in application level, wider adoption of battery systems has also been facilitated by recent battery developments.

Moreover, increased scientific interest and large investments by other industries (automotive, telecommunications, railways etc.) in the field of energy storage have resulted in high capacity batteries for electric vehicles and large-scale grid systems that were not available a few years ago. As can be seen by (Fig.5), modern li-ion batteries have improved their capacity per unit of mass from about 100Wh/kg to about 225Wh/kg in cell level. In practice, this means that larger capacity installations can be fitted at the same space onboard .

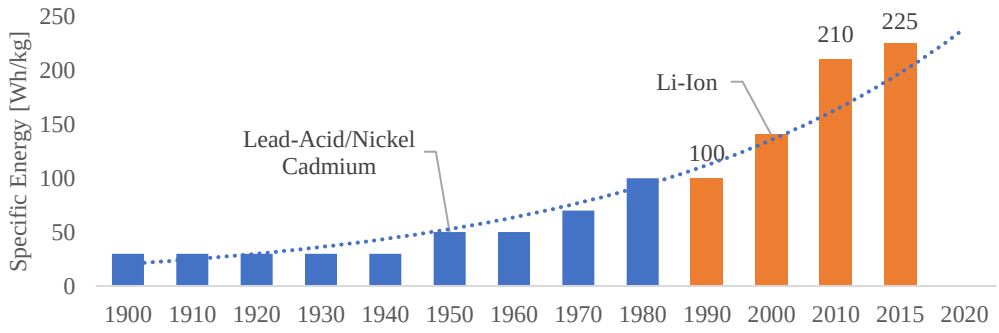

Figure 5 Historical Development of Battery Specific Energy in cell level [14]

However, the biggest driving factor is the significant price drop of li-ion batteries. Developments in the automotive industry have driven the technology and the scale of production. High production volumes, technical developments and increasing competition in the market have driven down the battery cost. Indicatively, Tesla Motor's new "Giga-factory" in Nevada, is expected to reach a li-ion battery production capacity of 35 gigawatt-hours (GWh) per year by 2020 [15]. This is nearly as much as the entire world's battery production combined in 2013.

As a result, DNV-GL reports that prices have declined in cell-level from 1,160 to 176 $/ kWh over the period from 2010 to 2018[16] . Impressively, these figures have already surpassed experts' projections on battery cost (Fig.6).

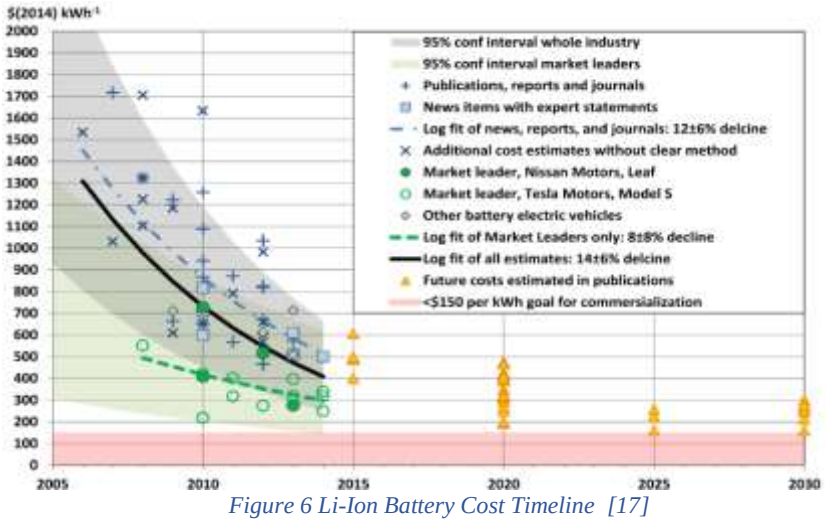

Figure 6 Li-Ion Battery Cost Timeline [17]

1.5 Li-Ion Battery Challenges

The documented success of existing battery-electric and battery-hybrid ship projects in terms of cost savings, environmental compliance and reliability has triggered the interest of the maritime industry for larger and more powerful electrical energy storage installations. To enable these larger installations, there are still significant challenges that first need to be addressed.

The first concern is related to battery capacity degradation or aging. Applications of transient power input/output such as propulsion dynamic assistance in ships or operation in heavy seas, have an adverse effect on battery lifetime meaning that the degradation of energy capacity over time is accelerated. When the capacity fading exceeds the 20% of initial nominal capacity then the battery can no longer meet application requirements and requires replacement [18].

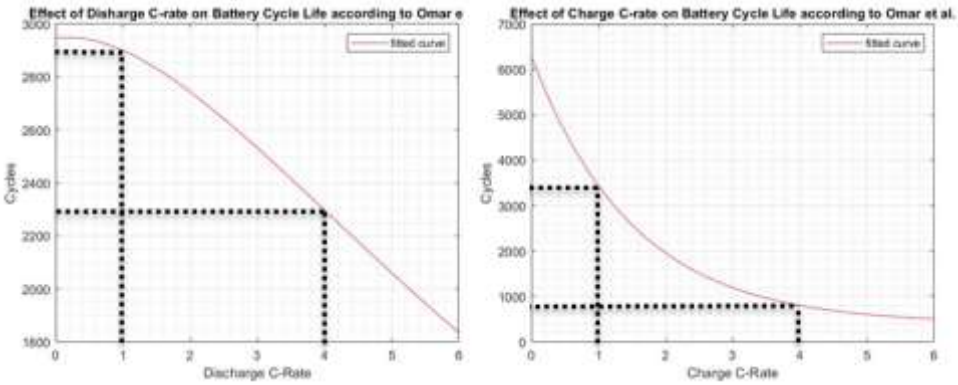

Figure 7 Effect of C-rates on LiFePO4 Battery Lifetime [19]

Operational parameters such as deep depth of discharge, high charging /discharging currents (C-rate[2]) and extreme temperatures that the battery may experience have been reported to affect the cycling aging behaviour of the battery [18, 21, 22].

[2] C-rate is a measure of the rate at which a battery is discharged relative to its maximum capacity. A 1C rate means that the discharge current will discharge the entire battery in 1 hour. 2C in 30 min and 4C in 15 min.

20. Team, M., *A guide to understanding battery specifications.* Academia. edu, 2008..

The single effect of C-rates on battery cycle life is shown in Fig. 7. Based on experiments conducted by Omar et al [19], if the battery is cycled in 1C it has an equivalent cycle life of 2900 full cycles. In the same graph it is shown that the battery can only achieve 2300 full cycles (20% less) when a C-rate of 4 is applied instead. From the same figure, it can be deduced that the effect is even worse for charging C-rates. Specifically, for a C-rate of 1 the battery has an equivalent of 3400 full cycles, while a charge C-rate of 4 is applied the same number drops to 800 cycles (82% less).

To reduce the effect of peak currents and large discharge cycles, current practise in marine installations involves the over-design of the battery system. Limited by their low specific power, Li-Ion batteries already need paralleling to reach high powers [23]. By paralleling additional battery modules, the max. C-rate is lowered while maintaining the same power ratings. By effectively reducing the max. C-rate, battery lifetime can be extended. However, an over-sized battery system will result in additional capital cost, space and system weight.

Finally, it has been reported that cycling aging can partially be controlled (slowed down) via operational measures that limit the energy storage utilization. Such measures include conservative energy management systems that restrict battery operation in high loads but at the expense of power system's performance and reliability[24, 25].

It is evident that despite the significant developments in battery technology there are still significant challenges that need to be addressed such as the undesirable trade-off between battery aging and battery size. In the following chapter, a practical approach to address these challenges is introduced while the aims and objectives of this thesis are clearly stated.

2 Problem Statement

2.1 Problem Definition

In the first chapter, the continuous growing interest of the maritime industry in battery installations, has been outlined as motivation for this thesis. The operational and environmental benefits of hybrid and battery-electric installations as well as the recent developments in battery cost and technology have enabled more shipboard applications of larger size.

However, it has also been stated that they are still significant challenges related to battery low specific power and cycling aging that need to be addressed. It has been mentioned ,that for peak load applications with high transients the battery degradation is accelerated. Additionally, limited by their maximum current rating, batteries cannot deliver effectively high C-rates and therefore are not able to fully absorb the load fluctuations. This results in a design trade-off dilemma; to over-size the battery by paralleling more modules to extend cycle life or to use a smaller battery but to accept shorter cycle life and compromised system's performance.

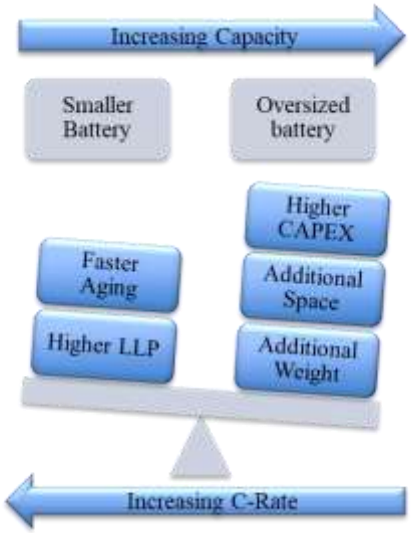

Figure 8 Battery Design Trade-off [3]

On the absence of an ideal energy storage system, there are several examples in literature from other industries that are examining the idea of combining storage technologies with complement features as an alternative solution to battery design trade-off [26-28]. By hybridizing the energy storage system, the aim is to exploit the strengths of each technology while hiding its weaknesses[29].

Supercapacitor, a high power device with ultra-high cycle life, has been proposed as an ideal match to the Li-Ion battery [30]. By placing the supercapacitor in parallel to the battery and by using it as a buffer for high peak currents, it has been suggested that it is possible to reduce the battery stress (and thus to extend battery cycle life) while improving the availability and the reliability of the power system. In addition, it has been reported that by taking advantage of the high specific power of the supercapacitor and the high specific energy of the battery there is potential to optimize sizing of the energy storage system for high power applications[26, 27].

Nevertheless, it has also been reported that even hybrid energy storage systems (HESS) might not be able to fulfil all these functions simultaneously. There are fundamental trade-offs that need to be considered, especially when considering a complex marine power system.

[3] Loss of Load Probability (LLP)

In compare to other industries such as electric vehicles and smart grids, there is very limited published work on marine battery/supercapacitor hybrid energy storage systems. This lack of research in the field of integrated and global design approaches for vessel applications, results in the necessity for further investigation of the HESS requirements, the dependencies between the key design and operating parameters and finally the performance trade-offs.

2.2 Research Questions

To address these considerations and based on the described potential of hybridized energy storage systems, the main research goal of this thesis is stated as follows:

"*To develop a design algorithm that combines sizing and energy management of hybrid energy storage systems in order to avoid battery oversizing for shipboard high-power applications with significant power fluctuations without compromising battery lifetime".*

The aforementioned main research goal can be analysed into research sub-questions as follows:

- What are the key design aspects of a Battery-Supercapacitor Hybrid Energy Storage System for a typical shipboard application?
  - What are the requirements?
  - What are the design constraints?
  - What are the trade-offs between design variables and desired outputs?
- How do we size a Hybrid Energy Storage System?
  - What is the ideal power and capacity split balance between the battery and the supercapacitor?
- How do these systems have to be managed to get the best of them?
  - What are the operation aspects of a Hybrid Energy Storage System?
  - How do we decide when and for how long to utilize each source (i.e. battery and supercapacitor) ?
- What is the impact of hybridization on system's overall efficiency and performance?

2.3 Thesis Objectives

To answer the research questions and to achieve the main research goal, the present master thesis will:

- Investigate the concept of Battery-Supercapacitor Hybrid Energy Storage Systems (for shipboard applications.
  - Review literature for any relevant work and identify the system requirements.
- Propose a design methodology for a Battery Supercapacitor Hybrid Energy Storage Systems that will extend cycle life of batteries ,in high power applications with significant fluctuations, without oversizing the system.
  - Define system design variables and constraints.
- Construct a design space with all feasible sizing combinations of Battery and Supercapacitor.
  - Compare the effect of different sizing combinations in system's performance for a benchmark operational load profile.
- Develop an energy management system to effectively allocate power between the hybrid energy storage system and a diesel generator as well as between the battery and the supercapacitor components of the HESS.
- Integrate sizing and energy management models to explore the performance regions and trade-offs between design variables and desired outputs for a battery supercapacitor hybrid energy storage system.
  - Integrate the hybrid energy storage system as a part of a benchmark ship's systems.

- Demonstrate the potential improvements of using the developed Battery-Supercapacitor Hybrid Energy Storage System with reference to battery-only baseline simulations.

2.4 Thesis Delimitations

Before describing the proposed approach, it is first necessary to also set the scope limitations of the thesis.

- The scope of present thesis is limited to power production and storage side of the electrical system; hence the energy management system has been designed following a backwards (effect-cause) approach. In this approach, the total load demand of all consumers is treated as an input to the power allocation controller and therefore no separate electric models of the consumers were created.
- The understanding of the proposed system will solely be based on the produced computer models and simulations. Therefore, no (real-world) experiments were conducted for the purposes of this thesis.
- MATLAB has been selected as the simulation environment due to the availability of generic component models that allow easy parametric changes and the relatively easy possibility to develop and run time-domain simulations.
- Calendar aging of the battery is not considered during the aging estimation of the battery. Calendar aging is not directly related to the operating profile of the battery and therefore it is expected that there will be no significant effect on it by the proposed solution.
- Supercapacitor lifetime is considered adequate for shipboard applications and therefore no estimation of remaining lifetime is required.

2.5 Thesis Approach

Given the problem statement and the definition of the thesis goals and objectives, the first step in the design process, is to outline the functional requirements that the Hybrid Energy Storage System must fulfil.

The next step is to translate the developed functional requirements into specifications for the selection of HESS topology.

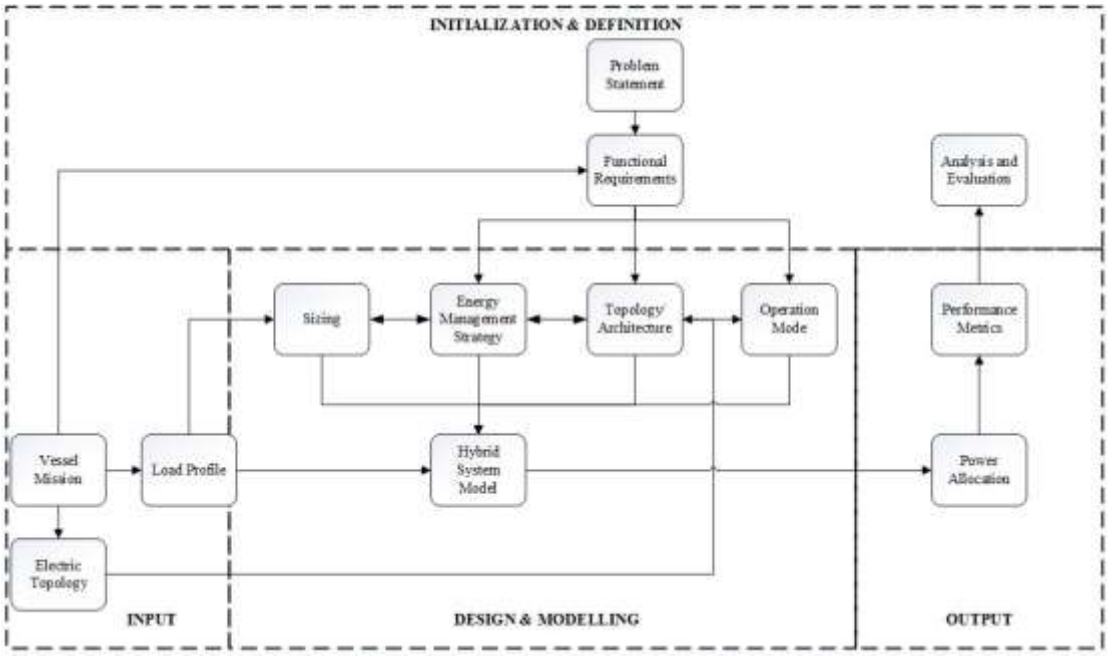

Figure 9 Thesis Approach

Following, a feasible design space of Battery-Supercapacitor sizing combinations is constructed using an Exhaustive Search Algorithm. After the construction of the design space and in order to correlate the design variables and static outputs of the sizing process with the dynamic phenomena of battery aging, HESS performance and total energy consumption, an energy management system is developed.

After the programming of the energy management strategy and based on a benchmark load profile, the HESS operation is simulated. In this backwards (effect-cause) approach, the load profile is used as an input to the model while power allocation between DG(s) and storage elements is the resulting output.

The system's performance is measured based on how well its function is fulfilled, its effectiveness and the trade-offs that must be made to fulfil these functions [31].

The static outputs of the sizing process and the dynamic outputs of the simulation are extracted in the form of design exploration maps and arrays and are used to correlate the key performance metrics with each sizing combination. Lastly, simulation outcomes are analyzed and evaluated before being returned as feedback to the stage of functional requirements.

2.6 Thesis Outline

The present thesis has been divided in 3 main parts. The first part, consisting of Chapters 1-3, is concerned with problem definition, project description and literature review of prior relevant work.

- In Chapter 1, status, trends and driving factors of energy storage maritime applications are discussed and presented as motivation to this project. Following, the practical challenges of battery aging and resulted oversizing in high-power applications are defined as a problem to be addressed.
- Chapter 2 outlines the research questions, the aims and objectives of the present thesis and the approach followed.
- In Chapter 3 battery and supercapacitor technologies are reviewed and compared to each other. Following, the concept of a battery-supercapacitor hybrid energy storage system is introduced and an analysis of relevant work on this topic is conducted.

The second part consists of Chapters 4-7 and represents the main body of this work, i.e. the design and modelling of the proposed battery/supercapacitor hybrid energy storage system.

- Chapter 4 outlines the design methodology including the functional requirements, the system topology and the performance parameters of interest.
- In Chapters 5, a methodology for sizing and dimensioning of the hybrid energy storage system is developed.
- Chapter 6 is concerned with the energy management system required to effectively operate the hybrid energy storage system.
- Following, in Chapter 7, modeling and analysis aspects of the conducted simulations are described.

The third and final part of this thesis comprises of Chapters 8 and 9.

- First, simulation results and findings are presented and analyzed in Chapter 8.
- Based on the derived conclusions, recommendations on future work are given in Chapter 9.

Finally, supplementary information and data related to the thesis, have been attached as appendices at the end of the report.

3 Battery-Supercapacitor Hybrid Energy Storage Systems

3.1 Li-Ion Battery Chemistries

With the term Lithium-ion we are referring to a broad range of different battery chemistries, each of which has very different performance characteristics [23]. The most common of which include: Lithium Iron Phosphate (LFP), Lithium Cobalt Oxide (LCO), Nickel Cobalt Aluminium Oxide (NCA), Nickel Manganese Cobalt Oxide (NMC) and Lithium Manganese Oxide (LMO). For the main battery chemistries, their performance is compared to each other for the key characteristics using a spider diagram fig.10.

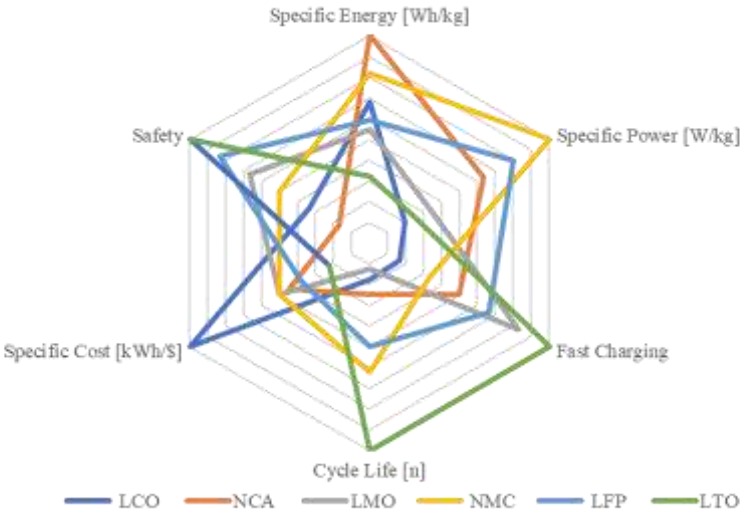

Figure 10 Comparison of most common li-ion battery chemistries adopted by [22, 23]

In a glance, LCO batteries have relatively high specific energy and are reported to be the most cost effective among all Li-Ion chemistries per unit of energy. On the other hand, they have a narrow life span of less than 700 cycles, and the lowest specific power among all types.

Next, NCA have the high specific energy with reported values up to 220 Wh/kg in cell level. However, optimizing for capacity will result in lower specific power and slower charging time. Additionally, it is reported as the second most expensive chemistry after LTO [23] while they score poorly in terms of safety due to thermal stability issues. Similarly, NMC chemistries have high specific energy between 140 and 200 Wh/kg. Again, drawbacks concern its cycle life and high cost.

LMO suffer from shorter cycle life making it an appropriate chemistry for portable power applications where this is not such a concern. On the other hand, LFP is one of the most popular chemistries due to its relatively high-power capability and moderately high life cycle. LFP is also considered to be more tolerant of abusive conditions such as overcharging the cell and high temperatures making it a safe choice for maritime applications [32]. Finally, (LTO) is the chemistry with both the highest cost per unit of energy and the highest cycle life. Moreover, its low specific energy makes it an unfavourable option for long range applications.

From the spider diagram, it is shown that no li-ion chemistry can fulfil simultaneously all desired characteristics. This is because there are fundamental trade-offs associated to the

electrochemical properties of each type. Table 3 summarizes some of the key trade-offs when it comes to battery specific power and specific energy.

High Specific Power	High Specific Energy
Thin Electrodes	Thick Electrodes
Porous Electrodes	Dense Electrodes
Nano structured electrodes	Large Particles
Low packing density	Large Packing density
Carbon Addition	Pure storage material

Table 3 High Power vs High Energy requirements for Li-Ion batteries [33]

A good example is the thickness of the electrodes used. Batteries assembled with thick electrodes can increase the proportion of active materials and thus increase their specific energy. However, it is reported that the battery with thicker electrodes has more intensive and uneven temperature response across the cell for the same discharge rates [34]. This causes the depletion of active materials and thus is accelerating battery aging. Zhao et al. also report that thicker electrode batteries have higher internal resistance which can result in lower power output[34].

3.2 The Supercapacitor

The supercapacitor also known as electric double layer capacitor and ultracapacitor [35] is a developing energy storage technology.

The supercapacitor differs from a regular capacitor in that it has very high capacitance. Indicatively, electrostatic capacitors have a low capacitance rated in pF, electrolytic capacitors are rated in μF (which is a million times larger than pF) and supercapacitors can reach capacitance values up to 3000F [35]. This is due to the layer of activated carbon on the electrodes, which increases the total surface area and eventually the charge storing capacity of the supercapacitor.

Contrary to electrochemical storage, supercapacitors store energy in the means of a static charge resulting to low heating losses and very high cycle life. The basic end-of-life failure mode for a supercapacitor is an increase in equivalent series resistance (ESR) and/or a decrease in capacitance. As can be seen in fig.11 commercially available modules can undergo more than 1,000,000 duty cycles before starting to deteriorate significantly[36]. Additionally, their low internal impedance enables them to effectively deliver high currents and thus achieve high specific power.

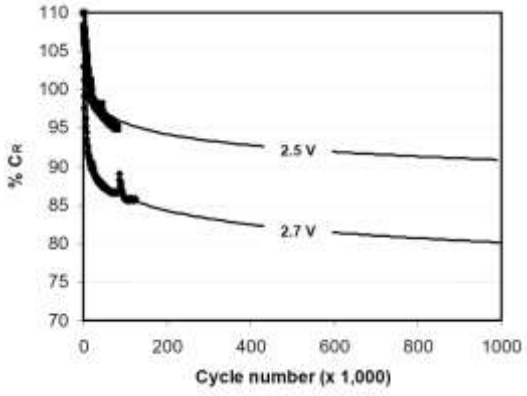

Figure 11 Capacity vs Cycling for Supercapacitors [Property of Maxwell Technologies[36]]

On the other hand, the amount of energy stored per unit weight of SCs is reported less than 10 Wh/kg. Another disadvantage of a supercapacitor is its large self-discharge rate. A supercapacitor may lose more than 20% of its stored energy per day even if no load is connected to it[37]. Therefore, it shouldn't be used in applications where medium- or long-term storage is required. Because of these characteristics, they are normally preferred in situations with frequent charging/discharging cycles or periodic high current pulses.

3.3 Li-Ion Batteries vs Supercapacitor

The Ragone plot is a tool used for performance comparison of various energy storing devices where the values of specific energy (in Wh/kg) are plotted versus specific power (in W/kg). Ragone plot is widely adopted for energy storage systems as it clearly demonstrates the trade-offs between these two magnitudes. For a given amount of energy, the higher the specific power and energy, the less the weight of the required energy storage system will be. Therefore, highly compact and light technologies suitable for high power mobile applications can be found at the top right corner of this plot. This tool adapted for li-ion batteries and the supercapacitor is shown below.

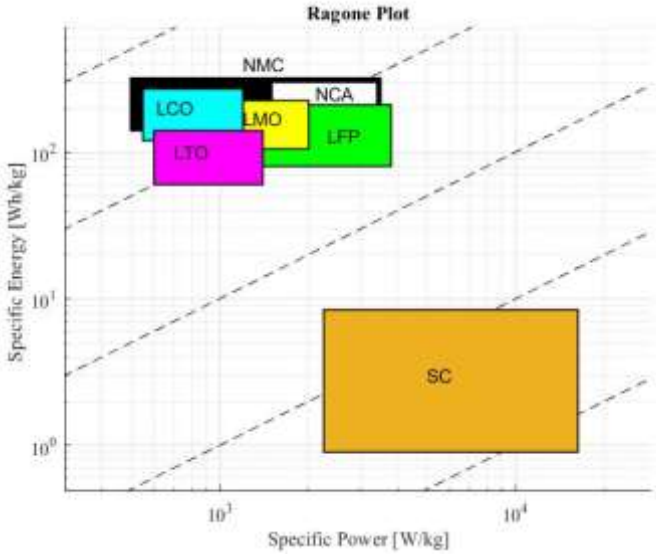

Figure 12 Ragone Plot – Li-Ion vs Supercapacitor. Partially adapted by [23, 38]

As expected, high on the specific energy axis, the li-ion batteries. Among them, NMC batteries are at the top with a range of 60-220 Wh/kg in cell-level. In the specific power axis, the same batteries lie within 500-3000 W/kg range. However, both the top values are for application optimized batteries meaning that there are no batteries optimized for both metrics. On the characteristic right-hand side of the graph, the supercapacitor may be found having a specific power range of approx. 5000 to 10000 W/kg. Nevertheless, the supercapacitor is placed towards the bottom of the y-axis meaning that it has a specific energy ranging between 1 and 10 Wh/kg. It is therefore seen that neither batteries nor the supercapacitor is located in the ideal region.

3.4 Hybridization of Energy Storage System

3.4.1 Definition and Philosophy

In the previous paragraphs, various energy storage systems, have been presented extensively. It has been demonstrated that no single type of ES element technology can fulfill all the desirable characteristics, such as high power/energy density, reasonable cost, high cycle efficiency, fast charging time and long cycle life at the same time due to fundamental trade-offs.

On the absence of an ideal energy storage system, there are several examples in literature discussing the idea of combining storage technologies with complement features in order to improve system's overall performance [26-28]. Hybrid ES systems (HESS), aim at exploiting the strengths of each technology while hiding its weaknesses[29].

For the purposes of the present thesis, a combination of lithium-ion batteries and supercapacitor has been decided. The concept of hybrid energy storage is introduced as a practical approach to overcome some of the limitations and thus to improve the performance characteristics of the entire system. Lithium-Ion batteries have been selected due to their high- specific energy, their higher cell voltage, their commercial availability, projections on declining prices and maturity in maritime applications. On the other hand, supercapacitors have been decided because of their higher-specific power, their significant life cycle, quick charging ability,

Function	Supercapacitor	Li-Ion (All types)
C-rate	<500	<6
Cycle life	500,000-1,000,000	500-5,000*
Cell Voltage	2.3-2.8V	3.6V nominal
Max. Efficiency	~95%	90-95%
Self-Discharge per day	20-40%	0.1-0.3%
Specific Energy (Wh/kg)	1-10	60-220
Specific Power (W/kg)	5,000-10,000	500-3,000

Table 4 Li-Ion Battery vs Supercapacitor Characteristics

By placing the supercapacitor in parallel with the battery it has been reported that is possible to maximize operational and cycle life of the batteries by limiting the currents which they discharge and recharge at. In this configuration, the battery is still used to supply a steady portion of the current to the load while the supercapacitor is used a power buffer to supply the bulk of the transient currents and currents in excess of those which are harmful to the battery. This way, instantaneous power input/output, can be served more effectively while protecting the battery from high C-rates.

In this subchapter, background work in battery/supercapacitor HESS is presented; with focus being given on potential benefit, on previous applications, and on design system characteristics such as sizing, architecture and energy management.

3.4.2 Hybrid Energy Storage Topologies (HEST)

Different structures of hybrid energy storage systems have been examined in scientific literature to date [39-41]. Each structure type is referred to as a Hybrid Energy Storage Topology (HEST) and is characterized by the coupling arrangement between the two storage elements and the wider power train configuration. The topology is a critical characteristic of a HESS system as it will define the system capabilities and restrictions with an application in mind.

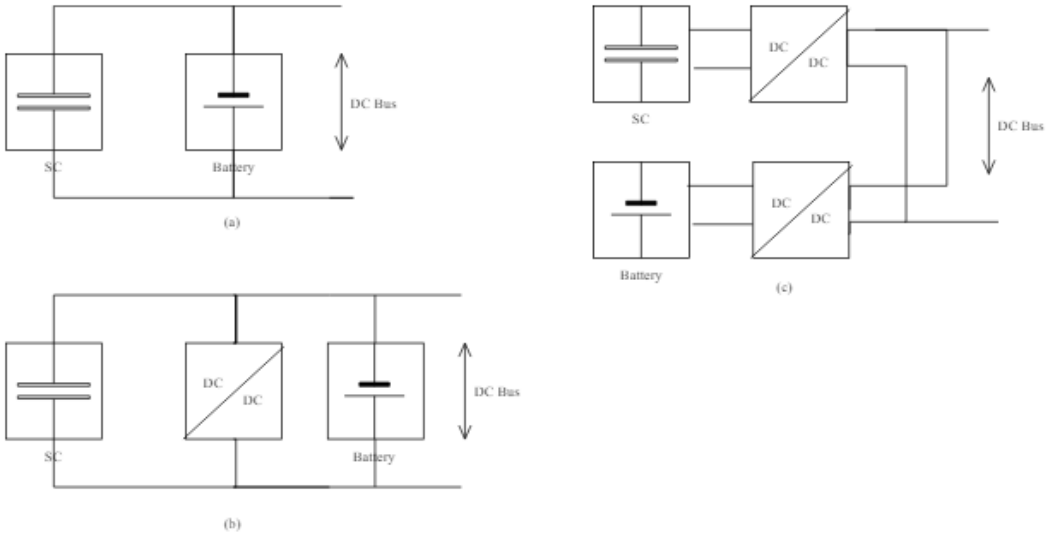

Figure 13 (a) passive HEST (b) semi-active HEST (c) parallel full-active HESS

Despite various design modifications, HEST can be classified into three main categories, based on the utilization or not of power electronic converters. These are namely passive hybrid energy storage topology (passive-HEST), semi-active hybrid energy storage topology (semi active-HEST) and full-active hybrid energy storage topology (active-HEST).

3.4.2.1 Passive HEST

Passive HEST is the simplest form of hybridization. It is achieved by direct parallel connection of the battery with the supercapacitor, without using any power electronic converters. By passively coupling the two devices, the battery is more protected from high currents in compare to the battery-only topology as these will be absorbed by the supercapacitor [40].

On one hand, the lack of power converters makes passive topologies more economical and less space intense but it consequences zero control capability over the distribution of power between the two storage devices. Without control over the supercapacitor or the battery, it is not possible to develop a complex energy management system that will fulfil multiple functions.

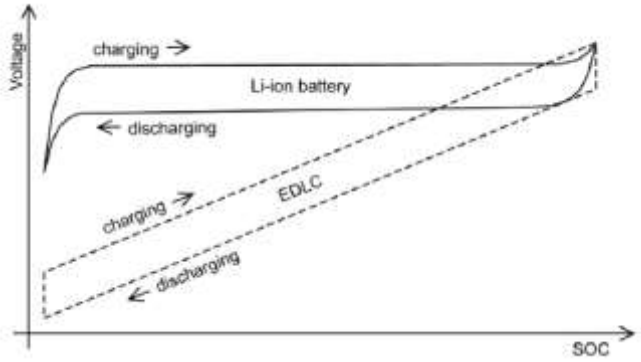

Figure 14 Exemplary voltage profiles for charging/discharging of Li-Ion Batteries and Supercapacitors[42]

In passive HEST, the voltage of the battery and the supercapacitor is identical to the voltage of the load meaning that the operating voltage window of both devices must match the load. Nonetheless, the charge and discharge characteristics of the battery and supercapacitor are very different resulting in the supercapacitor capacity utilization being limited by the voltage range of the battery [39]. Batteries have more constant voltage characteristics resulting in limited effect to the available capacity. However, in supercapacitors, the available capacity is a delivered as function of the voltage resulting in further limitations to its utilization as a result of the voltage drop.

$$E_{sc} = \frac{1}{2} C \cdot V^2$$

3.4.2.2 Semi-active HEST

In order to operate each energy storage in an optimal way and in accordance with its characteristics, the energy storage devices must be decoupled. The number of decoupled energy storage units defines a system as semi-active hybrid energy storage topology and full-active hybrid energy storage topology. A semi active HEST comprises of two or more different energy storage devices, from which one of the energy storage devices is decoupled using a power electronics converter [41].

Depending on which energy storage device is decoupled, semi-active HEST can further be analysed to various reported sub-topologies. Fig.13 (b) is showing a parallel semi-active HEST in which a bi-directional DC-DC converter is added between the battery pack and the supercapacitor. In case where the battery is decoupled from the load, it can be protected from short term power peaks and utilize its full capacity although the direct coupling of the supercapacitor with the power train will result in same limitations with the passive topology. In the reverse case (where the supercapacitor is decoupled from load), higher utilization of the supercapacitor energy is possible due to the extension of its voltage window. Again, the direct coupling of the battery with the load will result in limited controllability and higher balancing requirements (especially for high voltage applications), as the voltage of the battery will be following the voltage of the load.

3.4.2.3 Full-active HEST

In full-active HEST, both storage devices are decoupled by the load using power converters. In compare to the previous topologies, full-active is a higher cost solution as it incorporates two converters. Additionally, there are higher conversion losses and higher space requirements all because of the introduction of the additional converters. Regardless of these weaknesses, full-active topologies are becoming more popular as the power electronics technology progresses. This is because they allow the development of elaborate energy management strategies that will

enable both the supercapacitor and the battery to be operated optimally, based on their individual characteristics and thus to vastly improve the effectiveness of the whole system.

In Fig. 13(c) ,the two components of the HESS are placed in parallel and are decoupled from each other and from the load. Each connected to the load via its own bi-directional DC/DC converter. Another advantage of this arrangement is that each DC/DC converter can be power sized independently resulting in optimize sizing capabilities.

3.4.3 Hybrid Energy Storage Sizing

In conventional battery only storage systems, the sizing process is based on the estimation of the minimum power rating and energy capacity of the storage system to meet application requirements. Trade-offs such as system's overall efficiency, weight and CAPEX have also been reported to affect the sizing decision [25, 43-45].As there is only one type of energy storage technology, battery's capacity and power rating are equal to that of the storage's system and therefore battery dimensioning is a straightforward process.

On the other hand, dimensioning of a hybrid energy storage system is a more complex process as proportions between each storage device need also to be considered next to overall system's size. Depending on the optimization target, several different approaches have been proposed in past literature to address the sizing problem of HESS.

The most simplistic approach is to use the ragone plot to achieve a good compromise in terms of size. Nevertheless, this is a static approach where the system is not optimized [46]. Sadoun et al. focuses on the effect of different load profile in HESS sizing [47]. Another approach is to size the HESS components using a frequency filter method. The battery is optimized to handle low frequency while the supercapacitor is optimized for the higher part of the spectrum[48]. Jianwei Li et al. [49] have proposed a method in which the battery capacity is sized based on the system energy requirement and is connected to the system's required reliability. In the same work the high-power source is sized based on power requirements. Other performance metrics that have been reported to be optimized include minimum battery damage [50] or minimum weight [51].

L. Sun, P. Walker et al. [52] report that the main issue found within aforementioned sizing methods are related to them adopting a single objective optimization approach where cost is barely considered. As a consequence, fair comparisons and design trade-offs are difficult to be quantified. Additionally, they propose an analytical approach [52] in which the power converters are also considered as a part of the sizing process.

3.4.4 Maritime Experience on Battery/Supercapacitor Storage Systems

3.4.4.1 Literature & Studies

In compare to the extensive research on hybrid storage systems in applications such as EVs, smart grids and portable electronics, there is relatively limited published work on the integration of battery/supercapacitor HESS with marine power systems.

Most of the work is concentrated on naval All-Electric Ships (AES), where intermittent weaponry loads along with fluctuating propulsion loads are common [53]. This is because of their requirements to accommodate power fluctuations from the generators but also the intermittency between the load and power supply for a longer time. However, it is difficult for a single type of energy storage to satisfy both functions effectively. A high capacity energy storage is required for the steady power demand while a high-power source should be used to supply transient power demand. Combinations of these two systems, have been proposed as an alternative approach that can provide side benefits as well.

Tang et al. [54] have proved the feasibility of a li-ion battery/supercapacitor system for propulsion system and pulse power loads in "USS Arleigh Burke" class destroyer. A dual active bridge (DAB) topology was used to control the bi-directional power flow through phase shifting for charging and discharging batteries and supercapacitors. This configuration can provide high flexibility as each source can be sized at different power output and can be charged/discharged independently. Further work on this topology has been made on [55].

Active parallel topology with half bridge DC/DC bidirectional converters, has also been discussed in [56]. In this case, lead acid batteries have been used coupled with supercapacitors to improve the utilization rate and service life of the battery. The vessel type is however not specified.

Charpentier et al. [57] proposed an alternative hybrid propulsion power system for the passenger canal boat "FCS Alsterwasser". The ship originally driven by proton exchange membrane fuel cells (PEMFC), is modified to incorporate an HESS of lead-acid batteries and supercapacitors. The energy storage system is introduced to compensate for the limited dynamics and the slow response of the fuel cell systems during load transients and start-up time. Furthermore, to optimize power allocation between fuel cell and energy storage devices, a fuzzy logic energy management strategy is proposed.

On the other hand, in Trovao et al. [58], an indirect energy management strategy for a passive parallel topology connecting NiMH batteries and supercapacitors to the DC power distribution of a 160kW canal boat has been followed. This strategy was based on the stabilisation of the DC link voltage and showed that battery lifetime extension and lower using cost of the batteries was possible. The simplistic approach of selecting a passive parallel topology allows lower initial cost with single converters being used but at the price of no controllability of the storage devices. An overview of all prior relevant work of battery/supercapacitor HESS in maritime applications, is shown in Table in Appendix A.

By reviewing relevant literature, it is seen that most works are focused on a sole aspect of the system whether this is the energy management or the design of the converters. Important aspects like sizing are neglected using simplistic approaches such as load-averaging or are not discussed at all. Additionally, to the best of the knowledge of this thesis author, there is no work where the effect on battery aging has been quantified. Furthermore, the conclusions of these works are usually constrained by assumptions related to very specific applications such as military vessels that make their conclusions not applicable to other applications.

This lack of research in the field of integrated and global design approaches for vessel applications, results in the necessity for further investigation of the HESS requirements, the dependencies between its key design parameters and the performance trade-offs.

3.4.4.2 Applications

Ar Vag Tredan is is the first vessel of any type to be powered by supercapacitors. This full electric catamaran ferry was built in 2013 by STX France Lorient. The ferry serves a 20 minutes' round trip of around 1.7 nautical miles 28 times per day at a maximum speed of 10 knots crossing the Lorient bay between the city centre and Pen Mane, where she recharges her supercapacitors in just four minutes while the passengers enter and leave the boat [59]. The boat is equipped with 128 supercapacitors (modules) with a total weight of 6 tons.

Figure 15 Ar Vag Tredan is a zero-emission electric ferry using supercapacitors [Property: STX France]

The only reported maritime application combining both batteries and supercapacitors is an all-electric Chinese bulk carrier carrying coal down the Pearl river of the Guangdong province [60]. The ship is 70.5 meters long, 13.9 meters wide, 4.5 meters deep, 3.3 meters draft design, and it has a cargo capacity of 2,000 tons. According to [60], the powertrain is equipped with two 160 kW electric propellers and a mix of supercapacitors and lithium batteries for a total energy capacity of 2.4 MWh. Under full load conditions, the ship can reach a maximum speed of about 7 knots and a range of up to 50 nm on a single charge. Reported time for the ship to be fully charged is 2 hours, matching the time of berthing at the dock for cargo loading and unloading. Unfortunately, there are no publicly available information available on the design and the operation of this HESS to the knowledge of the author.

3.4.4.3 Guidelines

Finally, it should be mentioned that some classification societies have recently issued safety guidelines on supercapacitor systems for owners/operators, shipyards, designers & manufacturers. The American Bureau of Shipping has issued such guidelines that are "applicable to marine assets constructed or retrofitted with a SC system used as an additional source of power with a capacity >50 Wh" [61]. To get the corresponding class notation (ESS-SC), the system integrator need to submit for approval the system capacity calculation for intended application, a risk assessment report incl. failure modes, the system's configuration and topology and the power flows between all elements of power system and the supercapacitor.

3.4.5 Reported Benefits of HESS

Potential benefits based on literature could be summarized in:

Battery lifetime extension: Shipboard systems are in general power systems with high load fluctuations. High C-rates have an adverse effect on battery lifetime. In hybrid energy storage system, the battery is protected from high C-rates, since the current can be drawn from the supercapacitor. Therefore, an extension of battery lifetime can be achieved through an elaborate energy management system.[47]

Downsizing of Battery: Existing installations of battery energy storage in high-power applications are designed to meet peak power leading to over-sized systems. By using the supercapacitor to handle these peak loads, it is possible to downsize battery sizing for energy management applications. By combining these two devices, it is possible to reach a ''new'' area in the ragone plot and achieve an affordable compromise of power vs capacity.

Increased reliability: The quick charge and discharge ability of the supercapacitor enables transient loads to be effectively handled in cases where the battery or the prime mover are limited by their loading capacity.

Increased system efficiency: It has been reported that hybrid energy storage systems may achieve a higher overall system efficiency in compare to homogeneous battery systems, because of the higher roundtrip efficiency of the supercapacitors. This can be justified by the low internal resistance of supercapacitors and the direct energy conversion (electrical-to-electrical), that reduces heat losses. Nevertheless, this is a simplistic approach that does not consider the efficiency losses due to additional power conversion.

Improved dynamic performance: Can be used for dynamic stabilization of fuel cells during transient loads and for maintaining bus voltage within desired margins [62].

Stress reduction: Supercapacitor are more resilient to large DoDs, meaning that they can be used to relief stress from other sources. Besides, lifetime extension this could also result in lower maintenance costs for primary power source such as diesel engines or fuel cells.

Cost Savings: Operating cost benefits, can be related to reduced maintenance for the engine and to higher operating life of the battery. Also, in applications with high load fluctuations additional fuel saving might be possible by allowing the power source to operate in high efficiency region for longer time. In terms of CAPEX, there is a delicate balance in net benefits, as one should also consider the acquisition and installation cost of additional converters. Finally, it has also been reported that a combination of lead-acid with supercapacitor could be a more economical alternative to pure Li-Ion installations.

4 HESS Design Principles

4.1 Design Objective

As was seen in Chapter 3, potential benefits of battery/supercapacitor hybrid storage systems include effective handling of power pulse loads, battery life extension, optimized sizing, reduction of engine's dynamic loadings etc. However, it has also been reported that even hybrid energy storage systems might not be able to fulfil simultaneously all these functions. There are fundamental trade-offs that need to be considered, especially when considering a complex marine power system. This is because of the dependency of the system output on the dynamic characteristics of the load profile, the mode of operation and the energy allocation strategy, the system architecture and the sizing analogies of the sources. Without a prior knowledge of system behaviour it is difficult to optimize the design for a specific metric.

In chapters 4-7 of the present thesis, a Lithium-Ion/Supercapacitor hybrid energy storage system model is designed, sized and integrated via an Energy Management System to a typical DC shipboard power system. For the purposes of this thesis the focus is given on hybrid peak shaving applications.

The main objective is to increase understanding of the relationships between design and operating aspects of marine hybrid energy storage systems.

4.2 Design Approach

Function design distinguishes between innovation and improvement. Improvement usually only concerns the reorganization or reengineering of an existing system, which implies a re-arrangement of existing functions or a different interpretation of these functions. On the other hand, innovation concerns the extension, reduction or modification of function due to the introduction of new technology, resources and/or organization [31]. For the design of the concerned system, an innovation approach has been followed as innovative technology element (i.e. supercapacitor) is added to a conventional battery hybrid system.

Following the decision for a combined approach, the first step in the design process, is defining the functional requirements that the system must fulfil. The functional requirements should be based on prior knowledge and experience, vessel mission characteristics and exploitation of potential benefits. At the same time, technology constraints should be made clear.

The next step is to translate the developed functional requirements into system architecture both in HESS and power plant level.

Following, a feasible design space of Battery-Supercapacitor sizing combinations is constructed using an Exhaustive Search Algorithm. Sizing of a heterogeneous ES system is a complex process and should not be underestimated during the design phase.

Succeeding, the definition of requirements and the sizing, the energy management system is also developed in two levels. On the first level, decisions on the HESS utilization (charging/discharging) are being made in conjunction with the operation of the prime mover while on the second level, the EMS's primary function will be the power allocation between the storage devices, based on their state of charge, the prime mover strategy and on the momentarily load balance at the demand side.

Next, it is possible to simulate the system behaviour for a benchmark case. For each simulation, a different operating mode or energy allocation strategy can be tested.

Finally, the system's performance is measured based on how well its function is fulfilled, its effectiveness and the sacrifices that must be made to fulfil these functions[31]. To do so, key performance indicators for hybrid energy storage systems need to be previously defined.

The simulation outcomes are evaluated and returned to the stage of functional requirements. If all requirements are fulfilled and the system performance is adequate, then the process terminates. For the purposes of this thesis, the iterative character of the process, will be focused on the testing of various system inputs such as sizing analogies of ESDs and disturbances such as the energy management strategy.

4.3 Functional Requirements,

Before designing the proposed HESS in terms of component size, architecture and energy management strategy, one should first define the framework and the functional requirements as derived by the research objectives and by the type of application. The functional requirements can be analysed in design- HESS (local) level and in operation-energy management (global) level.

4.3.1 HESS Design Functional Requirements

1. *Reliability:* The hybrid energy storage power system should be designed to ensure full cover of the total demanded load in at least the 95% of total operation time.
2. *Aging*: The battery component of the HESS should be protected from high current loads to extend its battery lifetime. Battery aging should be expressed as battery damage percentage and be benchmarked for battery-only operation.
1. *Sizing*: The system energy capacity should be the minimum necessary to ensure fulfilment of reliability and battery aging criteria.
2. *Efficiency*: Overall system efficiency should be promoted where possible. External energy introduced into the system, conversion losses and engine fuel consumption should all be quantified to determine overall system's efficiency.
3. *Flexibility:* Adding, removing or modifying configuration of HESS elements should be easy, without a significant modification to the whole HESS system.
    a. System architecture should be able to accommodate increased number of ES elements. In this direction, battery and supercapacitor modules are designed in parallel/series strings to match applications requirements.
    b. Power allocation strategy should consider case when one of the components is not available (i.e. battery only operation).
4. *Controllability*: In order to operate each energy storage device optimally based on its charge and discharge characteristics while improving the performance of the system, a high degree of controllability should be allowed. Specifically, this can be analysed in:
    a. Control of battery charge/discharge with bi-directional power of flow.
    b. Control of supercapacitor charge/discharge with bi-directional power of flow.
    c. Power sharing of the required load between each the HESS as a whole and the primary source (i.e. diesel generator) should be possible.
    d. Individual assignment (sharing) of the required load between battery and supercapacitor should also be possible. The system should be designed in such a way that the battery and the supercapacitor can operate:
        i. Independently (series operation)
        ii. Simultaneously (parallel operation)
5. *Compatibility*: The system should be able to serve existing loads on-board the vessel and to be successfully integrated with the other components of the ship's power drive (i.e. DC architecture).
6. *Safety* & *Compliance*: The design should be in accordance with regulations/guidelines if applicable. Indicatively, classification societies of ABS and DNV-GL have released

guidelines on marine supercapacitor systems and can be used for [61, 63]. For the scope of this thesis, no further focus is being given on the safety guidelines of the system as this should be examined separately in a later realisation stage.

4.3.2 HESS Operational Functional Requirements

Expanding the design requirements into the operation of the system, another set of necessities is defined. These requirements will be used as guidelines for the development of energy management system on Chapter 6.

- The system should maintain the (power) balance between the loads and the supplied power. In other words, the system should be able to deliver all power required by the ship at any time. If for any reason the available power is not sufficiently enough to cover the load on the demand side this should be clearly declared as a loss of load instance.
- Utilization of the battery component of the HESS should be avoided under high current loads to extend its cycle life. Instead, supercapacitor should be preferred in these instances.
- Power allocation decision variables should be easy to obtain in an on-board application (i.e. measuring state of charge based on voltage and momentary electric load demand).
- System should be able to serve selected peak-shaving operating mode. These are identified as load levelling or load following.
- In terms of power flows:
    - The HESS should be charged from the excess available power of the diesel generator.
    - The HESS should be able to operate simultaneously/in-parallel (peak-shaving) with the primary source (i.e. the diesel generator).
    - Individual assignment of battery and supercapacitor should be possible.
- The system should use as an input the load profile (kVA or kWe) of the vessel expressed in time domain to simulate the energy management decisions that need to be taken in real time.
- The energy management system should be designed for normal operating mode of the diesel generator (no emergency).
- The engine(s) should operate in a reasonable and relatively high efficiency region to promote low fuel consumption and overall system efficiency where possible.

4.4 System Architecture

Following the definition of the functional requirements, the first step in shaping the design approach, is to decide the configuration of the power plant system that will act as a “testbed” for the design of the hybrid energy storage system and the topology of the HESS that will be incorporated to it.

4.4.1 Power Plant configuration

1.1.1.1. Benchmark configuration

For the purposes of this thesis, a generic full electric DC power plant topology consisting of a single diesel generator and a battery module has been selected as benchmark configuration (Fig. 16). Similar power plant configurations have been presented by Geertsma [8] and are already implemented in hybrid/full-electric applications such as world’s first full electric ferry MV Ampere [9]. As batteries are already DC-sources, it has been reported that DC architecture allows their easier integration to the power system [64]. Additionally, according to Geertsma [8] load sharing in DC systems is achieved by voltage droop control. By setting different values for voltage droop for different power sources the share of dynamics taken up by the different

types of power supply can be controlled. Thus, it is expected to lead into more DC architectures for hybrid powered systems in the future.

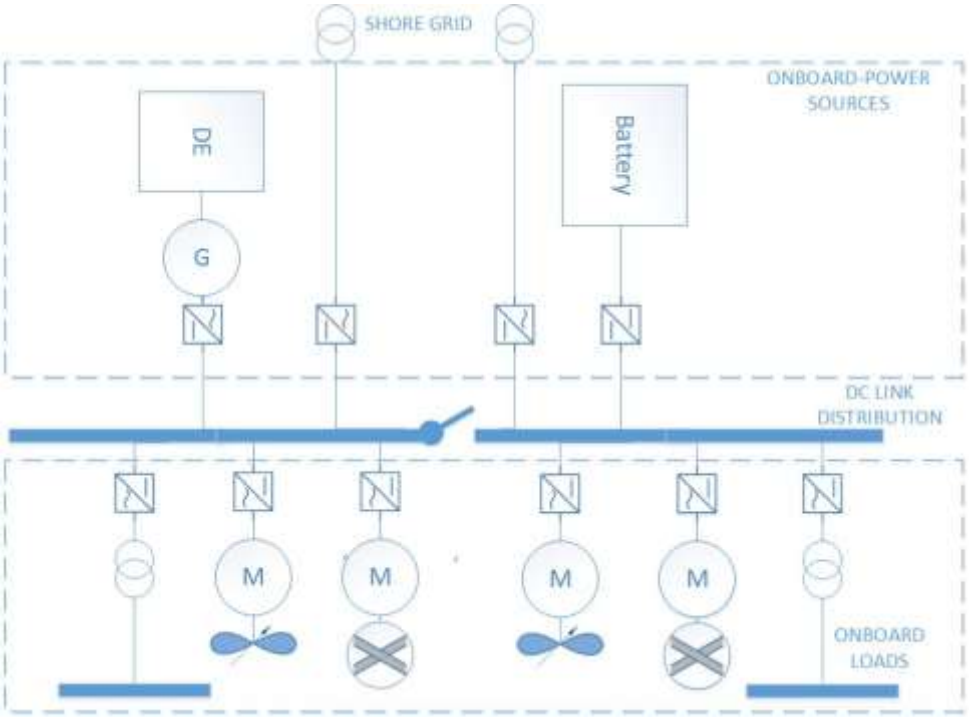

Figure 16 Basic architecture for battery-only hybrid installation

In the studied power plant configuration, the diesel engine is connected to an alternator than its turn is connected through an AC/DC inverter to the main DC bus bar.

For the purposes of this thesis, Wärtsilä 8V31 diesel engine is considered. This is a 4-stroke, non-reversible, turbocharged and intercooled diesel engine with direct fuel injection [12]. Wärtsilä 31 has been selected as it is designed to be suitable for a broad range of ship types and applications such as a main propulsion engine, in diesel electric configurations, in hybrid installations or as an auxiliary engine and therefore can serve in a generic purpose topology. Additionally, Wärtsilä 31 is reported to be the most fuel-efficient four-stroke engine in its class. At its optimum point the diesel version of the engine has been measured to consume as less as 165g/kWh[12, 65].

Voltage of the bus bar is assumed constant at 1000 VDC. The battery module is placed in parallel to the diesel generator and is connected to the DC bus bar via a bi-directional buck-boost DC/DC converter. The battery is used in peak shaving mode. Specifically, when the load demand is less than the engine available power as defined by the EMS, the excess power is used to charge the energy storage module. In this case, power is flowing from the diesel generator to the DC-bus and from there to the battery module via the DC/DC converter. Inversely , when engine power is insufficient to serve whole load demand, the battery is discharging and can directly supply power to some of the consumers through the DC-bus.

Potentially, shore grid connection capability is available for cold ironing mode while in port. In this mode that many passenger and cruise ships incorporate, the generators are shut off and all hotel loads are served by the shore grid when in port to avoid burning of polluting hydrocarbons near residential areas. Moreover, for vessels having shore grid capability it is possible to operate in hybrid plug-in mode meaning that they can fully charge their energy storage system while in port and utilize in a later stage.

4.4.2 HESS Topology

Considering the requirements in paragraph 4.3. the characteristics of different hybrid energy storage topologies in 3.3.2, and the benchmark power plant configuration, a parallel full-active HEST is selected. This is because the passive HEST and the semi-active HEST allow limited (if any) controllability over the two storage devices meaning that an elaborate system aiming to fulfill fuel efficiency, minimum sizing and battery lifetime extension is simply not compatible.

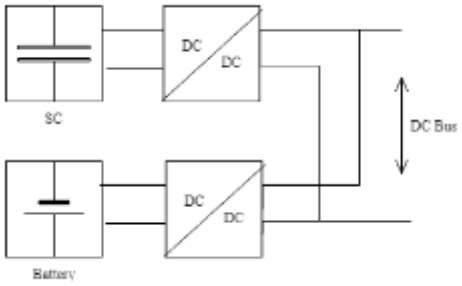

Figure 17 Parallel full-active hybrid energy storage topology

In the selected parallel-full active topology, the battery and the supercapacitor modules are connected to the same central DC bus through bi-directional DC/DC converters placed on independent power lines. Having independent DC/DC converters has the advantage that each storage device can be operated independently, based on its voltage characteristics. It is assumed, that both the battery and the supercapacitor modules can take-off / take-in 100% of power capacity in both charge and discharge directions. Another advantage of this arrangement is that a failure in one of the power lines can be tolerated because emergency operation using the other branch is possible.

By integrating the parallel full-active topology of the hybrid storage system into the benchmark configuration, layout of Fig. 18 is resulted.

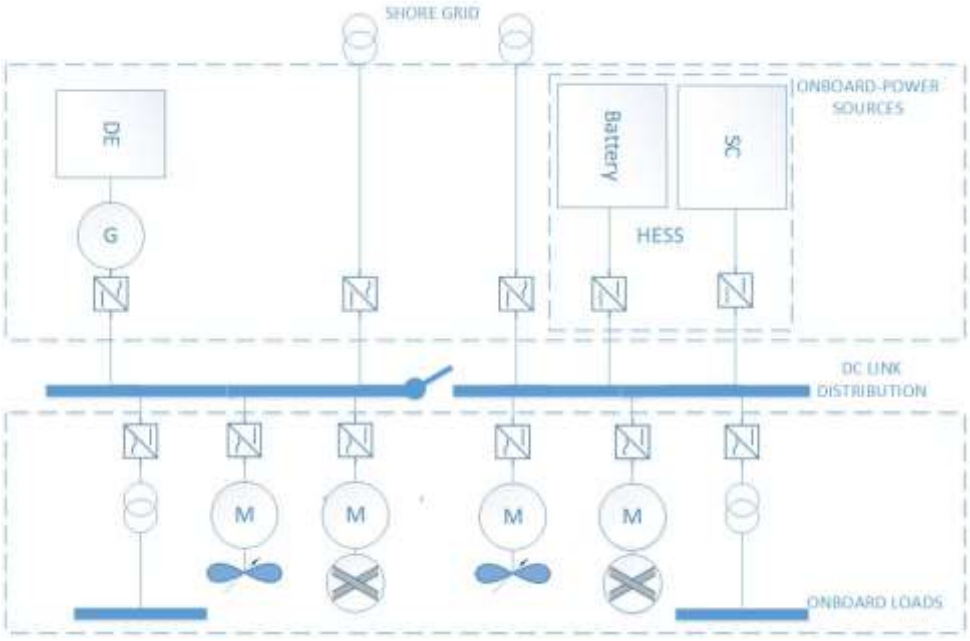

Figure 18 Basic system architecture with a single diesel generator and a HESS

Again, the battery-supercapacitor hybrid energy storage system is placed in parallel with the main diesel generator and is operated in a peak shaving mode. In charging mode, the power is flowing from the diesel generator to DC-bus where it is split between the HESS and the consumers. It should be mentioned that both the battery and the supercapacitor can only charge from the diesel generator and not from the other storage device. In discharge mode, the two storage devices can supply power combined or independently, but always in parallel with the diesel generator. Stand-alone operation of the HESS without the diesel generator although technically possible is out of the scope of this analysis and is not further examined. The operating mode and the power management system will be discussed in more detail in the Energy Management Section.

For future reference, this full electric DC topology can be scaled-up by adding more diesel generator sets in parallel similarly to prevailing diesel-electric architectures where four diesel generators are installed. In this case, equal load sharing among generators in proportion to their power rating is implemented. Another option for future reference, is the introduction of a second HESS modules replacing another diesel generator.

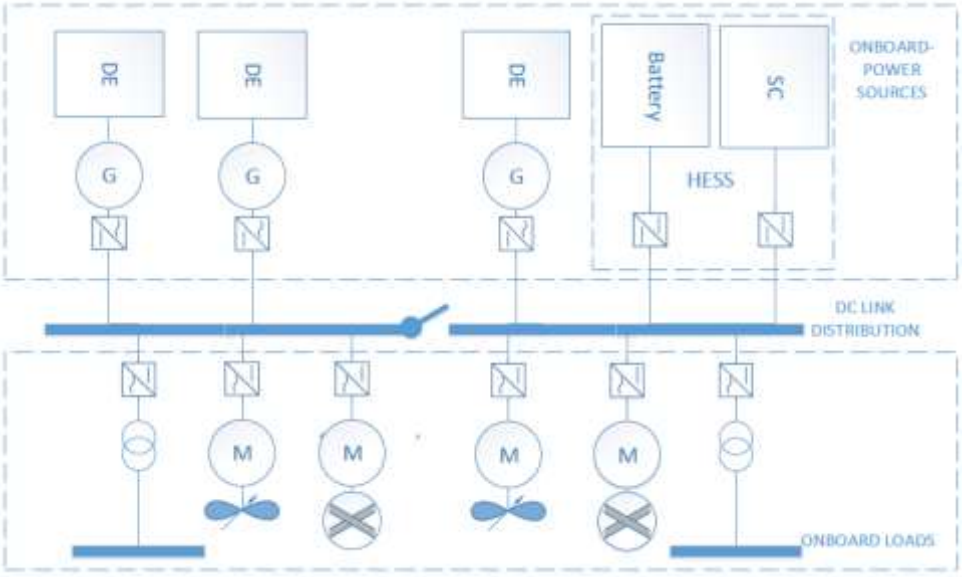

Figure 19 Expanded system architecture with HESS and multiple DGs.

4.5 Performance Metrics

To evaluate the performance of the developed sizing and energy management system, both static and dynamic performance parameters are being defined. As dynamic we define the parameters that are estimated using the Energy Management System and a time-domain simulation, whereas as static we define the parameters that can be calculated without the EMS following a steady-state approach.

4.5.1 Static Parameters

4.5.1.1 *Power and Capacity Split Ratios / Number of strings and cells*

For each feasible sizing combination resulted from the exhaustive search approach, a series of static parameters such as power and capacity split ratios, number of supercapacitor and number of battery cells in parallel and in series are estimated. These are indicators of the system's overall size and of the analogies between the two storage devices. Although, no direct conclusions can be made using these figures, they are used to estimate other static parameters such as cost and weight and they are particularly insightful when combined with dynamic parameters. Calculation of these parameters is discussed thoroughly in Chapter 5.

4.5.1.2 HESS Component Weight

By combining the high-energy density of the battery with the high-power density of the supercapacitor, it is theoretically possible to achieve an acceptable compromise in system's sizing by expanding to a new region of the Ragone plot. Estimating weight for each battery and supercapacitor combination including the effect of the power electronics, is a key metric to track any improvements between the suggested solution and the benchmark results.

4.5.1.3 HESS CAPEX

Capital expenditure include acquisition and installation cost of ESD elements. For batteries, this is typically expressed in cost per unit of energy ($/kWh) while for supercapacitors this is expressed in cost per unit of capacitance ($/F). Additionally, when considering a hybrid energy storage system, the cost of the power electronics should also be considered. For DC/DC converters this is normally priced based on the maximum power rating. Based on this, it is important to track both the impact of power rating and total system capacity on HESS CAPEX[51].

For the purposes of this thesis, no operational expenses including maintenance cost are measured for the HESS. It is however expected that higher capacity utilization of the energy storage system (i.e. slowdown of battery aging rate) could reduce the lifetime cost of the system. It should also be mentioned, that in most economic performance calculations of battery systems in marine applications, the battery is assumed to be depreciated fully (end of life) when they reach 80% of the original capacity or 80% of the original power [23]. This is because after this period, the batteries can no longer fulfil entirely their initial function. In this case, the ship operator should either accept a significant compromise in battery's useful energy capacity for a while or decide the replacement of it with a new module.

4.5.2 Dynamic Parameters

4.5.2.1 Battery Damage [%]

Considering the thesis objectives, battery aging expressed in life cycles is a key parameter to evaluate the performance of the system. A successful design incorporating the addition of a supercapacitor would theoretically result in the reduction of the experienced battery stress due to high peak currents and therefore an extension of the battery lifetime. In terms of estimating battery aging, the present thesis has focused on the effect of cycling aging and more specifically, on the effect of charge/discharge cycles (DoD) and charge/discharge currents (C-rate) to the battery capacity and remaining lifetime. A post analysis cycle counting procedure is followed where the output profiles of the simulation are used as inputs to the aging model.

Estimating cycling aging is considered adequate for proof of concept as this is the parameter that can be controlled through operational measures. Temperature effect has been excluded from modelling to keep computational time and model complexity reasonable. It is expected though that a model that is also including the temperature phenomena will be more favourable for the proposed approach as high rate operations contribute to an increase in heat generated internally in the cell [66]. The heat is generated because of joule heating which is proportional to the square of the current passing through the cell. This means that even a high-power lithium-ion battery with small internal resistance can generate a significant amount of heat when large quantities of charge flow through them. Finally, calendar aging, is not considered as it is not affected by operational parameters that can be controlled through energy management system and corresponding power allocation strategy and/or sizing process. The followed methodology is fully analysed in Chapter 7.

4.5.2.2 Loss of Load Probability (LLP)

As stated in the functional requirements , the HESS system should meet requested load in at least 95% total operation time.

Loss of load probability is introduced as a measure of system reliability and it is defined as the time the power system fails to deliver the demanded power over the time the system was designed to deliver power for:

$$0 < LLP = \frac{count_{fail}}{n} < 1 \tag{4.5.2}$$

Loss of load probability is an efficiency-alike defined factor varying between 0 and 1. Practically, a system with an LLP of 40% is only managing to meet load requirements at 60% of its operation making it less reliable in compare to a system with an LLP of 10% where the load is meet at 90% of operation time.

$$0\% \leq LLP \leq 100\% \tag{4.5.3}$$

Translating the 95% requirement, any HESS design should have an LLP equal or less than 5% to be accepted:

$$LLP \leq 5\% \tag{4.5.4}$$

As previously stated, as power system we consider the power production and storage system consisting of the diesel generator operating in normal operating mode ,the battery and the supercapacitor components of the hybrid energy storage system.

Commonly found in solar or wind integration applications where there is high uncertainty related to energy production [67], the concept of loss of load probability is being used to determine minimum required capacity of the energy storage system to reliably meet application requirements. In the case of ship applications, although diesel generator's power output can be controlled more effectively there are still some external factors on the demand side of the system (e.g. high wave induced load fluctuations) that might compromise the ability of the system to perform reliably.

Therefore, LLP can also be used in shipboard context as an appropriate metric that is correlating the size of the system with the Energy Management System in terms of reliability. Quantifying system's reliability is important when evaluating potential downsizing solutions, as in general larger capacity installations result in systems with lower LLP. Nevertheless, LLP can also be affected by the operating decisions on how each power source is utilized (e.g. if there is enough battery capacity at time t to cover load requirements). Therefore, a more detailed analysis is required as rate of improvement is not necessarily linear to system's size.

Calculation of loss of load probability is further discussed in Chapter 7.

4.5.2.3 Energy Consumption

Again, as identified during functional requirements stage, the hybrid energy storage system should promote overall efficiency where possible. This should be quantified and tracked for every sizing combination.

In hybrid systems, there is potential for fuel savings by effectively reducing the time in which the engine operates in non-optimum conditions. The aim is to produce the required electrical energy at the optimum point for the diesel generators, where the specific fuel oil consumption (SFOC) is a minimum [13, 68]. Nevertheless, the overall fuel consumption of an on-board hybrid power system will also be negatively affected by the additional conversion losses for charging /discharging of the energy storage system. Therefore, net effect on fuel consumption should be captured.

The developed tool has the capacity to obtain an accurate estimation of the diesel generator fuel consumption by using the dynamic load profile of the diesel generator as an output of the power

allocation and simulation process. Then diesel generator's fuel consumption can be estimated using engine shop test curves given by the manufacturer.

$$FC_{eng} = \sum_{t=0}^{t=n} P_{eng}(t) \cdot SFC(t)\, dt \tag{4.5.5}$$

However, when attempting to directly compare the fuel consumption of differently sized energy storage installations, it is important to specify whether external energy has been added to the system from the energy storage sources. Specifically, when simulation is assumed to start with the battery/supercapacitor storage system not empty, external energy (for which we have no information on what conditions it was produced) is introduced to an otherwise closed system.

For instance, a larger capacity battery is expected to have a higher energy throughput in compare to a smaller one as it can allow the diesel generator to absorb less fluctuations. In other words, it is expected that with a larger battery more already produced electrical kWh will be used during the same simulation span given it is adequately long enough. At the same time, less fuel will be converted by the diesel generator into new electrical kWh. This could be translated in lower fuel consumption for the diesel generator but not necessarily for the system.

Therefore, in order to reliably estimate the overall efficiency of the system it has been decided to evaluate it in terms of overall energy consumption including the HESS rather than direct fuel consumption alone.

$$\text{Energy consumption} = \mathrm{FC_{eng}} + \Delta \mathrm{E_{bat}} + \Delta \mathrm{E_{sc}} \tag{4.5.6}$$

where

$$\Delta \mathrm{E_{bat}}[\mathrm{kWh}] = \mathrm{E_{bat}}(\mathrm{t_n}) - \mathrm{E_{bat}}(\mathrm{t_0}) \tag{4.5.7}$$

$$\Delta \mathrm{E_{sc}}[\mathrm{kWh}] = \mathrm{E_{sc}}(\mathrm{t_n}) - \mathrm{E_{sc}}(\mathrm{t_0}) \tag{4.5.8}$$

With this expanded approach, it is possible to evaluate various HESS sizing's even if cold ironing capability for charging is added to the scope. Energy consumption modelling is further discussed in Chapter 7.

5 Sizing

In this chapter, a methodology for sizing and dimensioning of the battery-supercapacitor hybrid energy storage system is developed while an appropriate design space is constructed.

As mentioned in Chapter 3, dimensioning of a hybrid energy storage system is a more complex process than battery alone systems. This is because next to total system's outputs, proportions between each storage device need also to be considered.

Power and capacity split ratios between the two sources need to be introduced as additional problem parameters. As psr and csr can take any value between 0 and 1, there is there is a significant number of possible combinations that are making the decision on a HESS sizing configuration a trivia task.

	Power Rating	Overall Capacity	Power Split Ratio (psr)	Capacity Split Ratio (csr)
Battery System	P_{bat}	E_{bat}	1	1
Battery + SC System	$P_{bat} + P_{sc}$	$E_{bat} + E_{sc}$	$0 < psr < 1$	$0 < csr < 1$

Table 5 Sizing Problem Parameters

Moreover, constraints associated with the charge/discharge characteristics of the supercapacitors should also be considered as a part of the sizing process. Therefore, there is a delicate balance between component properties and system characteristics that should be well understood before designing a hybrid energy storage system.

5.1 Overview

The first step in narrowing down decision options is to construct an appropriate design by developing an Exhaustive Search Algorithm. Following a discrete space of valid sizing combinations can be obtained.

To do so, the two energy storage devices are treated initially as an integrated homogeneous system to determine the overall power rating (P_{hess}) for the hybrid energy storage system to meet application requirements. Through an iterative loop total power rating is incrementally increasing. For each (P_{hess}) iteration the power is split between the battery and the supercapacitor components for a range of different psr.

For each device, the max. power rating is used as an input together with a secondary constraint to obtain maximum capacity as well. For battery, max. C-rate is used as secondary constraint. On the other hand, minimum required duration for the discharge pulse is used as a secondary constraint for the supercapacitor dimensioning.

Following, for each feasible sizing combination resulted from the exhaustive search algorithm, the dimensioning for each source takes place. A series of static parameters such as energy capacity, power and capacity split ratios, number of supercapacitor and battery cells in parallel and in series, component weight and cost are estimated and exported in the form of design exploration maps and arrays.

Following, through a unified approach, where sizing process and energy management system are combined, the algorithm is returning the allocated load profiles for diesel generator, battery and supercapacitor for each of the examined sizing solutions. At this stage, the dynamic outputs such as loss of load probability, energy consumption and aging of the battery are also estimated and extracted.

A more detailed version of the algorithm's flow chart can be found in appendices.

5.2 Sizing Parametrization

To initiate the sizing parametrization process, application sensitive decision variables and constraints need to be known. In this approach, those include the system architecture, the battery and supercapacitor cell parameters and the load profile.

The parametrization process consists of three nested loops (fig.20). In the outer most loop, the total power rating of the hybrid energy storage (P_{hess}) is assigned a value. The hybrid energy storage system total power is equal to the sum of nominal power for the battery and the supercapacitor.

$$P_{hess} = P_{bat} + P_{sc} \tag{5.2.1}$$

Starting from a near-zero value, P_{hess} is incrementally increasing in each iteration and is terminated only when an upper bound value of P_{hess} is reached. At this stage, it is decided to select a low starting value and a high-end upper value for P_{hess} in order to expand the space of possible solutions. Later during the simulation stage any under-sized or over-sized combinations can be rejected and filtered-out from final results.

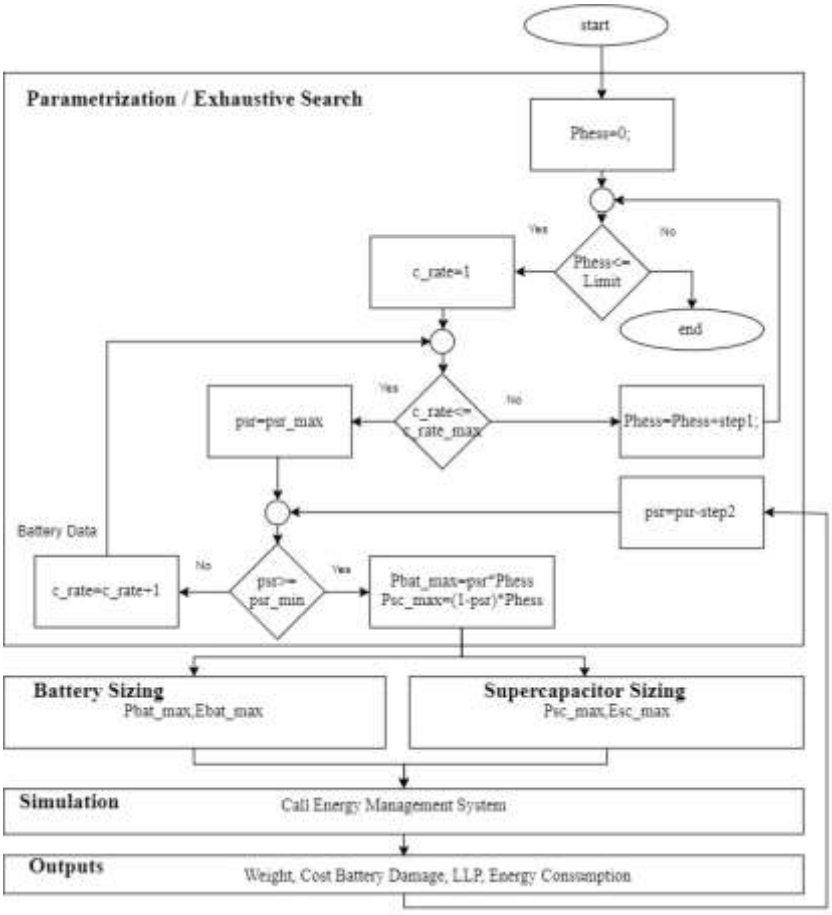

Figure 20 HESS Sizing Parametrization (Exhaustive Search Algorithm)

For each valid iteration of P_{hess} the algorithm triggers a second inner loop. Within this loop, dummy allowable C-rate is also pre-allocated for the battery and incrementally increasing in a set step till the maximum C-rate of the battery (given by the manufacturer) is reached. It should be mentioned that only integer step values are considered to reduce computational complexity of the algorithm. This step is critical for the purpose of the model as it will allow later comparison of batteries with same rating but with different capacities.

Finally, in the third loop a power split ratio (psr) is introduced to allocate system's overall rating to the battery and the supercapacitor. For each pass of the two outer loops, the power is split between the battery and the supercapacitor components for a range of psr.

$$P_{bat} = psr \cdot P_{hess} \tag{5.2.2}$$

Combining (5.2.2) and (5.2.1)

$$P_{sc} = (1 - psr) \cdot P_{hess} \tag{5.2.3.}$$

It can be deduced that for $\mathrm{psr} = 1$ the power rating of the battery is equal to the total power rating of the hybrid energy storage system and therefore the supercapacitor is rated to zero value. On the other hand, for $\mathrm{psr} = 0$, the power rating of the battery is equal to zero meaning that the supercapacitor power rating is equal to the total power rating of the hybrid energy storage system. This case is not aligned with the objective of the algorithm which is to protect the battery from experiencing high C-rates and therefore it is omitted by introducing a minimum power split ratio. The range of values tested for psr is set at:

$$0.10 \leq psr \leq 0.90 \tag{5.2.4}$$

For each HESS sizing combination resulted from the exhaustive search algorithm, the dimensioning for each source takes place. The parametrization process repeats till the outer most loop is finished.

5.3 Battery Dimensioning

To determine the dimensions of the battery component, it is first necessary to identify the required inputs. For each valid output of the exhaustive search parametrization, maximum power rating of the battery ($P_{bat,max}$) and max. C-rate are taken as basic inputs. Then, battery configuration can be estimated for a given commercial battery parameters.

For the purposes of this thesis, LFP battery modules commercially labelled as ''Seanergy''[32] have been assumed for all calculations and simulations. This battery system offered by SAFT batteries includes a built-in battery management system. According to the manufacturer, it has been designed to suit a large variety of marine applications such as passenger vessels, workboats, and inland shipping boat. [32]. Additionally, its modular design allows batteries to be configured to different energy and voltage levels in line with the flexibility objective of this thesis The final reason for the selection of iron phosphate chemistry is related to the high availability of experimentally validated cycle life models that can be used for later estimation of the battery damage [19]. Detailed specifications of the selected battery can be found in Appendix B.

LFP Seanergy SAFT Batteries [32]		
	Cell	Module
Nominal Voltage	3.3. V	46.2 V
Nominal Energy	272 Wh	3800 Wh
Max. Current	300 A	300 A
Number of cells	-	14
Max C-rate	~4	~4

Table 6 LFP Battery Parameters [32]

The first step in battery dimensioning, is to calculate the number of required cells in series and in parallel to meet capacity and power requirements of the application.

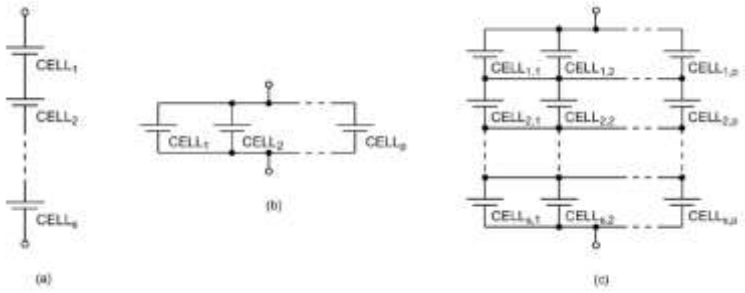

Figure 21 Basic interconnection topologies of battery elements (a) Serial interconnection, (b) parallel interconnection, and (c) parallel–serial interconnection. [41]

By connecting several cells in series, each cell adds its voltage potential to derive at the total terminal voltage that will equal the voltage of the DC-bus [69]. By dividing DC-bus voltage by the cell voltage:

$$N_{bat,series} = \frac{V_{DC,bus}}{V_{bat,cell}} \tag{5.3.1.}$$

It should be mentioned that in case $N_{bat,series}$ is non-integer, it is rounded-up to the nearest integer.

Next, the number of battery strings in parallel is estimated based on the parametrization outputs. For the selected battery, the max C-rate is 4. Therefore, sizing cases with all C-rate integer values between 1 and 4 are generated for each power rating.

$$N_{bat,parallel} = \frac{P_{bat,max}}{C_{Rate,max} \cdot N_{bat,series}} \tag{5.3.2.}$$

Finally, the overall energy capacity of the system is given by:

$$E_{bat,max} = N_{bat,parallel} \cdot E_{bat,cell} \tag{5.3.3.}$$

The process is repeated for all valid sizing combinations and the battery design space is constructed. Fig 22 shows all generated battery combinations expressed in terms of power rating vs energy capacity. For each power rating there are 4 corresponding capacities each representing a different C-rate.

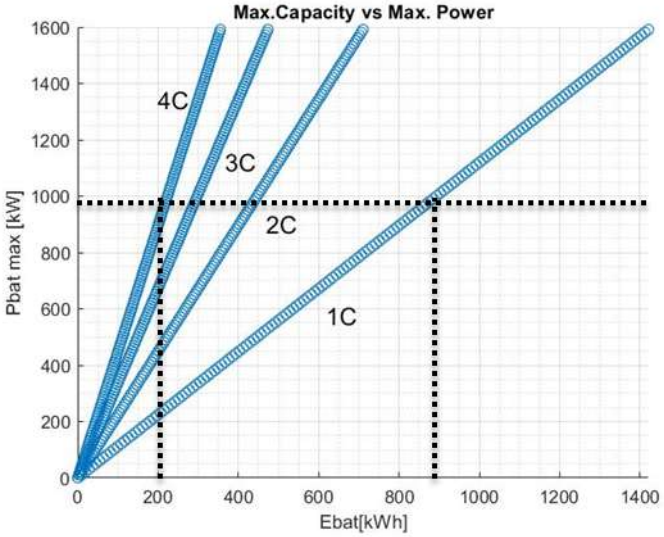

Figure 22 Produced Battery Sizings

5.4 Supercapacitor Dimensioning

For supercapacitor dimensioning, the basic input parameters used are the max. power rating ($P_{sc,max}$), the minimum required discharged capacity (dt_{req}) as well as the supercapacitor cell parameters. As outputs of this sizing process, supercapacitor configuration, actual max. discharge pulse duration and supercapacitor's system capacity are returned.

For the supercapacitor calculations, the BCAP3000 model of MAXWELL Technologies has been selected [70]. The key cell parameters are obtained by the manufacturer and are shown in table 7, while the detailed BCAP3000 specifications can be found in Appendix B.

Supercapacitor BCAP3000 Maxwell Technologies [70]	
	Cell
Capacitance	3000 F
Nominal Voltage	2.7 V
Equivalent Series Resistance (ESR)	0.29 mΩ

Table 7 Supercapacitor Cell Parameters [70]

Power rating is an output of the outer parametrization loop and is therefore different for every sizing combination. On the other hand, minimum required discharged capacity is taken constant for all runs and is set at 8 seconds for the studied load profile. This means that the supercapacitor system should be able to deliver power $P_{sc,max}$ for at least 8 consecutive seconds. Effect of dt_{req} on system performance is further discussed later as a part of the sensitivity analysis.

Contrary to battery sizing, the inner process of determining supercapacitor cells is iterative. Specifically, the actual duration of the discharge pulse of the supercapacitor (dt_{act}) depends on the total capacitance of the system. In its turn the capacitance is additive for parallel configurations[71]. Therefore, by adding strings in parallel higher capacitance and thus higher actual discharge pulse durations can be achieved. Hence, all calculations are initiated for a single string of supercapacitor cells for which dt_{act} is estimated. If actual duration of the discharge pulse is less than the minimum required duration, then a string is added, and the process is repeated.

$$\mathrm{dt_{act}} \geq \mathrm{dt_{req}} \tag{5.4.1}$$

The supercapacitor sizing process is outlined step by step below.

First the discharge current of the supercapacitor can be determined by calculating the current at maximum voltage and at minimum voltage and averaging these two values.

$$\mathrm{I_{avg}} = \frac{\mathrm{I_{max}} + \mathrm{I_{min}}}{2} = \frac{1}{2}\left(\frac{\mathrm{P_{sc,max}}}{0.5\ \mathrm{V_{DC,bus}}} + \frac{\mathrm{P_{sc,max}}}{\mathrm{V_{DC.bus}}}\right) \tag{5.4.2.}$$

To determine the number of required supercapacitor cells in series, the maximum application voltage ($V_{DC,bus}$) is divided by the maximum allowable cell voltage ($V_{sc,cell}$).

$$\mathrm{N_{sc,series}} = \frac{\mathrm{V_{DC,bus}}}{\mathrm{V_{sc,cell}}} \tag{5.4.3.}$$

Following, number of strings in parallel is initialized

$$\mathrm{N_{sc,parallel}} = 1$$

The capacitance and the resistance of the complete supercapacitor system are based on the number of individual capacitors in series or parallel.

For parallel the capacitance is additive while in series the capacitance is additive at 1/capacitance:

$$\mathrm{C_{total}} = \mathrm{C_{cell}}\,\frac{\mathrm{N_{sc,parallel}}}{\mathrm{N_{sc,series}}} \tag{5.4.4}$$

Total resistance is inversely proportional to the number of supercapacitor cells in parallel meaning the more cells in parallel the lower the resistance. For cells in series it is the opposite of capacitance as the more the cells the greater the resistance:

$$\mathrm{R_{total}} = \mathrm{R_{cell}} \cdot \frac{\mathrm{N_{sc,series}}}{\mathrm{N_{sc,parallel}}} \tag{5.4.5}$$

The total voltage change when charging/discharging a s supercapacitor has two components; a capacitive component due to discharge, and a resistive component due to the ESR[71]:

$$\mathrm{dV} = \mathrm{I_{avg}} \cdot \frac{\mathrm{dt_{act}}}{\mathrm{C_{total}}} + \mathrm{I_{avg}} \cdot \mathrm{R_{total}} \tag{5.4.6}$$

Solving for the actual discharge pulse duration:

$$\mathrm{dt_{act}} = \mathrm{dV} \cdot \mathrm{C_{total}} \left(\frac{1}{\mathrm{I_{avg}}} - \mathrm{R_{total}} \right) \tag{5.4.7.}$$

At this stage, dt_{act} is compared to dt_{req} and if is less, a string of cells is added in parallel. The process is repeated till the condition is fulfilled.

$$N_{sc,parallel} = N_{sc,parallel} + 1$$

Having determined the number of supercapacitor cells, the final step is to estimate the system's energy capacity. Based on the manufacturer instructions the supercapacitor can be used till the voltage reached half of the maximum voltage[71]. Depth of discharge of the supercapacitor i.e. usable capacity is given by the manufacturer as the capacity available till the voltage drop at half the maximum voltage. Therefore, maximum available capacity of the supercapacitor will be:

$$E_{sc,max} = \frac{1}{2} C_{total} \cdot \left({V_{max}}^2 - {V_{min}}^2 \right) = \frac{1}{2} \cdot \frac{3}{4} C_{total} {V_{DC.bus}}^2 \qquad (5.4.8.)$$

The abovementioned process is summarized in the flow chart of Fig.23

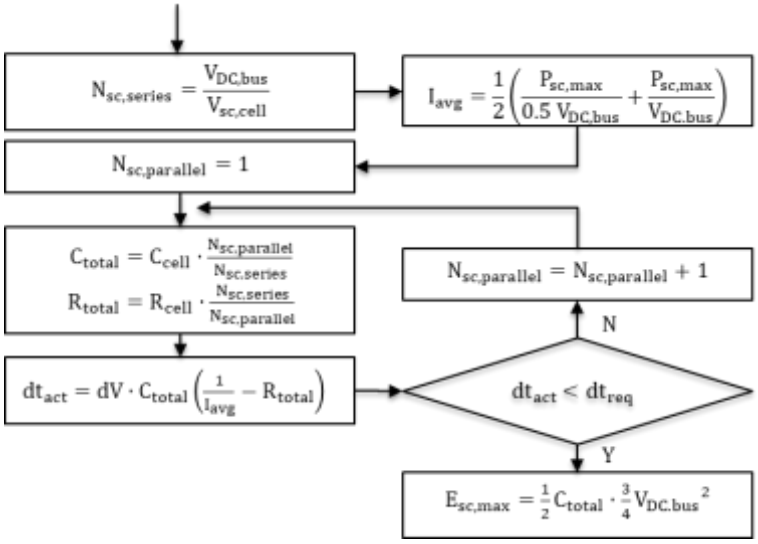

Figure 23 Supercapacitor Flow Chart for estimation of dt_{act}

By following the same procedure for all cases generated through the parametrization algorithm, the design space for the supercapacitor is constructed. In fig.24 the maximum power rating is plotted as a function of actual duration of the discharge pulse. For all plotted combinations the set minimum requirement of 8 sec for the discharge pulse is fulfilled. However, the actual value may vary significantly. For low power ratings, durations of up to 28 sec can be observed while for higher power ratings this number is decreased. Another, conclusion derived from this fig. is that the design space is discrete. Specifically, 6 independent subsets can be observed each representing the respective number of strings in parallel.

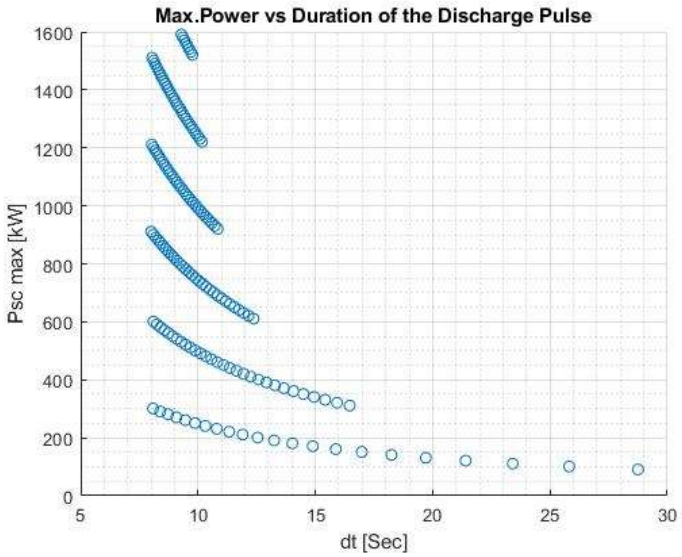

Figure 24 Supercapacitor Rating-Discharge Pulse dt

Finally, the same design space is expressed in terms of power rating vs capacity (fig.25). Again, the combinations are shaping 6 discrete vertical subsets. It is observed, that in compare to the equivalent diagram for battery combinations, the x-axis values (capacity) are much smaller for the same power ratings. Additionally, the diagonal lines representing the supercapacitor C-rates are ranging between 100C and 400C i.e. about 100 times higher than the battery.

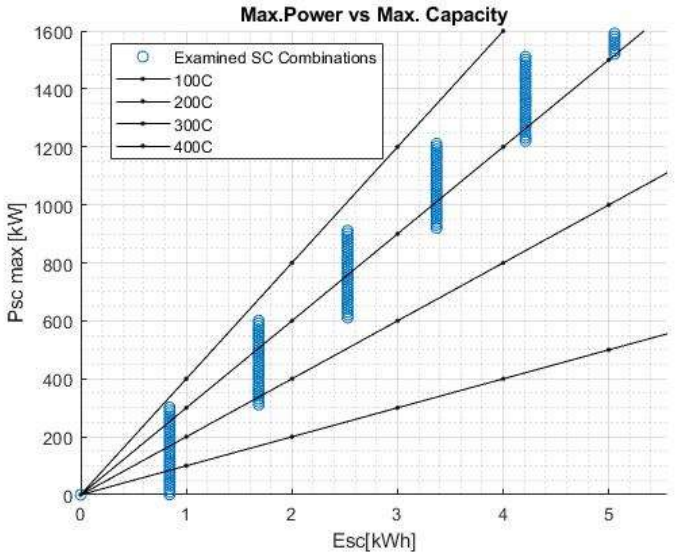

Figure 25 Supercapacitor Sizing Combinations

5.5 Power Electronics

The dimensioning criterion of the DC/DC converters coupled to each storage device is current. However, it has been stated that the charge and discharge characteristics of the battery and supercapacitor are different (Fig. 14).

For battery, the charge/discharge voltage curves are relatively constant with respect to its state of charge resulting in limited effect to the available capacity. Additionally, it is known that the power is given as the product of voltage with current.

$$P = V \cdot I \tag{5.5.1}$$

Subsequently, for constant voltage the battery current is a linear function of the maximum power rating of the battery. Therefore, the battery DC/DC converter can be dimensioned based on its maximum power rating.

$$P_{converter,max} = P_{bat,max} \tag{5.5.2}$$

On the other hand, the supercapacitor needs much larger converters than the Li-Ion batteries. This is because the voltage of supercapacitor is not constant with its state of charge.

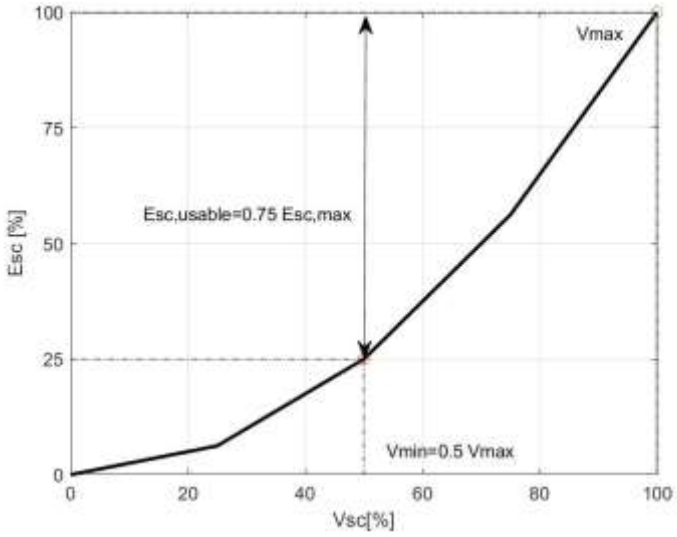

Figure 26 Supercapacitor Available Capacity Diagram [$E = \frac{1}{2} C V^2$]

Based on the manufacturer instructions [71] the supercapacitor can be used till the voltage reached half of the maximum voltage. Thus, supercapacitor depth of discharge is defined as capacity available till the voltage drop at half the maximum voltage.

$$E_{sc,usable} = E_{sc,max} - E_{sc,min} = \frac{1}{2} C\, {V_{max}}^2 - \frac{1}{2}\frac{1}{4} C\, {V_{max}}^2 = \frac{3}{8} C\, {V_{max}}^2 \Rightarrow$$

$$\Rightarrow E_{sc,usable} = \frac{3}{4} E_{sc\_max} \quad or$$

$$E_{sc,min} = 0.25\, E_{sc,max} \tag{5.5.3}$$

To utilize the supercapacitor with full power at 25% state of charge, then the converter needs to be sized 2x of current at full power.

$$P_{converter,max} = 2 \cdot P_{sc,max} \tag{5.5.4}$$

5.6 Combined Sizing

Next, step in the sizing process is to combine the individual valid outputs of battery and super capacity process into HESS paired outputs.

By combining figures 22 and 25, a ragone plot for the design is created. In fig. 26 the battery values are shown in blue scatters. All battery combinations are placed on the high specific energy side of the plot and can be grouped in four points representing C-rates from 1 to 4.

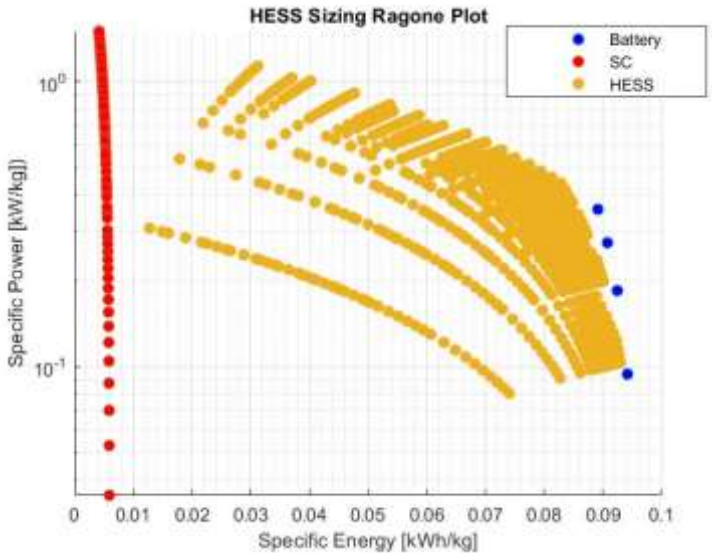

Figure 27 HESS Ragone Plot

On the other side of the spectrum, supercapacitor values are shown in red color. Following, battery and supercapacitor values are paired together, and overall specific energy and specific power is estimated. These are plotted in orange color. It can be seen that a whole new area of relatively high specific power and high specific energy is reached in the ragone plot through the hybridization of the system. It should also be noted that none of the HESS combination can have higher specific power than its supercapacitor component nor higher specific energy than its battery component.

Another split ratio is defined to indicate the capacity analogies of battery and supercapacitor with respect to the total energy storage system capacity. The capacity split ratio (csr) is defined as:

$$E_{hess} = E_{bat} + E_{sc} \tag{5.6.1.}$$

$$E_{bat} = csr\ E_{hess} \tag{5.6.2.}$$

$$E_{sc} = (1 - csr)E_{hess} \tag{5.6.3.}$$

By definition, for $csr = 1$, the battery's capacity is equal to maximum i.e. E_{hess} while the supercapacitor is set to zero. Respectively, for $csr = 0$, the battery is effectively omitted, and all energy capacity is assigned to the supercapacitor. In practice, supercapacitor have a small specific energy in compare to modern to lithium ion batteries, and therefore csr values are closer to 1. In the constructed design space (Fig. 27), possible solutions range from 10-90% for psr and from 60-99+% for csr.

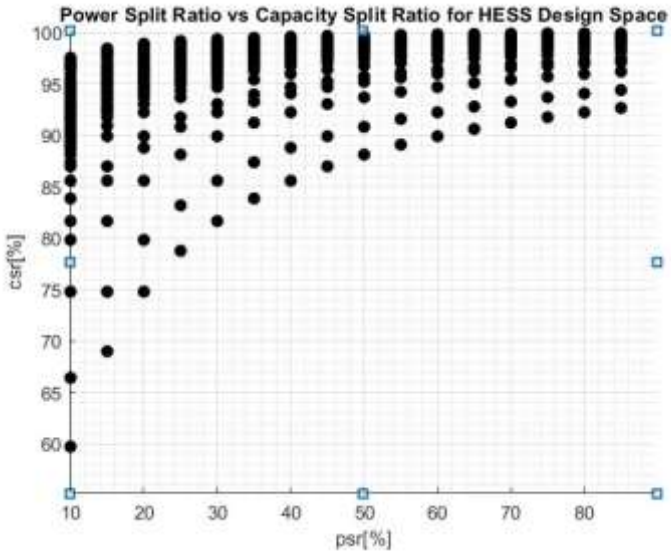

Figure 28 Power Split Ratio vs Capacity Split Ratio

In the following chapters each hybridized sizing combination will be fed as an input to the simulation to evaluate overall performance.

5.7 CAPEX and System Weight

From the defined performance metrics, total capital cost and total weight are static. Therefore, they can already be calculated at this stage for all combinations using specific unit factors for the key components.

	LFP Seanergy SAFT Battery	BCAP3000 Maxwell Technologies Supercapacitor	Bi-directional DC/DC Converter
Specific Power	-	-	5 kW/kg[51]
Specific Energy	96 Wh/kg [26, 32]	6 Wh/kg [70]	-
Specific Cost	800 $/kWh [23]	0.01 $/F [72]	140 $/kg[51]

Table 8 Specific Units

The specific energy factors have been adopted by the manufacturer's datasheets.

Selection of Li-Ion battery specific cost is arguably one the most trivia factors with a wide range of prices being suggested in literature[15, 73-75]. The first differentiator is the Li-Ion chemistry concerned. Different materials result in different prices. However, according to DNV-GL [16] these large differences can be explained by the fact that the quotes are referring to different integration stages of the battery installation [Fig 28]. A maritime installation is requiring battery management system, electrical connections and cabling, thermal runaway systems etc. resulting in a significant increase from cell level. All these concerned, for LFP batteries a system cost range of 400-1200$/kWh has been reported [23]. For the basic runs of this installation, a mean value of 800$ is selected. The effect of battery price on HESS cost is further examined as a part of the sensitivity analysis.

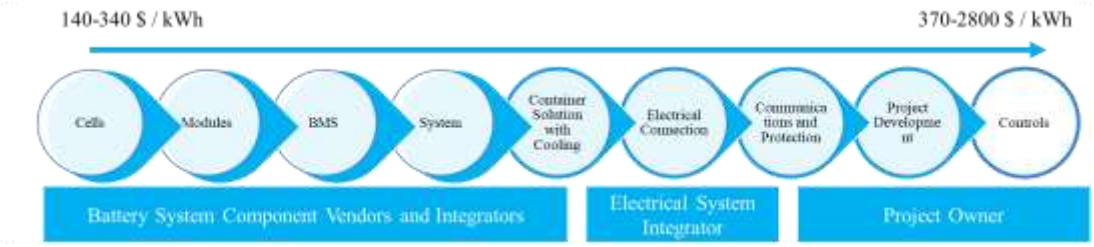

Figure 29 Battery Cost as a function of integration stage[16]

For the supercapacitor unit cost of as less as 0.005$/F has been suggested in literature [72]. Considering some buffer, a conservative value of 0.01$ /F is selected to account for supercapacitor's cost in module level.

With regards to overall system cost and weight the effect of power electronics is also considered. For both the bi-directional DC/DC converters, a simplified dimensioning approach has been followed as suggested by L. Sun, P. Walker et al. [52] . Specifically, it is assumed that the overall cost and weight of the DC/DC converter are linear function of the converter max. power rating.

All these considered, the total weight of the system is given by:

$$\text{weight}_{\text{total}} = \text{weight}_{\text{bat}} + \text{weight}_{\text{sc}} + \text{weight}_{\text{convert,bat}} + \text{weight}_{\text{convert,sc}} \quad (5.7.1.)$$

Similarly, the HESS overall cost will be:

$$\text{cost}_{\text{total}} = \text{cost}_{\text{bat}} + \text{cost}_{\text{sc}} + \text{cost}_{\text{convert,bat}} + \text{cost}_{\text{convert,bat}} \quad (5.7.2.)$$

Detailed calculations can be found in Appendix E.

6 Energy Management System

In previous chapter, a valid HESS design space was constructed. In order to evaluate the different sizing combinations within this space, it is necessary to develop an energy management system that will correlate the design variables and static outputs of the sizing process with the dynamic phenomena of battery aging, loss of load probability and system's energy consumption.

In practice, the hybrid energy storage system requires an energy management system, which will ensure proper energy flow from and to the DC-bus [76]. The energy management (or power allocation) strategy should determine the power split between the diesel generator, the battery and the supercapacitor while satisfying the load requirements with respect to dynamic constraints of the power system [77].

6.1 Overview

The scope of present thesis is limited to power production and storage side of the electrical system; hence the energy management system has been designed following a backwards (effect-cause) approach. In this approach, the total load demand of all consumers is treated as an input to the power allocation controller. Additionally, as only full electric topologies are considered, the load profile is assumed to be equivalent to the total electric power consumption (propulsion plus hotel loads) of the vessel as a function of time.

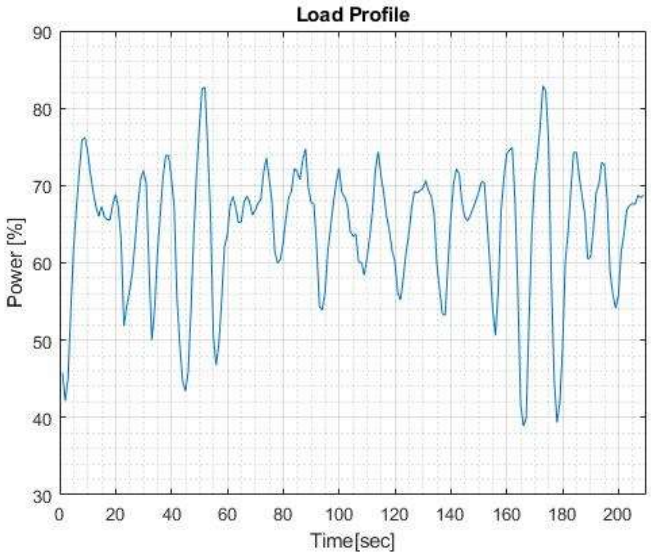

Figure 30 Load Signal as Input in Backwards Approach

The output combinations of the sizing process and specifically the maximum power rating and maximum capacity are typically also inserted as an input to the energy management system. Nevertheless, they are considered disturbances as they are variables that affect the process outputs but that cannot be adjusted by the power control system.

Following and as shown in fig. 30 , power allocation for HESS is defined in terms of the energy demands and the available energy on the HESS [78]. The latter is described through the state of charge of each device. The State of Charge of the Supercapacitor (SOC_{sc}), and the State of Charge of the Battery (SOC_{bat}) are a function of time and therefore knowledge of previous system's state is required. Subsequently, those are fed into the EMS as feedback inputs.

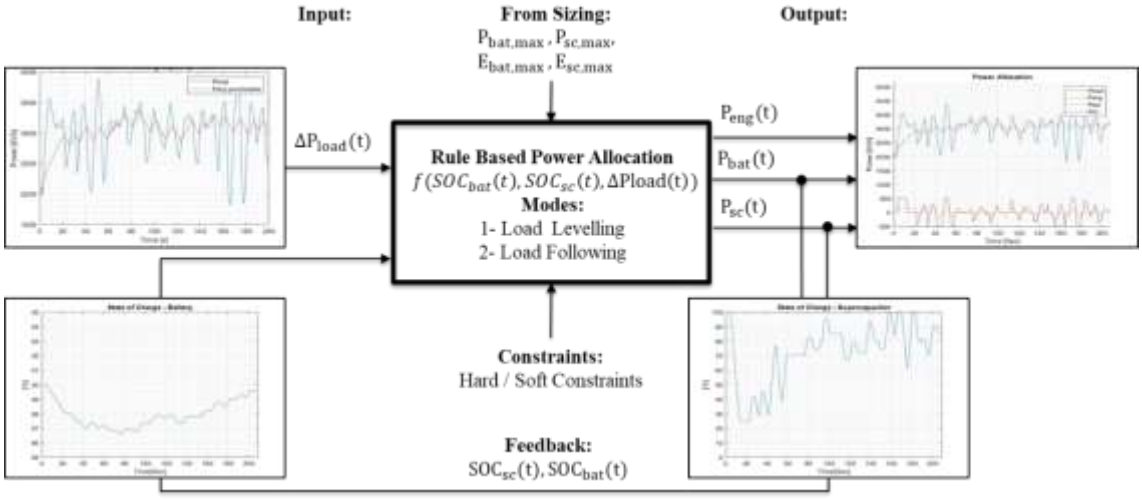

Figure 31 EMS Process Diagram

The power allocation is decided in two stages. In the first stage, the required load ,subjected to constraints, is split between the diesel generator and the hybrid energy storage system as a whole. In the second stage, decision is being made for the power allocation between the HESS components i.e. the battery and the supercapacitor. Following the consecutive power allocation stages, the power profiles for all sources over time $(P_{bat(t)}, P_{sc(t)}, P_{eng(t)})$ can be extracted as outputs of the simulation process.

6.2 Decision Variables

The three decision variables were namely identified as the State of Charge of the Supercapacitor (SOC_{sc}), the State of Charge of the Battery (SOC_{bat}) and the rate of change of the difference between required load and –preferred set point- engine load ($\frac{\boldsymbol{\Delta P}}{\boldsymbol{dt}}$), that is defined as follows:

$$\frac{\Delta P}{dt} = P_{load}(t) - P_{eng}(t) \tag{6.2.1}$$

Where $P_{eng}(t)$, is the pre-allocated power point of the diesel generator for the same time step. It should be mentioned that this is the preferred rather than the definite power allocated to the engine generator as it might be subjected to constraints for which corrections need to be applied. The pre-allocated engine set point depends on the primary power sharing approach(load levelling or load following).

State of charge for an energy storage device is an expression of the present capacity as a percentage of its maximum capacity and hence it is a measure of available energy stored. Their value is given by:

$$SOC_{bat}(t) = \frac{E_{bat}(t-1) - \int_{t-1}^{t} P_{bat}\ dt}{E_{bat,max}} \times 100 \tag{6.2.2}$$

$$SOC_{sc}(t) = \frac{E_{sc}(t-1) - \int_{t-1}^{t} P_{sc}\ dt}{E_{sc,max}} \times 100 \tag{6.2.3}$$

6.3 Boundary Conditions

With regards to the power allocation problem, besides the development of the functional requirements and the definition of key process inputs/outputs, it is also necessary to mathematically express the set conditions that are required to be satisfied by the controller that distributes the energy between the energy sources. These conditions can be distinguished to hard and soft constraints.

By identifying the hard constraints of the problem, which must always be satisfied and thus cannot be violated, candidate solutions can be narrowed down to a feasible region or search space of all possible points. On the other hand, soft constraints are desired conditions for which the user is prepared to accept their no satisfaction if the cost is too high or if there is a conflict with any of the hard constraints or goals [79]. Therefore, soft constraints are related to preferred solutions within the feasible region.

6.3.1 Hard Constraints

6.3.1.1 Engine System

The first set of hard constraints is derived from the capacity of the engine system.

For every moment t within the simulation time, the engine power output must be positive and less or equal to the engine maximum power output (MCR) as this is stated by the manufacturer:

$$0 \leq P_{eng}(t) \leq P_{eng,max} \tag{6.3.1}$$

Additionally, the load ramps taken by the engine should also be regulated and limited in accordance to its loading capacity diagram for normal operation.

In order to translate the engine loading capacity into tangible constraints, the loading capacity diagram need to be analysed based on the possible power allocation outcomes of the EMS.

Depending on the last known power output of the engine at time t, the maximum allowable movement within the pre-defined simulation time step is calculated:

$$\frac{\Delta P_{eng,permisible}}{dt} = P_{eng}(t_0) - P_{eng,permissible}(t_1) \tag{6.3.2}$$

The line equations for the loading capacity diagram and the detailed derivation can be found in the appendix section.

Following, the engine power corresponding to this maximum permissible movement is compared to the originally set engine power value as allocated by the EMS. Depending on the relative difference between EMS allocated and permissible engine power values and the requested mode (load-up or load-down) , four cases can be distinguished:

a) $P_{eng,permissible}(t_1) \geq P_{eng,allocated}(t_1)$ & $P_{eng,allocated}(t_1) > P_{eng}(t_0)$
b) $P_{eng,permissible}(t_1) < P_{eng,allocated}(t_1)$ & $P_{eng,allocated}(t_1) > P_{eng}(t)$
c) $P_{eng,permissible}(t_1) < P_{eng,allocated}(t_1)$ & $P_{eng,allocated}(t_1) < P_{eng}(t)$
d) $P_{eng,permissible}(t_1) \geq P_{eng,allocated}(t_1)$ & $P_{eng,allocated}(t_1) < P_{eng}(t)$

In the first two cases (a) and (b) the engine is requested to load-up between times t_o and $t_1 = t_0 + 1$ while in the latter two the engine load set by the EMS is reduced (load-down).

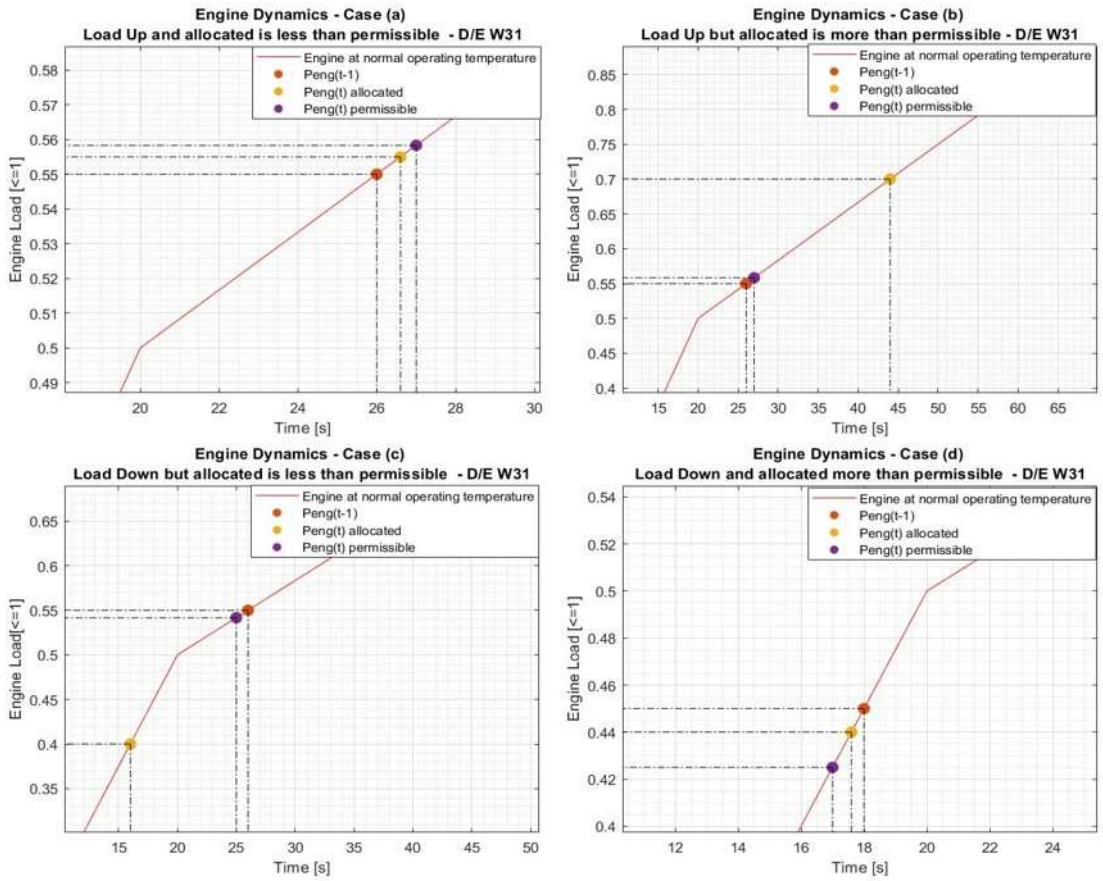

Figure 32 Engine Load Capability Cases for Wartsila E31 DG [12].

Going a step further, in cases (a) and (d) the allocated power is within permissible margins and therefore assignment operation is not restricted by engine's loading capacity (Figure 31). Conversely, this is not applicable for cases (b) and (c) in which the allocated engine load value is exceeding the permissible. For these instances, respective hard constraints need to be introduced:

Load-Up:

$$P_{eng,allocated}(t_1) - P_{eng}(t_0) \leq P_{eng,permissible}(t_1) - P_{eng}(t_0) \tag{6.3.3}$$

Load-Down:

$$P_{eng}(t_0) - P_{eng,allocated}(t_1) \geq P_{eng}(t_0) - P_{eng,permissible}(t_1) \tag{6.3.4}$$

6.3.1.2 Battery System

The energy management controller is also subjected to constraints related to the battery characteristics and design.

First limitation is related to the max. power rating of the battery system as determined during the sizing stage. The momentarily load assigned to the battery cannot exceed the absolute value of its power rating for neither charging nor discharging operations:

$$-P_{bat,max} \leq P_{bat}(t) \leq +P_{bat,max} \tag{6.3.5}$$

Next, a constraint linked to the battery available capacity is introduced. As per industry's common practice (and manufacturer's advice) a maximum operating depth of discharge of 60% is pre-allocated to avoid additional cycling aging. With respect to battery's relative capacity this constraint can be written as:

$$30\% \leq \mathrm{SOC_{bat}}(t) \leq 90\% \tag{6.3.6}$$

6.3.1.3 Supercapacitor System

As with the battery system, the momentarily supercapacitor load assigned from the EMS controller cannot exceed the max. power rating that was determined during sizing:

$$-P_{sc,max} \leq P_{sc}(t) \leq +P_{sc,max} \tag{6.3.7}$$

Additionally, by considering a Depth of Discharge of 75% (i.e. capacity available till the voltage drop at half the maximum voltage), the supercapacitor operating window is determined as:

$$25\% \leq \mathrm{SOC_{sc}}(t) \leq 100\% \tag{6.3.9}$$

6.3.2 Soft Constraints

As mentioned, soft constraints concern the preferred properties of the system and should be fulfilled as much as possible. For the developed power allocation controller, soft constraints are associated to the power balance between production and consumption sides of the system. Ideally, the system should be in equilibrium meaning that all users can be fully satisfied after losses are counted.

For charging conditions, available power i.e. the difference between engine power and requested load should be greater than energy storage associated consumed power:

$$P_{eng}(t)\text{-}P_{load}(t) = P_{bat}(t) + P_{sc}(t) + Losses_{bat}(t) + Losses_{sc}(t) \tag{6.3.10}$$

It should be mentioned that under charging conditions P_{bat} and P_{sc} have by definition a negative sign.

In case of violation of this constraint, where the left-hand side of the equation is less than the right-hand side, the allocated power of the storage elements for time t must be re-calculated to match the available power.

Violation of this constraint can also occur in case, where the left-hand side is greater than the right-hand side. In this instance, the available power is higher than the absorption capacity of the storage system and therefore there is an excess of energy. This redundancy although not desired, could occur in instances where the storage elements are either fully charged or the engine cannot load-down quick enough to balance the system.

Equivalently, for discharging operations the power balance is given by:

$$P_{load}(t)\text{-}\mathrm{P}_{eng}(t) \leq -P_{bat}(t) - P_{sc}(t) + Losses_{bat}(t) + Losses_{sc}(t) \tag{6.3.11}$$

This condition can be violated if the requested load is greater than the supply capacity of the hybrid energy storage system at time t. Failure to fully meet load requirements , will result in an undesired loss of load instance where power supply cannot correspond to the instantaneous demand. For a carefully designed system, loss of load instance should be a rare occasion nevertheless it could happen if there is a sudden increase in load demand while the engine and storage system are limited by their dynamic capability and/or available capacity.

6.4 Primary Power Allocation

As discussed in section 4.3 , the energy management system should be able to fulfill certain functional requirements. The battery component should be protected from high current loads to extend its lifetime. Additionally, the HESS and the diesel generator should be able to operate in parallel with the diesel generator, in peak shaving mode. Other controllability requirements include the individual assignment and/or power sharing between the battery and supercapacitor. Finally, system's overall efficiency should be promoted where possible. Given these requirements, a careful selection of operating mechanisms should be made.

According to Shabbir [80], there are two distinct approaches to determine the power share between a primary source (i.e. the diesel generator) and a secondary source (i.e. hybrid energy storage system). These are namely: load leveling, load following. For the purposes of this thesis, peak shaving strategies of both load levelling and load following have been developed and simulated.

6.4.1 Load Levelling

In load levelling the basic principle is to run the diesel generator at a selected constant load and have the energy storage system act as an equalizer that is absorbing all fluctuations above this point. For fuel consumption optimization, the selected point is typically set to be the MCR of the engine as this is normally the point with the lowest specific fuel consumption. Lower points are however possible depending on the load profile characteristics.

$$\Delta P(t) = P_{load}(t) - P_{eng@loadpoint} \tag{6.4.1}$$

With

$$\Delta P(t) = P_{hess}(t) = P_{bat}(t) + P_{sc}(t) + Losses_{bat}(t) + Losses_{sc}(t) \tag{6.4.2}$$

In load levelling the primary source profile is relatively constant or slow varying, with the exception of limited HESS power absorption (or release) capability or insufficient available capacity where the diesel generator has to (partially) follow the load.

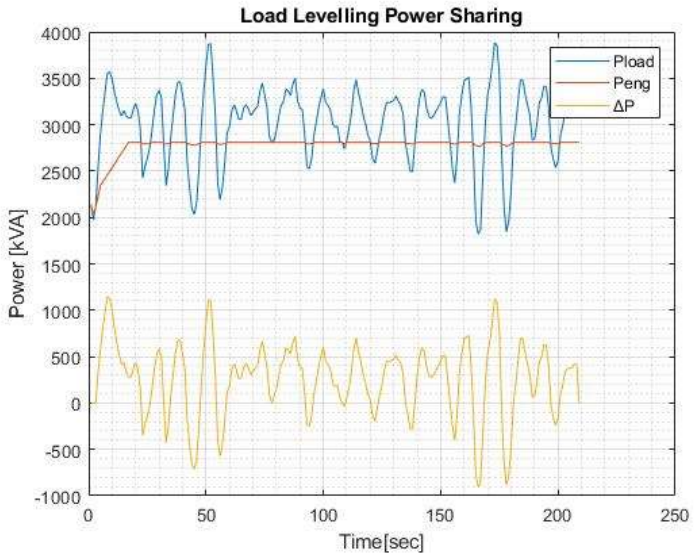

Figure 33 Load Levelling Power Sharing

In this approach, there is potential for fuel saving as engine's efficiency can be optimized. Another reported benefit is associated to improved maintainability as it gives the engine a smoother operation by reducing load variations.

On the HESS side, load levelling requires larger installations in general. This is because the energy storage system is responsible to stand-alone handle all system fluctuations without the assistance of the prime mover. This can lead into higher battery damage and potentially loss of load instances. Impact of load levelling on performance metrics is further examined in the results section.

6.4.2 Load Following

The principle in load following is to have the diesel generator "following" the load power only limited by its loading capacity mode (emergency or normal). In this reliability-oriented approach, the HESS is set to compensate only the remaining fluctuations. This is given by:

$$\Delta P(t) = P_{load}(t) - P_{eng,permissible}(t) \tag{6.4.3}$$

Again, $\Delta P(t)$ is assigned to total power requested by the HESS. In this approach the engine is already covering a big part of the load. If for any reason the HESS is not able to fully absorb/compensate for all $\Delta P(t)$ the engine limited by its capability cannot further follow resulting in a loss of load instance. Fig 34 outlines the logic of load following approach in pseud-code form.

```
function [ Peng_t1_permissible ] = load_following(Pload,n,Engine_Range)
% *Load Following Power Sharing*
% *DG "following" the load power only limited by its loading capacity*
% *Based on Normal Operation Loading Capacity for Wartsila 31*
% *Engine at normal operating temperature*
Peng_t1_permissible=zeros(n,1);
for ind=1:n-1
    Peng_t0=Pload(ind);
    Peng_t1_allocated=Pload(ind+1);

    if Peng_t0<=0.50
        t0=Peng_t0/2.5*100;
    else
        t0=((6/5)*Peng_t0-(1/3)*(6/5))*100;
    end

    if Peng_t1_allocated<=0.5
        t1_allocated=Peng_t1_allocated/2.5*100;
    else
        t1_allocated=((6/5)*Peng_t1_allocated-(1/3)*(6/5))*100;
    end

    Delta_Peng=Peng_t1_allocated-Peng_t0;
    if Delta_Peng>=0                                          % Load-up
        t1_permissible=t0+1;
        Peng_t1_permissible(ind)=Engine_Range(t1_permissible);

    else
        t1_permissible=t0-1;
        Peng_t1_permissible(ind)=Engine_Range(t1_permissible);  % Load-down

    end
    % Remaining Load for HESS
    Delta_P=Pload(ind)-Peng_t1_permissible;
end

end
```

Figure 34 Pseudo-code for Load Following Power Sharing

In load following approach, fluctuation handling is split to both HESS and diesel generator. On the positive side, this results in smaller capacity installations and potentially to less battery damage. On the other side, this approach does not guarantee the operation of the engine in the high efficiency region as this as this will depend on the varying load. Again, these trade-offs are quantified and discussed further in the results section.

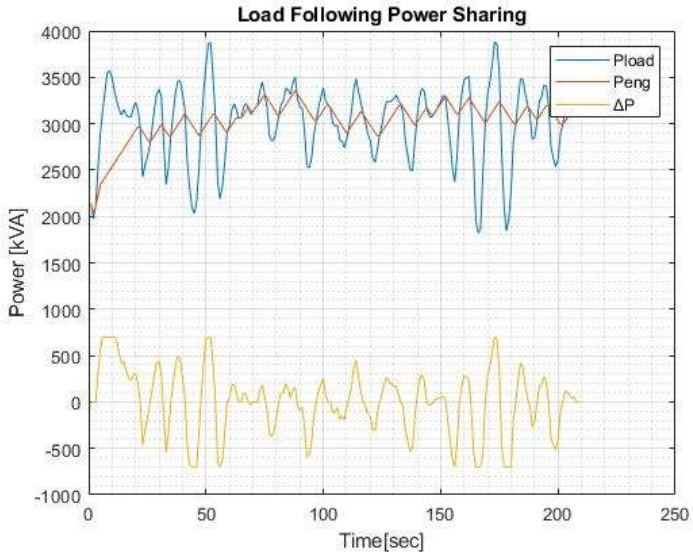

Figure 35 Load Following Power Sharing

6.4.3 HESS Employment Mechanisms

In the first level of the energy management system a decision is being made on the employment or not of the HESS.

Depending on the sign of $\frac{\Delta P}{dt}$, the energy management system can return either of three output states namely ''Charging'', ''Discharging'' and ''Neutral'' for the battery and the supercapacitor.

Primarily, "Charging'' state is activated in situations where $\frac{\Delta P}{dt}$ is negative or in other words where $P_{load}(t) < P_{eng}(t)$ in combination with a non-fully-charged storage element. By applying this condition, the system is only directing energy from the diesel generator to the storage elements when there is a surplus of available power (difference between power generating capacity and load requirements) after satisfying all load requirements.

On other hand, "Discharging" state is activated in situations where $\frac{\Delta P}{dt}$ is positive or in other words where $P_{load}(t) > P_{eng}(t)$ and therefore the available power from the diesel generator is not adequate to serve all loads. In this condition and given that the energy storage elements have a state of charge within allowable limits, the deficit between available and required load is satisfied by the energy storage system.

Lastly, in ''Neutral'' state, the system is in perfect balance between the available diesel generator power and the required load. During this state, the diesel generator system is acting as a stand-alone system with no inflow or outflow of energy to the energy storage system.

6.5 Secondary Power Allocation

Through the load levelling and load following power allocation approaches, a top-level decision on the operation of the HESS can be made. Nevertheless, introducing a supercapacitor to the system is adding significant complexity to the lower-level power sharing between the two energy storage devices.

Given the scope of this thesis to explore the design space for HESS systems, the objective is to develop a relatively simple and reliable set of bespoke power allocation rules that will satisfactorily fulfill the application requirements for the primary source and the energy storage system.

6.5.1 Power Allocation Modes

For the HESS consisting of the battery and the supercapacitor, 9 different power allocation modes have been identified based on the utilization decision on each storage device. Power allocation modes (1)-(4) are concerned with charging operations where there is a surplus of available power by the diesel generator. In the first mode the battery is the only medium allowed to charge. For the second mode, the concept of priority is introduced. Specifically, both devices can be charged nevertheless battery is set as priority one while supercapacitor as a secondary. Inversely, for power allocation mode three, the supercapacitor is set as a priority one while the battery is set as a secondary choice.

	Charge				Neutral	Discharge			
	(1)	(2)	(3)	(4)	(5)	(6)	(7)	(8)	(9)
Battery	CH	CH_1	CH_2	-	-	DIS	DIS_1	DIS_2	-
Supercapacitor	-	CH_2	CH_1	CH	-	-	DIS_2	DIS_1	DIS

Table 9 HESS Power Allocation Modes [1= First Priority . 2*=Secondary Priority]*

If a device is set as of secondary priority, it will only be activated if the other device is fully satisfied first. For charging operations, an activated secondary priority source implies that there is still available power in the system after priority one option has absorbed power equal to its maximum capacity.

Last allocation mode for charging operations is (4), in which only the supercapacitor can charge while the battery is at stand-by.

Power allocation mode (5) is activated when there is no charge or discharge requirement for any of the hybrid energy storage system media and therefore can be considered as a ‘Neutral’ or ‘stand-by’ mode.

Next, power allocation modes (6)-(9) are associated with discharge operations. In mode (6), battery is supplying part of the load requirements while the supercapacitor is at stand-by. In modes (7) and (8) the battery is assigned as priority one and two respectively while the supercapacitor the vice versa. For discharge operations, priority two is activated only if the priority one device is unable to fully cover the requested load difference by itself. Finally, in power allocation mode (9) the supercapacitor is the only storage medium allowed to discharge a part of its stored energy.

Detailed coded function for modes (3) and (7) can be found in the appendix section.

6.5.2 Power Allocation Strategy

Due to its simplicity and practicality, a rule-based energy management strategy is developed to realize real-time control of the power system. In this approach, the decision on power split between the engine, the battery and the supercapacitor, is pre-defined in a set of logical rules that describe the operational conditions under which a power allocation mode is employed.

In practise, these rules are presented in the form of a decision matrix where power allocation is determined depending on the relationship between the three earlier defined decision variables (inputs). Those are namely the State of Charge of the supercapacitor (SOC_{sc}), the State of Charge of the Battery (SOC_{bat}) and the rate of change of the difference between required load and pre-allocated engine point.

6.5.3 Power Allocation Decision Space

A logical threshold is also introduced to enable split between the battery and the supercapacitor. This threshold is expressed as a percentage of engine's installed power and will be used to distinguish the rate of change of the difference between required load and engine point into rapid and slower fluctuations. In accordance with this thesis aims and objectives, the supercapacitor will preferably be handling the rapid fluctuations exceeding this threshold to protect the battery module.

It should be mentioned that the logical threshold can take positive or negative value to cover both charging and discharging operations.

The threshold value is manually determined by the user as it requires some prior knowledge of the system's behaviour. For the purposes of this thesis, a threshold value of 15% has been selected for basic simulation runs. Any uncertainty caused by this decision is further examined in the next chapters as a part of the model's sensitivity analysis.

Derived from the problem's constraints, the SOC_{bat} variable is only examined for values between 30% and 90% of battery's maximum capacity while SOC_{sc} variable is only valid between 25% and 100% of supercapacitor's maximum capacity.

The SOC_{bat} is further analysed in two intervals to increase system's resolution. The first is 30-60% and is considered as lower charged while the second is 60-90% and is considered as adequately charged. Similarly, SOC_{SC} is divided into two classes; 25-75% and 75-100% respectively.

6.5.4 Decision Matrix

Having defined the decision space for the three variables, the returned power allocation outputs can be associated.

		Charge		Neutral	Discharge	
SOC_{bat} (%)	SOC_{sc} (%)	$\frac{\Delta P}{dt}$<-Threshold	-Threshold<$\frac{\Delta P}{dt}$<0	$\frac{\Delta P}{dt}$=0	0<$\frac{\Delta P}{dt}$<Threshold	$\frac{\Delta P}{dt}$>+Threshold
30-60	25-75	(3)	(3)	(5)	(7)	(8)
	75-100	(2)	(2)	(5)	(8)	(8)
60-90	25-75	(3)	(3)	(5)	(7)	(8)
	75-100	(3)	(2)	(5)	(8)	(8)

Table 10 Decision Matrix (Rule-Based)

Table 10 shows an overview of the power allocation rules. The logic of the rules is further elaborated in the following paragraphs.

If $\frac{\Delta P}{dt}$ is exceeding max. negative threshold then supercapacitor charging is set as priority 1 (power allocation mode 3). The only exemption is if the supercapacitor is already highly charged and the battery is at the same time in its lower capacity class. Reasoning behind these rules can be summarised in that we want the supercapacitor to always be available and to handle high peak currents on the charging side.

For lower negative values of $\frac{\Delta P}{dt}$, the supercapacitor is set as priority for charging only in instances where its capacity is less than 75%.

Moving towards the centre of the table 10 $\left(\frac{\Delta P}{dt} = 0\right)$, the system is in equilibrium. In this state, no charge or discharge operation can be activated independently of what the state of charge is (power allocation mode 5).

On the discharge side of the decision matrix $\left(\frac{\Delta P}{dt} > 0\right)$, the power allocation is depending on the measure of the power deficit rate. For high deficit rates exceeding the set threshold the system needs quick discharging. Therefore, the supercapacitor is activated in priority (power allocation 8). Supercapacitor can also be activated first for lower deficit rates given that SOC_{sc} is above 75%. This is done to protect battery from unnecessary loading cycles even for low peak currents. On the other hand, battery is activated in priority for lower power deficit rates for the remaining cases where SOC_{sc} is below 75%. This is to ensure that the supercapacitor will have available capacity for higher peak currents.

6.6 Power Flows and Efficiency Losses

For each operation incorporating an energy storage device there is a loss of energy to the surroundings. As a part of the EMS, it is important to account for these conversion losses during power allocation. By quantifying the discharge efficiency of the storage devices, the HESS supplied power can be normalized to ensure that the correct amount of energy is anticipated by the consumers. Similarly, charging efficiency is needed to ensure that the HESS received power is not exceeding the available power.

6.6.1 Roundtrip efficiency

Regarding bi-directional DC/DC converters of supercapacitor and battery, the model assumes the energy efficiency evolution is a function of the power loading. The advantage of a parametric approach is that as converters are sized to match maximum power rating of each device, the effect of sizing into system losses can be captured more precisely. The values of the look up table are based on [80] for both the supercapacitor and the battery.

Considering full bi-directional flow of energy through the DC/DC converters, efficiency curves are ‘’mirrored’’ for charging and discharging operations as shown in Fig. 36

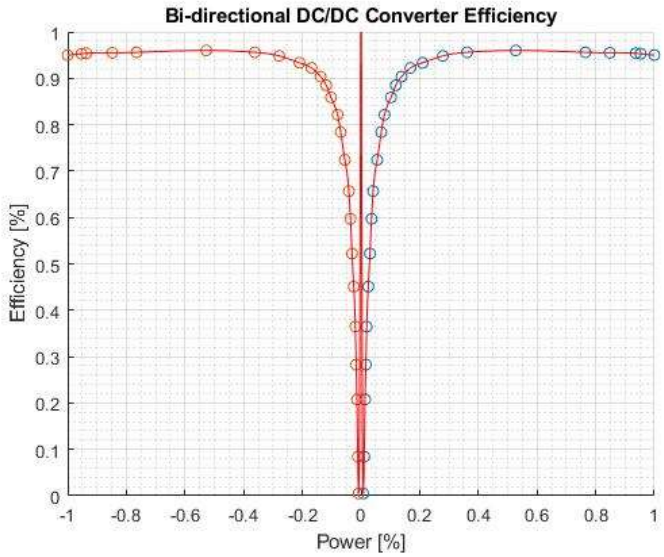

Figure 36 DC-DC Converter Efficiency Curves

For battery charging and discharging efficiency can be expressed as:

$$\eta_{ch,bat} = f\left(\frac{-P_{bat}(t)}{P_{bat,max}}\right) \mid \eta_{dis,bat} = f\left(\frac{+P_{bat}(t)}{P_{bat,max}}\right) \qquad (6.6.1 - 6.6.2)$$

Similarly, for supercapacitor the efficiency for each operation is given by:

$$\eta_{ch,sc} = f\left(\frac{-P_{sc}(t)}{P_{sc,max}}\right) \mid \eta_{dis,sc} = f\left(\frac{+P_{sc}(t)}{P_{sc,max}}\right) \qquad (6.6.3 - 6.6.4)$$

Having estimated the individual efficiencies for each operation, the roundtrip DC-to-storage-to-DC energy efficiency of the storage devices, or the fraction of energy put into the storage that can be retrieved is estimated as follows:

$$\eta_{\text{roundtrip}} = \eta_{ch} \times \eta_{dis} \qquad (6.6.5)$$

Assuming maximum efficiency of 95% for both operations, maximum roundtrip efficiency will be:

$$\eta_{\text{roundtrip,}} = \eta_{ch,max} \times \eta_{dis,max} = 0.95 \times 0.95 = 90\%$$

6.6.2 HESS Losses

After estimating the efficiency for each charging/discharging operation, the corresponding losses can be calculated. All power flows concerned are depicted in fig.37. On the charging side, the power requested by the energy storage devices is divided by the corresponding efficiency. As efficiency is a number between 0 and 1 this results in more available power to be supplied from the engine. On the discharge side the power supplied by the energy storage devices, is multiplied by the discharge efficiency and therefore less energy is arriving to the consumers.

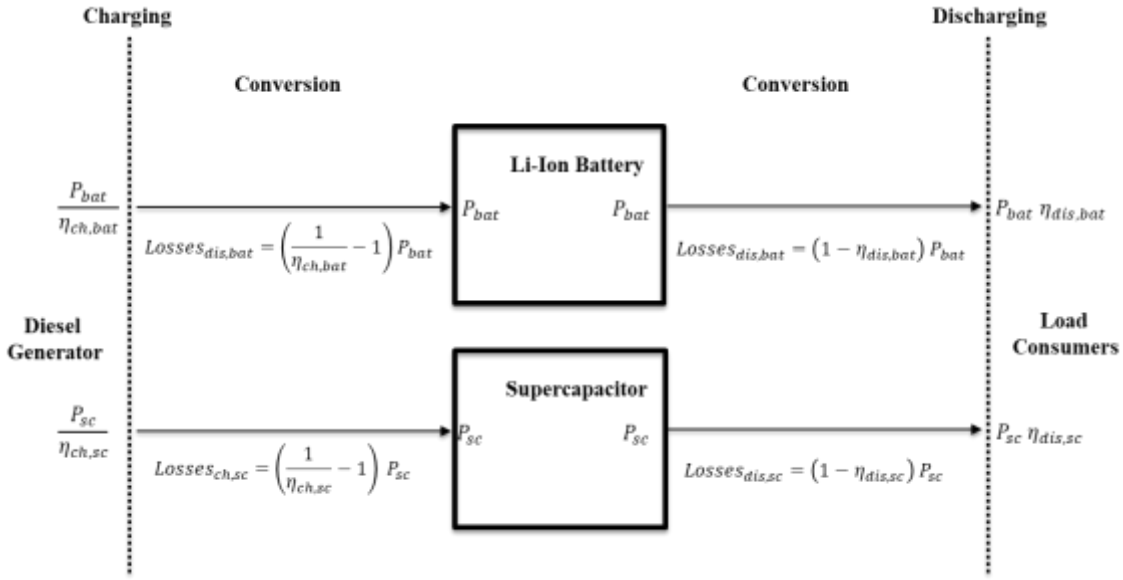

Figure 37 HESS Power Flows

Total battery losses for the entire simulation are given by:

$$Losses_{ch,bat} = \int_{t=0}^{t=n} \left(\frac{1}{\eta_{ch}, bat} - 1\right) \cdot P_{bat}(t)\ dt \tag{6.6.6}$$

$$Losses_{dis,bat} = \int_{t=0}^{t=n} \left(1 - \eta_{dis,bat}\right) \cdot P_{bat}(t)\ \ dt \tag{6.6.7}$$

For supercapacitor total losses are given by:

$$Losses_{ch,sc} = \int_{t=0}^{t=n} \left(\frac{1}{\eta_{ch,sc}} - 1\right) \cdot P_{sc}(t)\ dt \tag{6.6.8}$$

$$Losses_{dis,sc} = \int_{t=0}^{t=n} \left(1 - \eta_{dis,sc}\right) \cdot P_{sc}(t)\ \ dt \tag{6.6.9}$$

7 Modelling & Simulation

To capture the behaviour and performance of the proposed hybrid energy storage system, a time-domain simulation is required for each sizing combination.

This chapter is concerned with (a) the model development for the calculation of the dynamic performance outputs of the simulation such as loss of load probability, battery aging and energy consumption and (b) with the description of the conducted simulations including parametrization and assumptions.

MATLAB has been selected as the simulation environment due to the availability of generic component models that allow easy parametric changes and the relatively easy possibility to develop and run time-domain simulations.

7.1 Model Development for Dynamic Performance Metrics

7.1.1 Loss of Load Probability – Verification

As defined in section 6.3.2. the system should ideally be in equilibrium meaning that all users can be fully satisfied after losses are counted. This condition can be violated if the requested load is greater than the supply capacity of the hybrid energy storage system at time t. Therefore, verification of the system's ability to meet the load is required.

A combined profile (P_{val}) for all power sources including conversion losses is calculated as a measure of verification. This is given by:

Charging:

$$\mathrm{P_{val}(t) = P_{eng}(t) - P_{bat}(t) - P_{sc}(t) - P_{bat,losses}(t) - P_{sc,losses}(t) \geq P_{load}(t)} \quad (7.1.1)$$

Discharging:

$$\mathrm{P_{val}(t) = P_{eng}(t) + P_{bat}(t) + P_{sc}(t) - P_{bat,losses}(t) - P_{sc,losses}(t) \geq P_{load}(t)} \quad (7.1.2)$$

For the system to achieve balance, $P_{val}(t)$ must be equal or greater than the requested load $P_{load}(t)$ for both charging and discharging operations.

$$\mathrm{P_{val}(t) \geq P_{load}(t)} \quad (7.1.3)$$

In other case, there is a loss of load instance (LLI) and the power system is unable to meet demand.

$$\mathrm{P_{val(t)} < P_{load(t)} \Rightarrow LLI}$$

Subsequently, loss of load probability will be the sum of all LLI over simulation time. It is logically derived that the more the LLI the higher the LLP.

$$\mathrm{LLP} = \frac{1}{\mathrm{n}} \sum_{\mathrm{t=0}}^{\mathrm{t=n}} \mathrm{LLI\ dt} \quad (7.1.4)$$

In Fig. 38, a run for load following ($P_{hess} = 800\,kW$ and $psr = 30\%$) is presented. The profiles resulted from the power allocation process are plotted as a function of time for each power source. The input load profile (P_{load}) for all consumers is highlighted in blue colour. On the output side, the engine profile for load following mode (normal operation), the battery profile and the supercapacitor profile are shown in red , purple and light green colours respectively. Finally, the combined verification profile (P_{val}) of all power sources including conversion losses is shown in yellow colour.

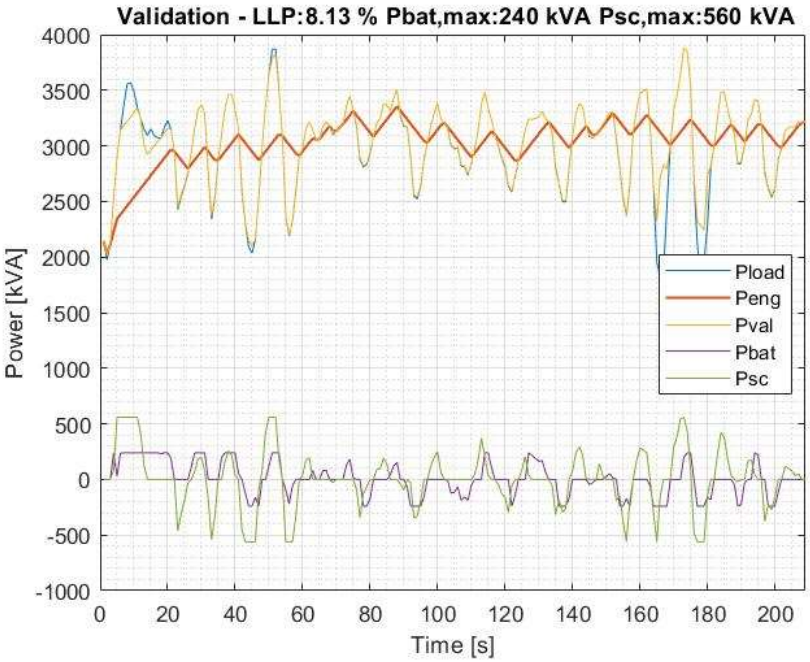

Figure 38 Load Following - Validation (LLP=8.13%)

In Fig.39 loss of load instances can be seen between 7-22 sec, and 51-53 sec . This is resulting in an LLP of 8.13% that is not accepted based on the reliability criterion of 5%. In compare, another run resulting in an acceptable LLP is shown in fig. Again, the engine is set in load following mode and the total power rating of the system is set at 800kW. However, a higher power split ratio of 40% has been used for this run. Therefore, it is deduced that loss of load probability is affected by both the overall power rating of the system as well as from the power split ratio.

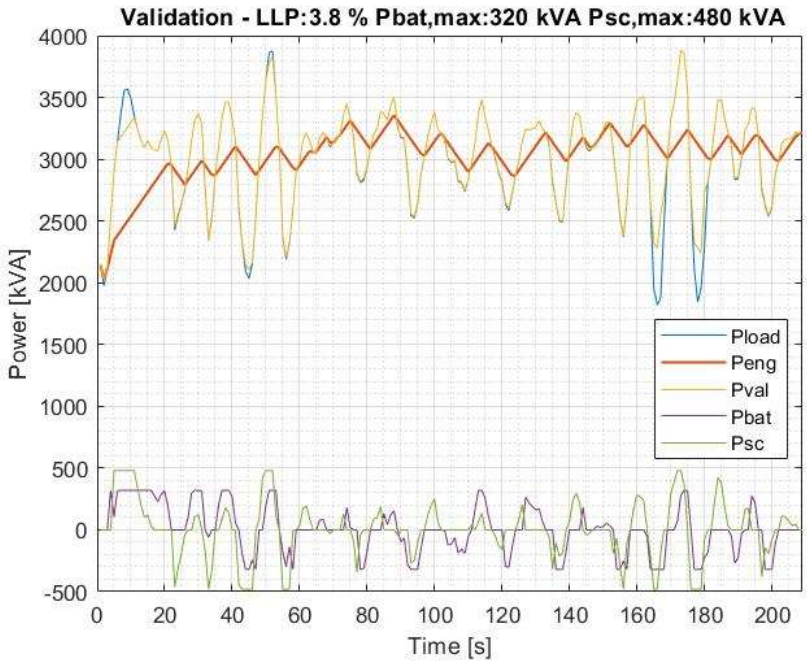

Figure 39 Load Following - Validation (LLP=3.8%)

The reasons resulting in loss of load instances, can be identified in:

a. Limited capability of the diesel engine in normal mode to follow quick load ramps.
b. Failure of the HESS to supply all required load because of:
    i. Undersized power rating of the battery and/or supercapacitor.
    ii. Insufficient available charge in the battery and/or supercapacitor at time t.
    iii. HESS sources being utilized in low efficiency region resulting in high conversion losses.

In order to capture the full effect of sizing decisions on LLP , performance maps of all combinations are plotted in the results section.

7.1.2 Battery Aging (Damage)

In terms of estimation of battery aging, the present thesis has focused on the effect of cycling aging on battery capacity and remaining lifetime.

Estimating cycling aging is considered adequate for proof of concept as this is the parameter that can be controlled through operational measures. Calendar aging, is not considered as it is not affected by operational parameters that can be controlled through energy management system and corresponding power allocation strategy and/or sizing process.

7.1.2.1 Cycle Counting Model

For the estimation of the battery aging and damage a cycle counting model ,where the output profiles of the simulation are used as inputs to the aging model, has been developed similar to those reported in [18, 78, 81]. The obtained profiles for battery state of charge and for battery C-rate are shown in for one of the combinations in Fig. 40.

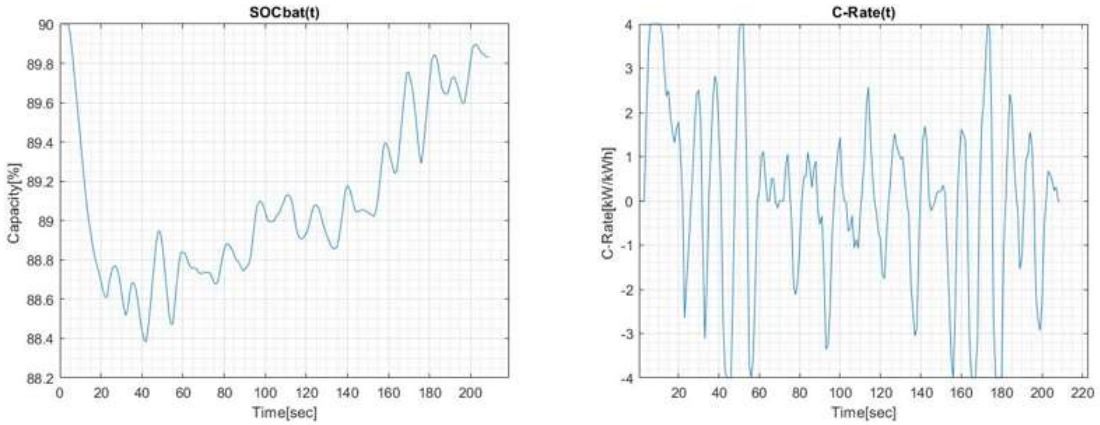

Figure 40 Input Signals to Battery Aging Model [SOCbat(t) / C-rate (t)]

Assuming that the battery is able to achieve an overall number of cycles throughout its lifetime, cycle counting models, link some battery parameters or stress factors to the End-of-life. The main advantage of this method is that deviations from the standard operating conditions can be considered, making the real-life battery simulation more accurate [22]. In the developed model, the concerned stress factors are namely the charge and discharge C-rates and the depth of discharge. Their stress models are designed using the experimentally validated model of Omar et al [19] for LFP batteries. The stress model co-efficients are given in Table 11.

	Coefficients			
Cycle Life vs constant stress factor	a	b	c	d
$f_{DoD}(DoD) = a \cdot e^{b \cdot DoD} + c \cdot e^{d \cdot DoD}$	4464	-0.1382	-1519	-0.4305
$f_{C_{rate,ch}}\left(C_{rate,ch_i}\right) = a \cdot e^{b \cdot C_{rate,ch}} + c \cdot e^{(d \cdot C_{rate,ch})}$	5963	-0.6531	321.4	0.03168
$f_{C_{rate,dis}}\left(C_{rate,dis_i}\right) = a \cdot e^{b \cdot C_{rate,dis}} + c \cdot e^{d \cdot C_{rate,dis}}$	6.009 E9	-0.011869	6.009 E9	-0.01879

Table 11 Coefficients of Battery Stress Models [19]

7.1.2.2 Rainflow Counting

As suggested by the name, in cycle counting model the signal is analysed into cycles with the same stress. To count cycles from an irregular SoC or C-rate profile , rainflow cycle counting algorithm is used to fulfil this task. Specifically, Adam Nieslony's [82] rainflow function in MATLAB has been adopted accordingly to fit the battery profiles.

The first step in the rainflow cycle algorithm is to extract the local minimums and maximums for each of the signal input profiles. These extremums are classified to measure cycles of the same stress. Some cycles are not completed (fully) cycles, those are considered half cycles. The effect of full or half cycle is simply modelled as that one-half cycle causes half of the degradation of its identical full cycle.

In the second step the individual cycles are grouped into classes of equal size. A subroutine is being used to create histograms of absolute frequency for each stress factor [Fig. 41]. The number of groups (bins) is input by the user, representing the number of divisions of the stress profile.

Next, each group of cycle is assigned to a stress factor weight using the Wohler curves generated from the data of table 11. These are shown in Fig. 42.

7.1.2.3 Palmgren-Miner's Stress Level Estimation

Following cumulative battery damage is calculated using the Palmgren Miner's rule. Palmgren Miner's states that the lifetime of a component after undergoing a series of loads is reduced by a finite fraction corresponding to each one of these load events. This reduction fraction is the ratio between the number of cycles that the element has undergone under a stress factor divided with the number of cycles that the element was supposed to last until reaching EOL when operating continuously under this specific stress factor [83].

$$D = \sum_{i=1}^{E} \frac{n_i}{N(\sigma_i)} = 1 \tag{7.1.5}$$

Where,

- n_i: Number of cycles spent under a stress factor σ_i
- $N(\sigma_i)$: Total Number of Cycles for the EOL to be reached
- E: Number of events taken place until the EOL condition is reached
- D: Damage at the battery for each one of these events

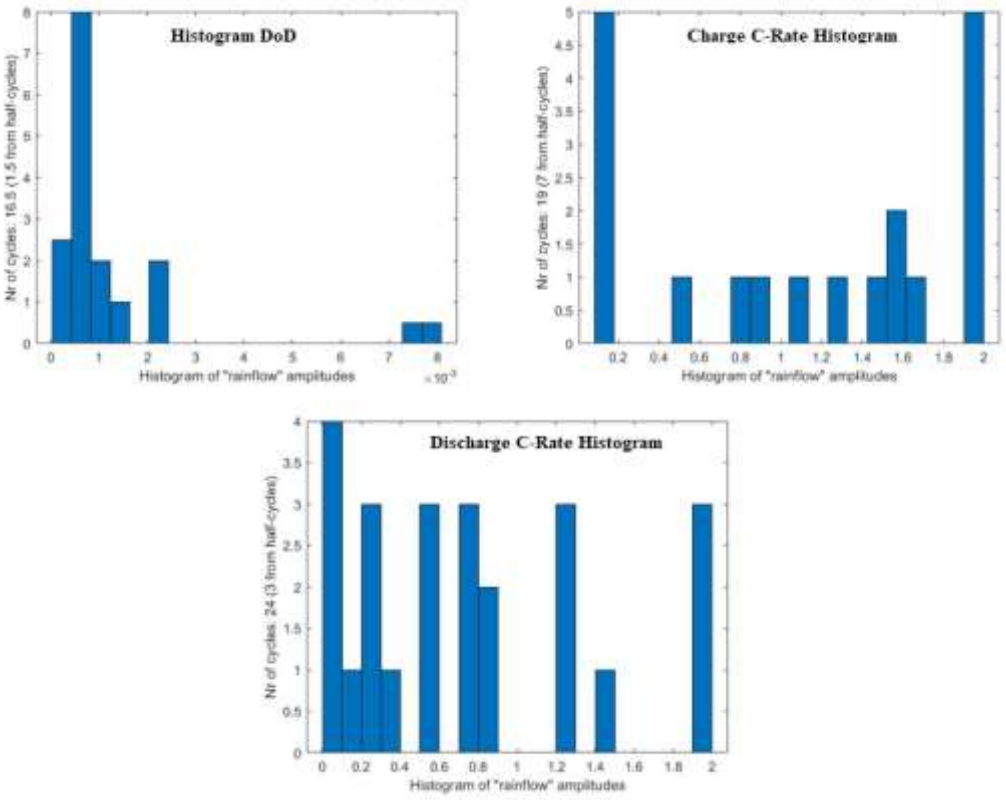

Figure 41 Histograms of Rainflow Amplitudes for each stress factor

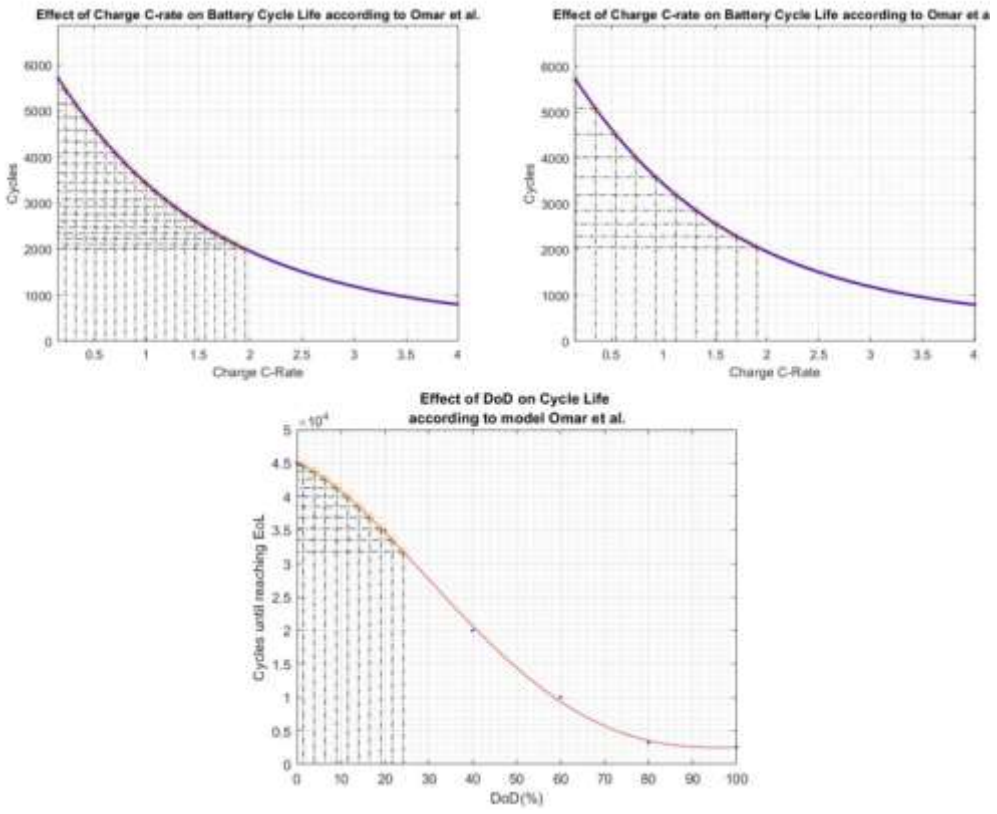

Figure 42 Stress factor Wohler Curves adapted by [19]

The End-of-life of the element is reached when the Damage (D), which is the cumulative of the fractions of life reduction, reaches the 1.

It should be mentioned that a limitation of the Palmgren-Miner rule is that it does not consider sequence effects, i.e. the order of the loading makes no difference in this rule.

7.1.2.4 Aging Model Synthesis

The final step in estimation of battery damage is to combine the individual effect of each stress factor into a single cumulative damage model.

The cumulative damage model is expressed as the summation of each single cycle's degradation with the assumption that cycles affect degradation independently to each other as suggested by Xu [18].

$$f\left(DoD, C_{rate,ch}, C_{rate,dis}, n, N\right) =$$

$$\sum_{i}^{N} f_{DoD}(DoD_i) \cdot f_{C_{rate,ch}}\left(C_{rate,ch_i}\right) \cdot f_{C_{rate,dis}}\left(C_{rate,dis_i}\right) \cdot n_i \qquad (7.1.6)$$

Finally, a process overview is given in Fig. 43. This post simulation analysis is repeated for all valid sizing combinations.

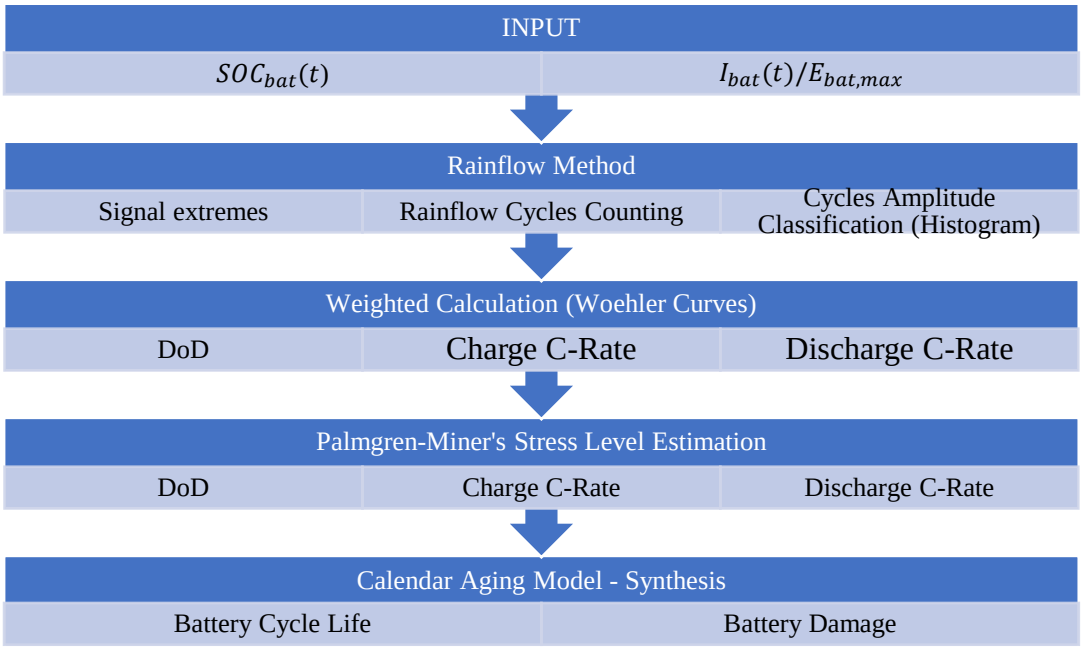

Figure 43 Battery Aging Estimation Process

7.1.3 Energy Consumption

Earlier energy consumption was selected as a more insightful performance metric than fuel consumption when comparing differently sized energy storage installations.

From (4.5.6) energy consumption is given by:

$$\Delta E_{total} = \Delta E_{fuel} + \Delta E_{bat} + \Delta Esc$$

For the selected Wärtsilä 8V31 diesel-electric engine, the specific fuel consumption curve has been derived out of four given load points given by the manufacturer [12].

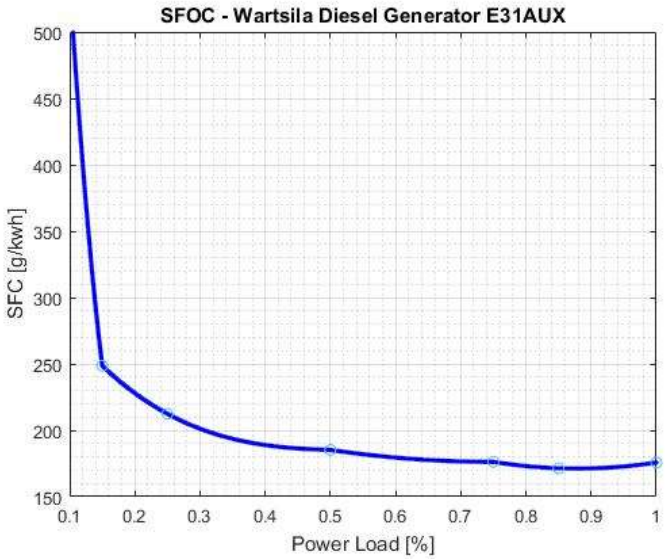

Figure 44 Wartsila E31 MDO Specific Fuel Consumption

The fuel consumption curve is used for the estimation of engine's fuel consumption for each case produced by the sizing and power allocation process. It is assumed that these values are also accounting for the losses from the alternator and the AC/DC converter.

$$FC_{eng} = \sum_{t=0}^{t=n} P_{eng}(t) \cdot SFC(t)\, dt \tag{4.5.5}$$

Assuming an initial deposit of 100 kg of MDO for all runs, a remaining fuel capacity at the end of the simulation can be estimated:

$$\mathrm{Fuel_{eng}(t_n) = Fuel_{eng}(t_0) - FC_{eng}[kg] = 100 - FC_{eng}[kg]} \tag{7.1.7}$$

Having estimated diesel engine's fuel consumption in terms of mass, a conversion in energy units is required. For marine diesel oil, a lower calorific value (LCV) of 42700 kJ/kg is taken as per IMO guidelines [84].

$$\mathrm{FC_{eng}[kJ] = FC_{eng}[kg]} \cdot 42700 \left[\frac{\mathrm{kJ}}{\mathrm{kg}}\right] \tag{7.1.8}$$

Converting kilojoules into kWh units

$$\mathrm{FC_{eng}[kWh] = FC_{eng}[kJ]} \cdot \left(\frac{1}{3600}\right) \tag{7.1.9}$$

It is assumed that both battery and supercapacitor are having the maximum allowable charge before the beginning of the simulation.

$$SOC_{bat}(t_0) = 90\% \ | \ E_{bat}(t_0) = 0.9\ E_{bat,max}$$

$$SOC_{sc}(t_0) = 100\% \ | E_{sc}(t_0) = E_{sc,max}$$

From equations (4.5.6 -4.5.8), total energy consumption is given by:

$$\Delta E_{total}[kWh] = FC_{eng} + \Delta E_{bat} + \Delta E_{sc} \quad (4.5.6)$$

$$\Delta E_{bat}[kWh] = E_{bat}(t_n) - 0.9\ E_{bat,max} \quad (4.5.7)$$

$$\Delta E_{sc}[kWh] = E_{sc}(t_n) - E_{sc,max} \quad (4.5.8)$$

Energy consumption can be modelled as the differential between the beginning and the end of the simulation for each storage medium including fuel deposit. In Fig. 45 energy consumption is visualized. Two of the thousands valid sizing combinations are selected to illustrate energy differential concept.

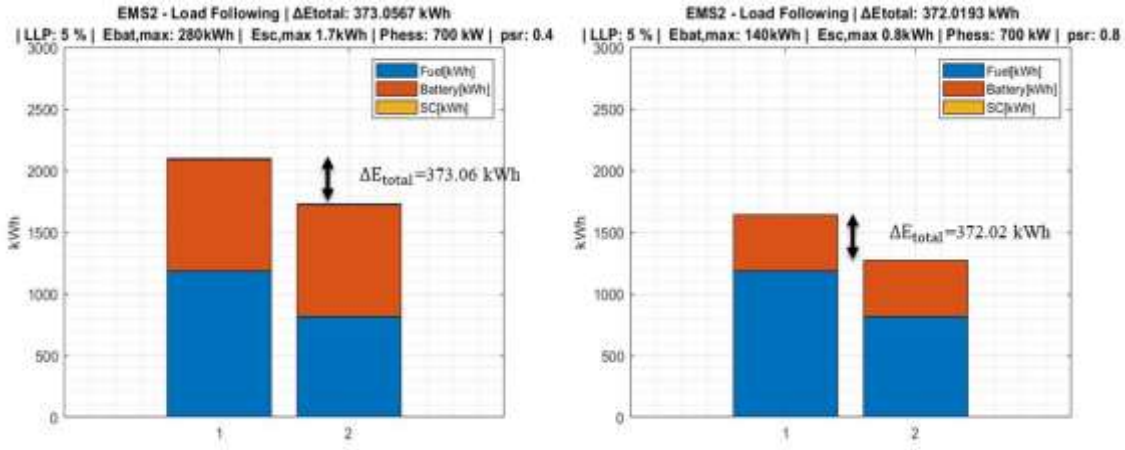

Figure 45 Energy consumption before-after breakdown for two different sizing combinations

For both cases, total power rating and LLP are the same. On the left side however a larger capacity system is depicted. Additionally, although system's overall rating is the same at 700 , the power split ratio is different (40% and 80% respectively). Stacks labelled "1" are representing the total stored energy at the beginning of the simulation while stacks labelled "2" represent the total remaining energy stored at the end of it. Logically derived, stack number "2" has a lower magnitude than "1". This is because a part of the system's initial energy has been converted into work while another part has been dissipated to the environment in the form of losses. Derived by the figure, it is shown that differently sized systems are resulting in different energy consumptions. In this instance, the larger system is consuming more energy. Another quick remark derived by the two graphs is that supercapacitor's capacity is barely visible in compare to battery and fuel. However, this should not be confused with the energy throughput as a storage medium might charge and discharge many times within the time of span of the simulation. Due to the multi-variable nature of the problem, a clear correlation can be only obtained when all runs are considered. Therefore, the impact of sizing combination on overall energy consumption is furthered discussed in the following results & discussion chapter.

7.2 Benchmark Case

The profile used for the simulation is concerning a product tanker from Wärtsilä E4PS project. The load profile is the result of real-life measurements in the open sea at the South of Norway and it has been selected because of its significant dynamic fluctuations that facilitate the examination of the HESS behaviour. As can be seen from Table 13, the ship was operating in heavy sea conditions with a wind speed of 20.4 knots and an average wave height of 4.5m.

Date	1.12.2011
Time	22:15
Vessel Speed	14.3 kn
Latitude	N 57°58‘
Longitude	E 6°4'
Heading	100°
Wind Speed	10.5 m/s – 20.4 knots
Wind Direction	290°
Wave height (avg)	4.5 m

Table 12 Benchmark Case Measurements Data

As can be seen from Fig. 46, because if the wave-induced loads the engine was asked to follow ramp up its load from 37% to 83% in less than 8 seconds. It should be mentioned that according to Wärtsilä, the diesel generator managed to cope up with this ramp rate by operating in the emergency load curve near its maximum capacity.

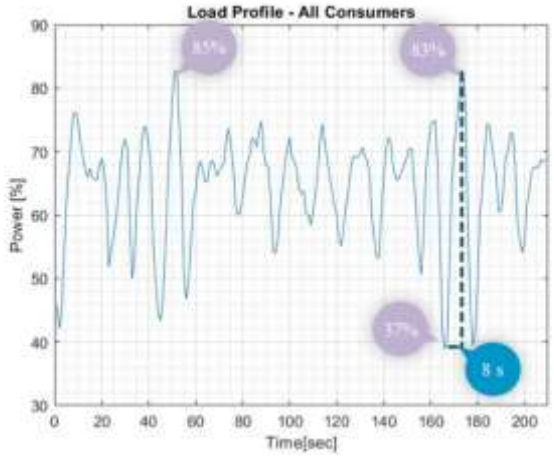

Figure 46 Load Profile Dynamics

In order to use the abovementioned profile for the purposes of this simulation, the following assumptions are being made:

- The load profile is the equivalent of the total electric power demand (propulsion plus hotel loads) of the vessel as a function of time. By this assumption it is possible to use the outlined power plant configuration of Chapter 3.
- It is assumed that load profile is repetitive. Then it is extrapolated by a factor of 3 to increase simulation running time to about 10 minutes. By increasing the duration of the input signal, it is possible to examine the behaviour of the battery and the supercapacitor for larger DoD cycles.
- For all simulations, Wärtsilä 31 Diesel Generator MDO is assumed. The engine is only allowed to operate in normal operating mode to allow for the HESS to absorb the fluctuations.
- Assuming all load is served by a single diesel generator, the total fuel consumption is calculated as benchmark for the HESS performance.

7.3 Simulation Runs

7.3.1 Basic Runs

In line with the objective of this thesis for demonstration of potential improvements, two battery-only peak shaving hybrid systems have been simulated as baseline cases. The two battery only simulations are (a) for load levelling and (b) for load following power sharing approaches between the diesel generator and the energy storage system. For reasons of convenience, all cases concerning load levelling will be referred to as "EMS1" and all cases concerning load following will be referred to as "EMS2".

Moreover, for the baseline cases, the design space is limited to battery-only cases (as defined in section 5.3.), while the supercapacitor rating is set at zero ($psr = 1, csr = 1$) for all combinations. Additionally, the energy management systems used in these simulations operate in the same principle as in Chapter 6 although secondary power allocation is not being triggered.

Following, and as a part of the main objective of this thesis to increase understanding of battery-supercapacitor hybrid energy storage systems in ship applications, the equivalent two peak shaving cases for HESS are simulated for all design solutions resulted from Chapter 5.

Detailed flow charts depicting each basic simulation run can be found in the Appendices.

Finally, the parameters shown in Table 13 are selected for the basic simulations runs. As was stated in section 5.6., battery cost of 800$/kWh is taken for all basic runs. For both "EMS1" runs, the engine set load point is set at 60% of engine MCR. This point has been selected as it matches the average load of the benchmark profile.

	Battery Only		HESS	
Run	EMS1	EMS2	EMS1	EMS2
dt_{req}	N/A	N/A	8	8
Engine Set Loadpoint [% MCR]	60%	N/A	60%	N/A
HESS Decisive Threshold [% MCR]	N/A	N/A	15	15
Battery Cost [$/kWh]	800	800	800	800
Simulation Duration	x3	x3	x3	x3

Table 13 Parameters for Basic Simulation Runs

Next, some additional parameters that are only applicable to the HESS runs are defined. Specifically, the minimum required discharged duration for the supercapacitor is set at 8 seconds to match the transient characteristics of the benchmark load profile. Lastly the decisive threshold for the secondary power allocation between the battery and the supercapacitor is set at 15% of engine's installed capacity.

7.3.2 Sensitivity Runs

In order to narrow down the uncertainty of model outputs that is related to input or disturbance assumptions, some additional sensitivity runs are conducted.

First minimum required duration of supercapacitor discharge pulse is identified as a parameter whose behaviour should be further examined. Specifically, two additional runs have been conducted for both a smaller $dt_{req} = 4\ sec$ and a larger value $dt_{req} = 12\ sec$.

Next, the HESS decisive threshold is also tested for values of 10 and 20% of installed engine capacity. Again, these cases are not applicable to battery-only cases and thus they are only simulated for the HESS.

Another parameter whose effect is further examined is the engine load point % for the load levelling runs. As the energy consumption is not only a function of the engine specific fuel oil consumption, it is interesting to see what the effect of other MCR points on system's overall performance is. The engine load point is tested for values of 55% and 65%.

Finally, the single effect of battery cost is also investigated. Having in mind that further improvements in batteries cost are likely, the effect of a 50% reduction in battery price is simulated.

A summary of all runs can be found in Appendix.

8 Results & Discussion

After the conduct of the basic simulation runs, those are compared to each other with regards to the defined performance metrics. First, the results of HESS load levelling run are presented extensively and then compared to the battery-only load levelling. Then HESS load following results are summarized and compared to the battery-only case. Finally the two HESS cases are compared to each other.

At this point, the reader should be advised that battery-only cases are always shown on the left-hand side of the page while the proposed hybridized system at the right-hand side.

8.1 EMS 1 – Load Levelling (Extensive Analysis)

8.1.1 Global View

Starting from load levelling approach, the two simulations are visualised in 4D plots (Fig. 47-48). On the x-axis and y-axis, the overall sizing dimensions (i.e. overall capacity and power rating) of each examined combination can be seen. The loss of load probability as calculated from the simulations is shown in the z-axis. Any value exceeding 5% should not be accepted in accordance with the set reliability criterion. Finally, battery damage percentage is expressed using coloured scale. Orange or yellow colours depict high damage (or fast aging) percentages while low damage is shown in shades of blue. The colour scale is kept consistent for all graphs shown in this chapter.

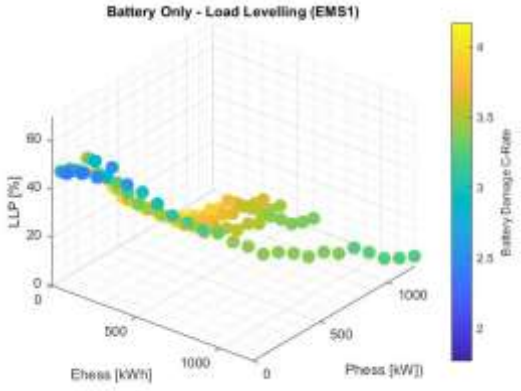

Figure 47 EMS1 – Battery Only 4D

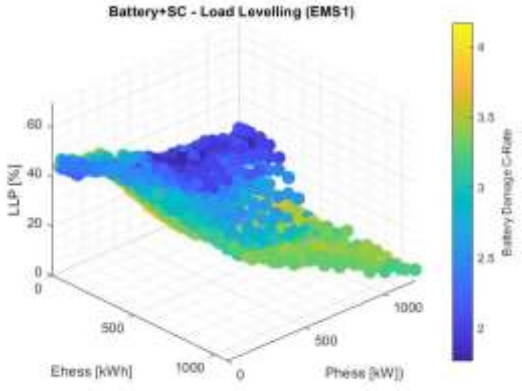

Figure 48 EMS 1 - HESS 4D

By having a section view of the same diagrams (Fig. 49-50), it can be logically derived that blue scatter points on the bottom left part of the chart represent low capacity systems with acceptable LLP and low battery damage. Therefore this can be considered as the desirable performance region.

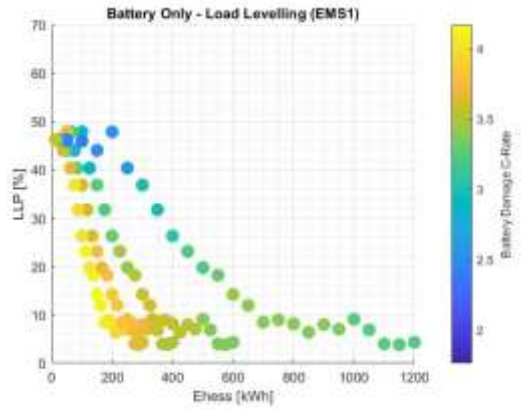

Figure 49 EMS1 Battery Only LLP vs Ehess

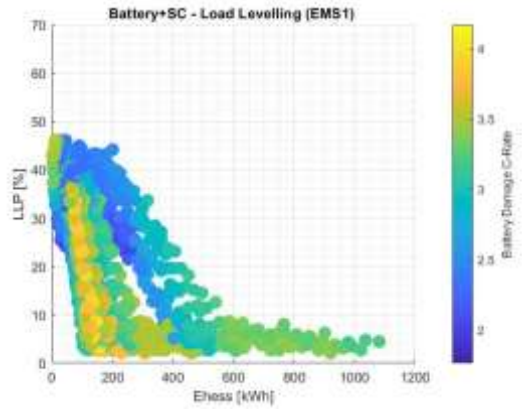

Figure 50 EMS1 HESS LLP vs Ehess

On the battery only diagram (Fig. 49), the 4 distinct lines represent 4 different C-rates. It can be seen that the higher the C-rate (i.e. left-most line), the steeper the slope is. Hence, smaller capacities are required to meet the LLP criterion. At the same time, it is seen that high C-rate combinations experience very high battery damage. By over-sizing the battery system, the battery damage is moderated. Nevertheless, as energy storage size increase rate surpasses a certain threshold both the LLP and battery damage rates of improvement start to converge near a constant value. For LLP this is represented by a flat line, while for battery damage this is shown by low color variations. On the other hand, in the proposed HESS solution (Fig. 50) it can be seen that there is a design region below 600kWh for which battery damage is much less in compare to battery-only case. By doing this analysis we can identify the convergence patterns and determine the minimum capacity that satisfies both criteria.

This trend is also observed with respect to the system's overall weight (Fig.51-52). By reducing the system's overall capacity, it is possible to also optimize the weight of the system despite the addition of the supercapacitor and its converter. Specifically, it can be seen that there are hybridized design options in the range of 2-2.5 tonnes (Fig. 52) that are performing at the same level with battery only installations of 3+ tonnes (Fig. 51).

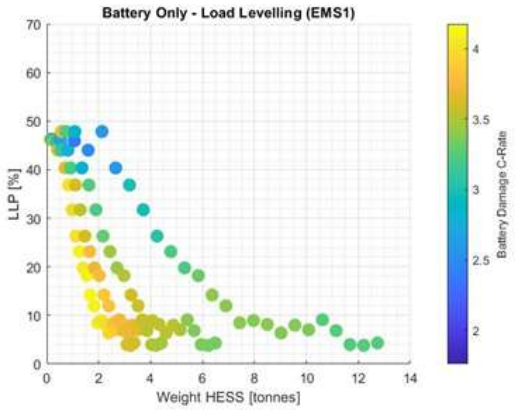

Figure 51 Battery Only Weight EMS1

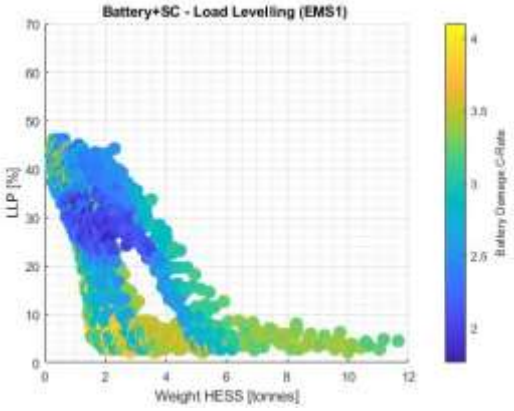

Figure 52 HESS Weight EMS1

Next, the ragone plot of Chapter 4 is expanded to include the dynamic outputs of the simulation. On fig. 53, it is seen that in order for the battery system to achieve moderately high specific power its cycle life is significantly compromised. Fig 54 shows that by hybridizing the energy storage system it is possible to meet application goals while optimizing for specific power.

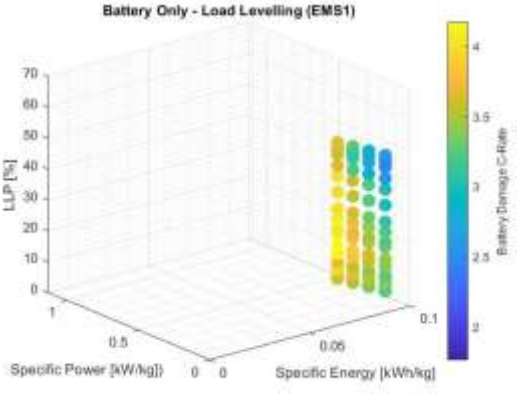

Figure 53 EMS1 -HESS Ragone Plot

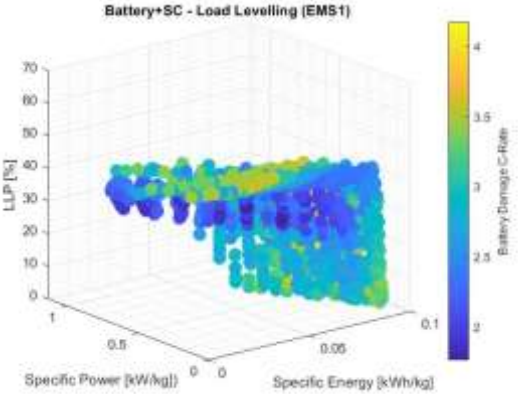

Figure 54 EMS 1 - Battery Only Ragone Plot

8.1.2 Filtered Results

Next step in the results analysis, is to apply certain filters to remove "noisy'' values from the design space. First filter is concerning acceptable LLP values:

$$\text{LLP} \leq 5\%$$

Another filter is concerned with battery damage percentage. This is set to a relatively high threshold of 4%. Any values exceeding this number are eliminated and are not further considered for the analysis.

$$\text{Battery Damage} \leq 4\%$$

Lastly, a third filter is introduced with respect to system's overall weight. Based on Fig. 52 the threshold is set at 6.5 tonnes.

$$\text{HESS Weight} \leq 6.5 \text{ tonnes}$$

Since, the algorithm is checking a range of solutions (where the power has been split in different proportions for different C-rates), it is derived there are multiple sets of available HESS combinations for which the LLP and battery damage criteria are meet (Fig. 56).

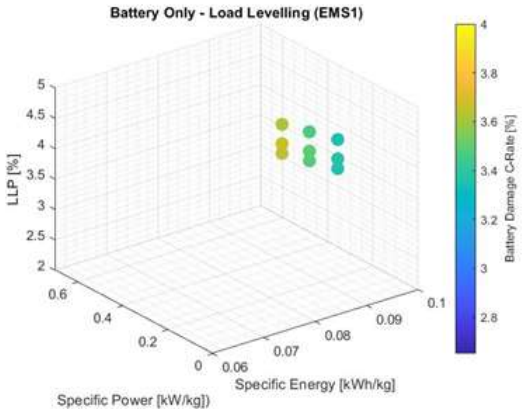

Figure 55 EMS 1 Battery Only - Filtered Ragone Plot

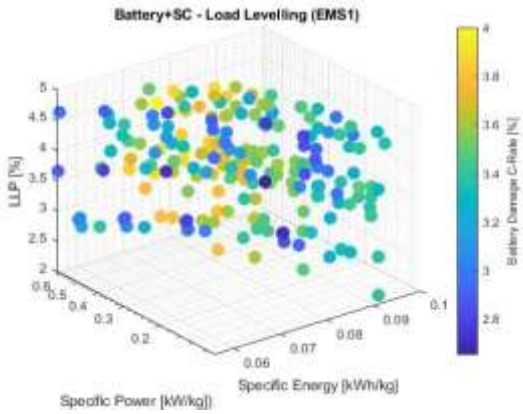

Figure 56 EMS 1 HESS - Filtered Ragone Plot

To facilitate further selection, performance metrics such as weight, cost and energy consumption need also to be considered and plotted against the overall HESS power rating, the power and capacity split ratios.

In Fig. 57 the weight of each combination is plotted against the capacity split ratio. It is shown that all preferred solutions (after filtering) are given for csr values between 97.5% and 99.5%. This means, that battery needs to be dimensioned close to the hybrid system's overall energy capacity while the supercapacitor should only account for a small fraction of it.

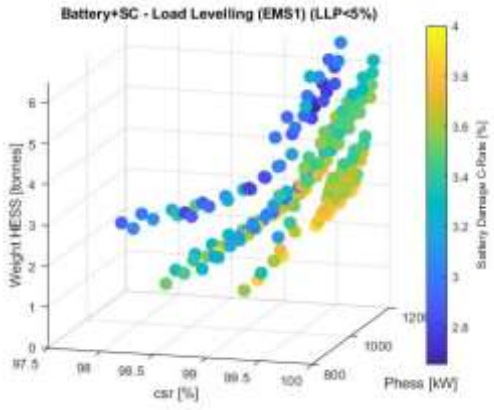

Figure 57 EMS 1 HESS - Weight vs capacity split ratio

In Fig. 58, it is identified that all combinations that result in low battery damage (dark blue colour) lie within 40-55% region of the power split ratio. It is observed that the split of power rating between battery and supercapacitor components of the HESS, is relatively balanced with a slight bias in favour of the supercapacitor. Practically, this means that neither battery nor supercapacitor devices should be sized to stand-alone serve most of overall power rating (i.e. values near 0 and 100%). Specifically, when reliability, battery aging and system's weight are all considered, the corner value combinations of power split ratio can be omitted.

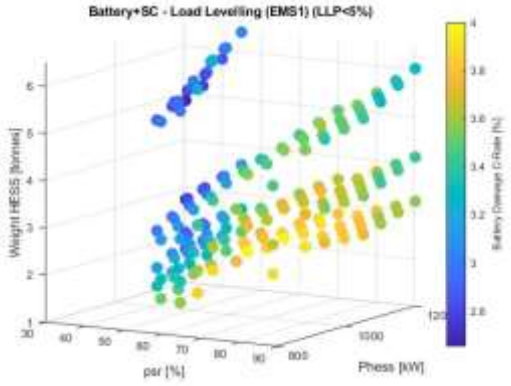

Figure 58 EMS 1 HESS - Weight vs power split ratio

Another conclusion that can be derived by Fig 58 is about the effect of power electronics weight on overall system's weight. As stated in paragraph 5.5., the supercapacitor is requiring larger power electronics in compare to batteries because of its voltage drop characteristics. Therefore, for lower power split ratios, heavier power electronics are required. Based on this, we would expect that system's overall weight would be lower towards 90% of psr. Nonetheless, it is observed that HESS overall weight tends to decrease for smaller psr, meaning that the effect of power electronics in overall system's weight is limited. This is because the high specific power of the supercapacitor outweighs the necessity for heavier converters resulting in a net reduction in system's weight for $psr > 40\%$.

Having established that reliability, weight and aging criteria are fulfilled, the analysis is expanded on system's cost. For both battery-only and hybridized cases, the overall cost is a linear function of system's overall weight. Figure 59 and 60 show that range of cost efficient and light solutions is also expanded. By having this expanded design space, it is possible to optimize for different primary objectives. If capital cost or weight is the primary concern, then values as low as 1.6 tonnes and 150k$ can be achieved respectively. For comparison the equivalent minimum in battery-only cases are 3 tonnes and 350k$. By elaborating, if somebody wishes to optimize battery lifetime with a damage of less than 3% for a given budget of 400k$ (or max. weight value of 5 tonnes) this is only possible in the HESS.

The equations describing these relations are given below.

Battery-only:

$$\text{Weight}_{\text{total}}(\text{Cost}) = \frac{13.01 \cdot \text{Cost}_{\text{total}} - 185.9}{1000} \tag{8.1.1}$$

Hybrid energy storage system:

$$\text{Weight}_{\text{total}}(\text{Cost}_{\text{total}}) = \frac{13.04 \cdot \text{Cost}_{\text{total}} - 258.2}{1000} \tag{8.1.2}$$

Where cost is expressed in ($,000) and weight in tonnes.

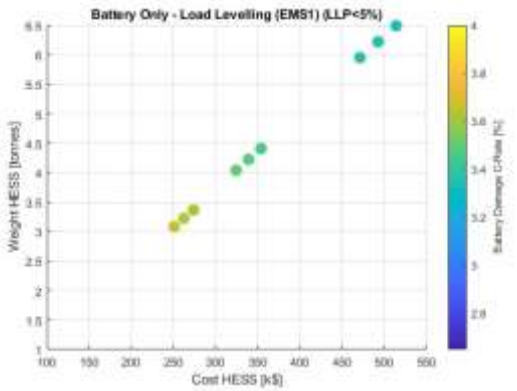

Figure 59 EMS 1 Filtered - Battery Only Cost

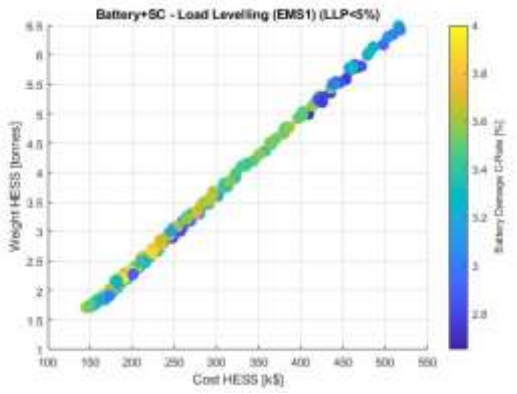

Figure 60 EMS1 Filtered- HESS cost

8.1.3 Energy Consumption

At this stage, benefits of hybridization with respect to battery damage, system reliability, overall weight and cost have already been demonstrated. Nevertheless, the effect of hybridization on system's energy consumption must also be considered.

8.1.3.1 Energy Consumption Comparison with Engine Benchmark

To evaluate the overall energy consumption, we distinguish three cases namely no energy storage (benchmark), battery only and HESS.

In the benchmark case, the diesel generator is in emergency load mode and is serving all load without any assistance from the energy storage system. It has been estimated that in this case 93.5 kg of MDO or equivalently 1109 kWh of work, have been consumed. It should be reminded that the selected Wartsila 31 DG is already very efficient with a minimum specific fuel consumption of 171.4 g/kWh. Therefore, if the engine is allowed to operate in emergency load mode (at the expense of engine stress) a satisfactory consumption can already be achieved.

In comparison, all battery only load-levelling combinations with acceptable LLP (<5%) are consuming a minimum of 1186 kWh for the basic case (Fig. 61). This can be translated in a raise of +6.9% in overall energy consumption for the engine to be able to operate in normal operating mode. The additional losses can be explained by the fact that the introduced conversion losses are exceeding any savings from operation in higher SFC.

	(1) DG Emergency	(2) Battery Only	(3) HESS
Total Energy Consumption [kWh]	1109	1186	1181-1189
Difference with (1) [%]	-	+6.95	(+6.5) - (+7.2)
Difference with (2) [%]	-	-	(-0.50) - (+0.25)

Table 14 Load Levelling EMS1 - Energy Consumption (filtered results) for each case

For the proposed battery-supercapacitor energy storage system, the acceptable energy consumption values for load-levelling, vary between 1181kWh and 1189kWh depending the performance metric we wish to optimize for (Fig. 61). Again, energy consumption is higher in compare to the Diesel Generator stand-alone operation in emergency mode. With respect to battery only case, marginal differentiations between -0.5% and +0.25% of the battery-only energy consumption are observed. Positive variations can be explained by the developed energy management strategy that is preferentially operating battery and supercapacitor near their maximum power output (high efficiency region).

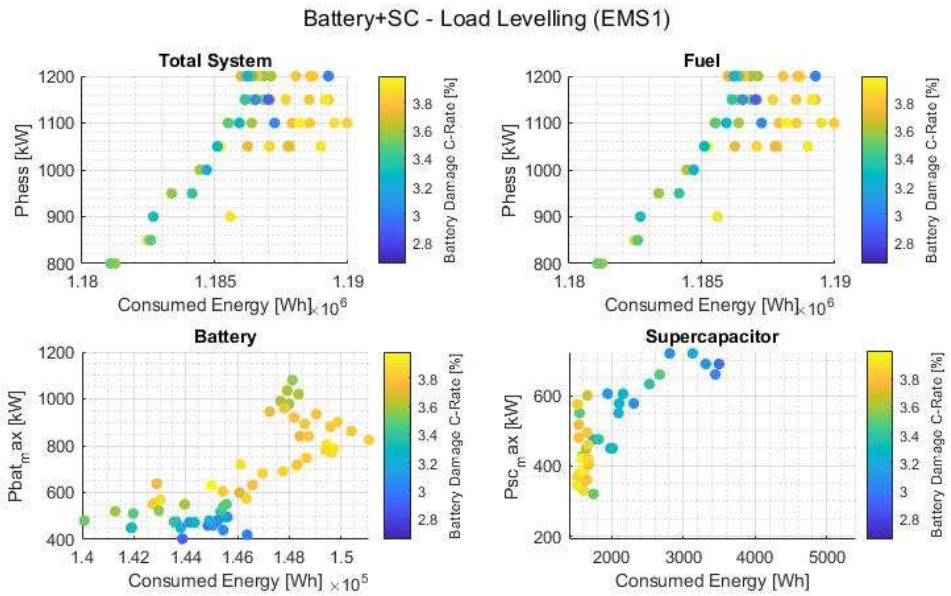

Figure 61 HESS EMS 1 - Energy Consumption Breakdown

8.1.3.2 Excess Energy Utilization

When it comes to overall energy performance of the system, excess energy is another important aspect. High utilization of the excess energy produced by hybrid systems is a measure of system's effectiveness rather than efficiency [85]. As outlined in chapter 6, if P_{load} is less than P_{eng} then the energy storage system should charge. Nevertheless, an amount of non-utilized excess electrical energy is observed in occasions where:

a) both battery and supercapacitor are fully charged
b) their combined power receiving capability is insufficient to fully absorb all the available power

According to the developed EMS, if the HESS is unable to absorb all available power then the allocated engine load is set to be reduced till power balance is achieved. However, the load reduction rate is also constrained as per section 6.3.1.1. If the reduction rate is set too fast, then the correction is automatically regulated as per engine's normal mode loading capacity diagram. In this case, surplus or excess energy is generated by the power system and is dissipated based on the tolerance of each load consumer [86].

For excess energy the maximum power rating P_{hess} is identified as the design factor with the most influence. In Fig. 62, excess energy is expressed as percentage of total produced energy by the diesel generator and is plotted against P_{hess} for HESS load levelling runs.

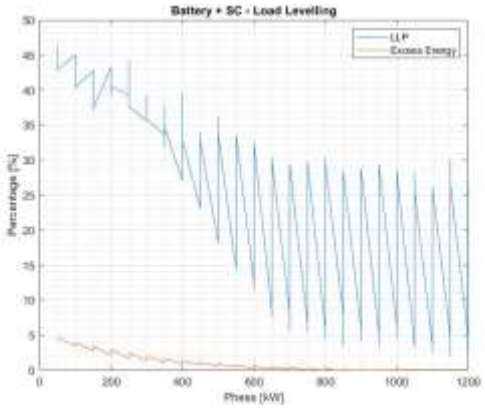

Figure 62 HESS Load Levelling - Excess Energy vs Simulation Runs

For time spans in the range of minutes such in the conducted simulation, insufficient power rating of the HESS is the most often cause for engine generated energy to not be absorbed. The high frequency oscillations of the diagram are representing the different power split ratios tested for each P_{hess} step. The low spikes represent low power allocation ratios (i.e. $P_{sc,max} > P_{bat,max}$). For P_{hess} ratings up to 450 kW, the excess energy is having a generally linear behaviour. Above this value, the non-utilized energy starts to converge in values well below 1%. In fig. 63 the LLP over P_{hess} is also shown. The minimum P_{hess} value resulting in an acceptable LLP of below 5% is appearing after 800kW.

Therefore, it is shown that percentage of non-utilized excess energy is negligible for the range of solutions meeting the LLP criterion. This mean that above a critical power rating value, energy saving potential due to higher absorption of engine excess power by HESS starts to get limited. For any further reduction in energy consumption, a more elaborate energy management strategy needs to be developed. Any further upsizing is only beneficial for other objectives such as extension of the battery lifetime and for further LLP improvement.

8.1.4 Selected Solutions

To demonstrate the clear effect of the proposed solution on system's performance direct comparison with battery-only configuration must be conducted. Best solutions are selected for each configuration for a given power rating value of 1100kW and for C-rate values of 3 and 4 respectively (Table 15). It should be mentioned that all combinations discussed in this section satisfy the minimum set criteria for reliability, battery damage and weight and therefore further optimization can be achieved.

EMS1- Load Levelling - Battery Only											
Phess [kW]	Ehess [kWh]	C-rate	Spec. Power [kW/kg]	Spec. Energy [kWh/kg]	psr	csr	Total Cost [k$]	Total Weight	Battery Damage [%]	Consumed Energy [kWh]	LLP (%)
1100.0	366.7	3	0.27	0.09	100%	100%	324.13	4039.44	3.50	1186.46	4.0
1100.0	275.0	4	0.36	0.09	100%	100%	250.8	3084.6	3.7	1186.5	4.0
EMS1- Load Levelling - Battery and Supercapacitor (HESS)											
Phess [kW]	Ehess [kWh]	C-rate	Spec. Power [kW/kg]	Spec. Energy [kWh/kg]	psr	csr	Total Cost [k$]	Total Weight	Battery Damage [%]	Consumed Energy [kWh]	LLP (%)
1100.0	203.4	3	0.41	0.08	55%	99%	228.3	2700.5	3.6	1185.5	2.6
1100.0	185.0	3	0.44	0.07	50%	99%	215.1	2520.5	3.3	1185.5	4.0
1100.0	166.7	3	0.47	0.07	45%	99%	202.0	2340.5	3.1	1185.9	3.8
1100.0	149.2	3	0.48	0.06	40%	98%	200.0	2300.9	2.9	1187.2	2.9
1100.0	139.2	4	0.54	0.07	50%	99%	178.5	2043.1	3.5	1185.5	4.0
1100.0	125.4	4	0.58	0.07	45%	99%	169.0	1910.8	3.3	1185.9	3.8
1100.0	112.5	4	0.57	0.06	40%	98%	170.7	1919.0	3.1	1187.2	2.9

Table 15 Selected Best Solutions forEMS1 - Battery Only and HESS

From Table 15, it is derived that the psr values for the hybridized system range between 40% and 55% meaning that the supercapacitor rating should be between 495kW-660kW. Any values outside this range fail to meet at least one of the set criteria and therefore are not considered feasible solutions. With regards to static characteristics, another quick conclusion is that despite the higher specific energy (~90 Wh/kg) of the battery-only system, all hybridized solutions are lighter in terms of total installation weight. This is because at the same time the overall specific power is improved. Given adequate range (shown from LLP) the system is sensitive only to the power rating. Weight reduction of 33-43% for C-rate of 3 and 29-34% for a C-rate of 4 are achieved.

In absolute values, total capacity is not exceeding 2700 kg and 1910 kg respectively while minima are found for psr of 40% . Similarly, cost savings of 30-38% for C-rate of 3 and 25-33% for a C-rate of 4 are demonstrated. It is observed that with increasing C-rates, the relative capital cost saving potential is decreasing although still significant. This is because smaller batteries are being used in the baseline battery-only configuration.

Returning to the basic design dilemma between oversizing and battery aging. It is shown that:

a) By hybridizing the system in an analogy of $40\% \leq psr \leq 50\%$, battery damage can be reduced by 5.7%-17.4% in compare to the battery only configuration for 3C. Specifically, the battery degradation is slowed down for the same period from 3.5% EoL to 2.9%.
b) By sizing the HESS for a C-rate of 4 battery experiences faster aging in compare to a C-rate of 3. The relative improvement is also dropping (although still significant) to 5.4%-16.2% in compare to the battery only case. This results in 3.7% and 3.1% if EoL respectively.
c) For lower the csr, the battery damage is smaller. As the supercapacitor energy capacity increases, the battery can be utilized less and thus extend its lifetime.

Moving on, the effect of hybridization in energy consumption is considered more complex. Specifically, for $45\% \leq psr \leq 55\%$, a marginal improvement of 0.08% is observed. However, as the psr drops to 40% (where battery damage, overall weight and cost are optima) a turning point appears, and the energy consumption deteriorates by 0.06%. This behaviour is observed independently of the C-rate.

Finally, with regards to loss of load probability all combinations meet the set criterion and therefore no further analysis is required.

8.2 EMS 2 – Load Following

In order to evaluate the effect of power sharing approach on the performance of the hybridized energy storage system, results of EMS2 -Load Following simulations are being discussed in this paragraph. As stated, the principle in load following is to have the diesel generator "following" the load power only limited by its loading capacity mode (emergency or normal). In load following approach, fluctuation handling is split between battery, supercapacitor and diesel generator.

Fig. 63-64, show the effect of system's overall capacity on battery damage and on loss of load probability. The colormap axis is set on same scale with Fig. 49-50 to demonstrate the differences between the two power sharing approaches. From the overall color of the two graphs, it can be seen that load following approach is resulting in faster battery degradation (in compare to load levelling) due to higher utilization of the energy storage system. When comparing the two load following cases (Fig. 63-64), it is derived that it is possible to control battery aging while downsizing the installation.

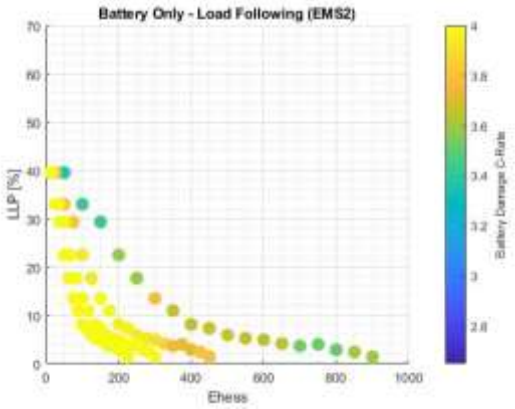

Figure 63 EMS2 Battery Only LLP-Ehess

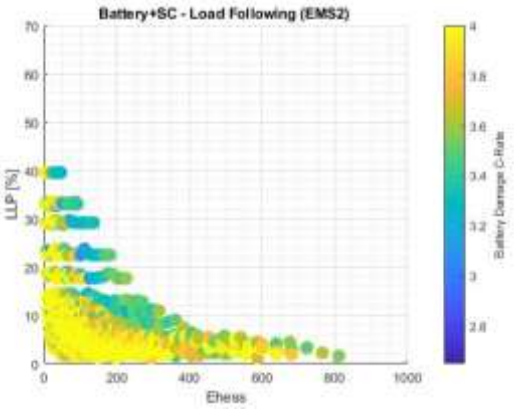

Figure 64 EMS2 HESS LLP vs Ehess

It is also clear that load following approaches result in smaller power installations. According to Fig. 65, it is possible to have reliable installations rated as little as 700-800 kW. For reference, load levelling required over 1000kW to achieve same LLP. This is because diesel generator is absorbing a part of the fluctuations itself.

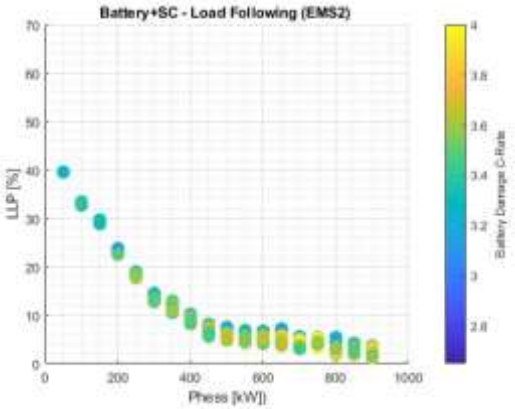

Figure 65 EMS2 HESS LLP vs Phess

For load following mode, the total energy consumption is estimated at 1129 kWh which accounts for 2% increase in compare to the baseline case. This means that load following is 5% more efficient than the equivalent load levelling approach. Lower energy consumption is mostly justified by the lower diesel generator fuel consumption (Fig. 66) as a result of the engine's more effective utilization and thus lower energy throughput of the storage system.

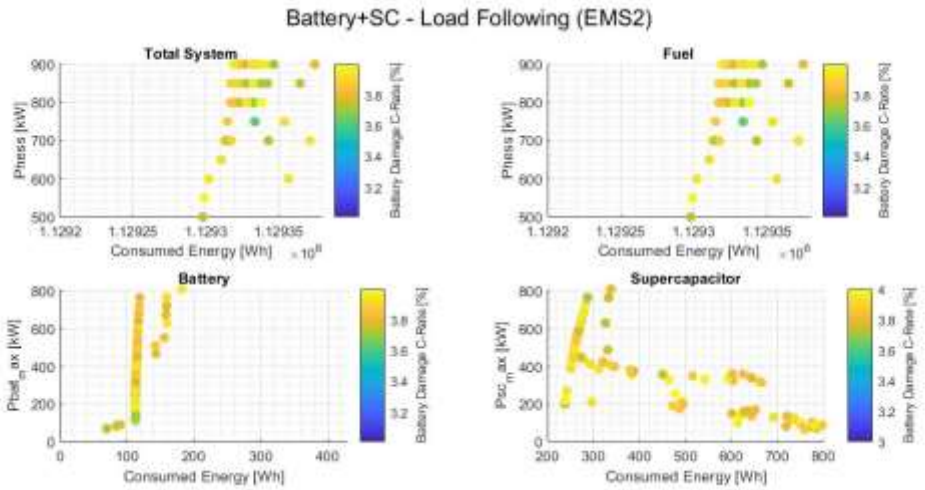

Figure 66 HESS EMS 2 - Energy Consumption Breakdown

Finally, with respect to excess energy (Fig. 67.), differences in compare to load levelling can be found in:

a) Excess energy percentage being a bit higher than in load levelling but still acceptable
b) Loss of load probability curve being steeper resulting in smaller HESS installations.
c) Effect of power split ratio on excess energy is very small, allowing the designer to optimize power split ratio for another metric.

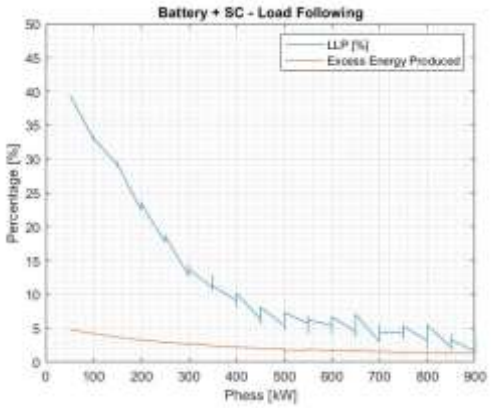

Figure 67 HESS Load Following - Excess Energy vs Simulation Runs

8.2.1 Selected Solutions

For Load Following, the best solutions were identified for a given power rating value of 800kW and for C-rate values of 3 and 4 respectively (Table 16).

EMS2- Load Following - Battery Only											
Phess [kW]	Ehess [kWh]	c-rate	Spec. Power [kW/kg]	Spec. Energy [kWh/kg]	psr	csr	Total Cost [k$]	Total Weight [kg]	Battery Damage [%]	Consumed Energy [kWh]	LLP (%)
800.0	266.7	3	0.27	0.09	100%	100%	235.73	2937.8	4.0	1129.36	2.9
800.0	200.0	4	0.36	0.09	100%	100%	182.4	2243.3	4.3	1129.36	2.9
EMS2- Load Following - Battery and Supercapacitor (HESS)											
Phess [kW]	Ehess [kWh]	c-rate	Spec. Power [kW/kg]	Spec. Energy [kWh/kg]	psr	csr	Total Cost [k$]	Total Weight [kg]	Battery Damage [%]	Consumed Energy [kWh]	LLP (%)
800.0	161.7	3	0.37	0.07	60%	99%	181.6	2171.4	3.9	1129.72	2.6
800.0	148.4	3	0.39	0.07	55%	99%	172.1	2040.6	3.8	1129.66	3.2
800.0	121.7	3	0.45	0.07	45%	99%	153.0	1778.8	3.9	1129.34	2.4
800.0	108.4	3	0.49	0.07	40%	98%	143.4	1647.9	3.8	1129.32	1.9
800.0	95.0	3	0.53	0.06	35%	98%	133.9	1517.0	3.8	1129.32	2.7
800.0	81.7	3	0.58	0.06	30%	98%	124.3	1386.1	3.8	1129.32	4.0
800.0	68.4	3	0.64	0.05	25%	98%	114.8	1255.2	3.6	1129.33	4.1
800.0	51.7	4	0.74	0.05	25%	97%	101.5	1081.6	4.0	1129.33	4.1
800.0	32.5	4	0.78	0.03	15%	92%	98.8	1029.7	4.0	1129.34	3.7

Table 16 Selected Best Solutions forEMS1 - Battery Only and HESS

First of all, it is observed that the power split ratio range of solutions is extended to $25\% < psr < 60\%$. The smaller overall power rating in combination with the higher supercapacitor proportions, lead into very compact and cost effective hybridized installations. Specifically, for C-rate of 3C, savings range between 23% and 51.3% while weight can be reduced 26%-57.3%. For the same combinations, battery degradation is slowed down from 4% to 3.6% EoL for the same period of time (10% relative reduction). Similar trends exist for C-rate of 4C, although battery damage percentage is still exceeding 4%. Finally, another turning point is observed for the consumed energy. For $psr > 45\%$ higher consumption is observed in compare to the load following battery-only case.

8.3 Sensitivity Analysis

Lastly, and to narrow down any uncertainties related to input or disturbance assumptions, a sensitivity analysis is conducted and presented for load levelling.

8.3.1 Minimum Discharge Pulse Duration

First minimum required duration of supercapacitor discharge pulse is examined. Specifically, two additional runs have been conducted for both a smaller $dt_{req} = 4\ sec$ and a larger value $dt_{req} = 12\ sec$. By increasing dt_{req} for a fixed maximum power rating, a higher system capacitance is required and therefore more stacks need to be added in parallel. Higher capacitance will result in larger energy capacity which in turns results in heavier installations of higher initial capital expenditure.

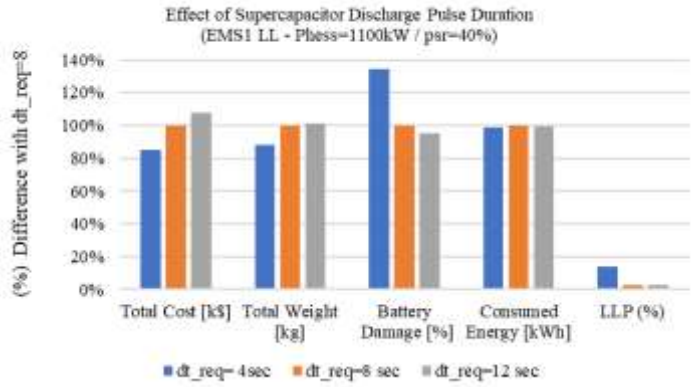

Figure 68 Sensitivity Analysis Minimum Discharge Pulse Duration of Supercapacitor

From the sensitivity analysis performed for dt_{req} it is derived that it is positively correlated to system's performance while negatively correlated to system's size, weight and CAPEX. By reducing the duration of dt_{req} LLP deteriorates and less combinations are meeting the set constraints. For dt_{req} is 4 sec we see that LLP deteriorates in compare to the 8 sec. Same with battery aging as the supercapacitor is able to handle peak loads for less time.

It is also observed that the rate of improvement of the system is starting to converge between 8 and 12 seconds and any supercapacitors above these thresholds result in disproportionally heavy and expensive systems. It is therefore deduced that the assumed discharge pulse duration of 8 sec is a reasonable design choice.

8.3.2 Decisive Threshold

Next, the HESS decisive threshold is tested for values of 5%, 10% and 20% of installed engine capacity (Fig. 69). Again, these cases are not applicable to battery-only cases and thus they are only simulated for the HESS.

The logical threshold has been introduced to enable split between the battery and the supercapacitor. This threshold is expressed as a percentage of engine's installed power is used to distinguish the rate of change of the difference between required load and engine point into rapid and slower fluctuations. The threshold value is connected to the priority decision. High values will require larger fluctuations for the supercapacitor to be employed. A low value can compromise the reliability of the system as it will limit too much the operation of the battery. On the other hand, a too high value would cause battery to be utilized too much with an adverse effect on its lifetime.

As this is an assistive measure to the energy management system it does not affect the HESS weight and cost. The most significant conclusion derived from Fig. 69, is that the loss of load

probability highly depends on the value of this threshold. It is seen that for Threshold values of 5% and 10%, the LLP is taking non-acceptable values of 16% and 13% respectively. The relation between these two figures is found to be non-linear as it starts to converge near 3% (acceptable LLP) for decisive thresholds larger or equal to 15%. Given, the large LLP values (application goal is not meet) for the first two values, no further comments can be made about the battery damage and the consumed energy.

It is therefore deduced that further increase in the decisive threshold value would have limited effect on the system's performance.

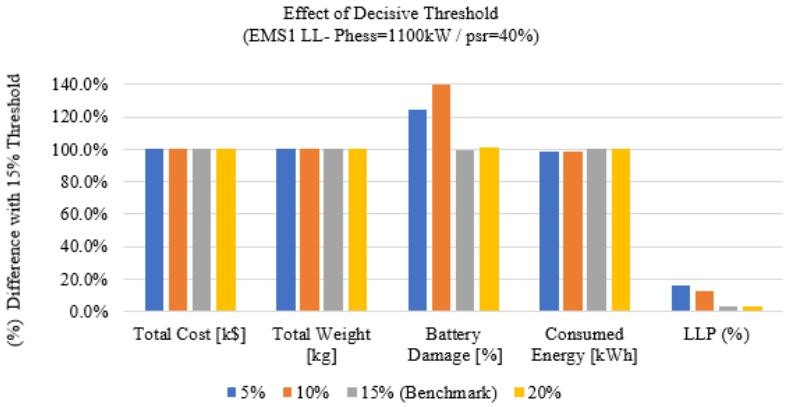

Figure 69 Sensitivity Analysis Decisive Threshold for Power Allocation

8.3.3 Load Levelling – Engine Set Point

Another parameter whose effect is further examined is the engine load point percentage for the load levelling runs. The engine load point is tested for values of 55% and 65% in addition to the base case of 60%.

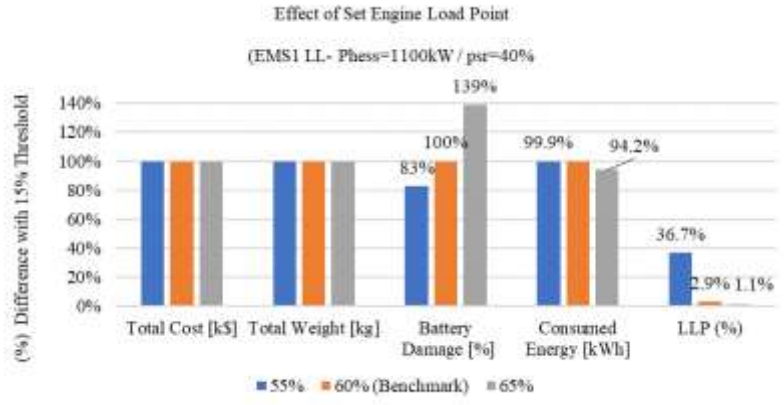

Figure 70 Sensitivity Analysis Engine Set Load Point (Load Levelling)

Again, this is a tuning parameter of the energy management system and therefore overall weight and cost are not affected. With regards to energy consumption, it is observed that the overall value for the HESS configuration can be reduced by an additional 5.8% by setting the load point value at 65%. This is translated to an additional consumption of only 0.8% with respect to the engine-only benchmark. With further tuning of the energy management system parameters, further optimization of the energy consumption might be possible. On the other hand, it is clearly demonstrated that by increasing the engine set load point and moving away of the load profile average value, the battery is experiencing higher c-rates (and higher utilization) resulting in the battery degradation being accelerated by 40%.

8.3.4 Battery Cost

Finally, the single effect of battery cost is also investigated. Having in mind that further improvements in batteries cost are likely, the effect of 50% and 75% reduction in battery price (from \$800/kWh to \$400/kWh and to \$200/kWh respectively) is examined. It should be reminded that aforementioned battery price represents system level cost.

Figure 71 depicts cost as a function of power split ratio for the three different scenarios. Colour scale represents battery cost as a percentage of total system cost and is not to be confused with the battery damage shown in previous graphs.

In the baseline \$800/kWh scenario, the battery represents the critical component with respect to cost for psr combinations exceeding 25%. This number is increasing to approx. 35% for a battery cost of \$400/kWh and to psr of more than 50% for battery price of \$200/kWh.

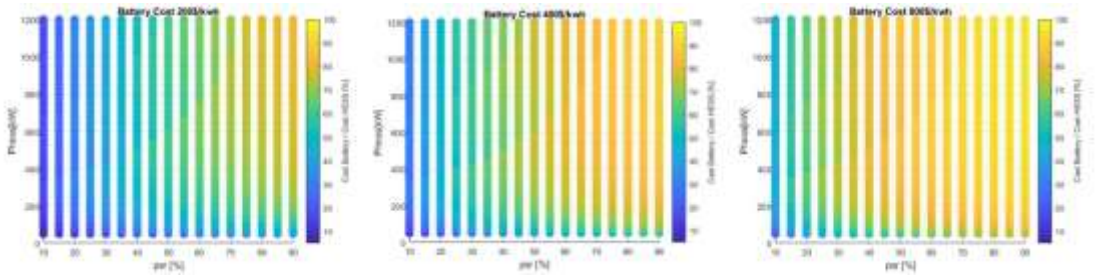

Figure 71 Battery Cost Sensitivity Analysis (\$200, \$400 and \$800)

The absolute cost values are shown in Fig. 72. It is observed that with dropping battery prices, the relative capital cost saving potential is decreasing although still significant. This does not imply that hybridized systems are becoming more expensive than battery-only. It indicates that less cost savings can be achieved. This is because battery oversizing becomes cheaper.

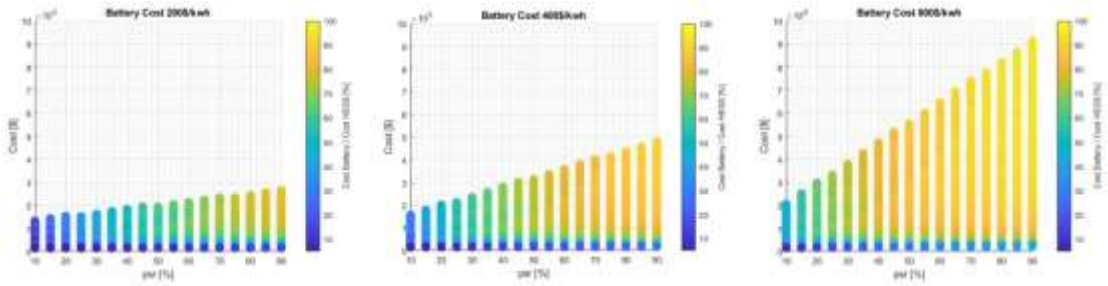

Figure 72 Absolute Cost vs Power split ratio (\$200, \$400 and \$800)

9 Conclusions & Recommendations

This work proposes a battery-supercapacitor hybrid energy storage system as a practical approach to overcome challenges related to battery aging and battery oversizing in shipboard applications of high power with significant fluctuations. This is attempted by a parametric approach of combined sizing and energy management. The potential and limitations of this work are summarized in this Chapter, as well as the author's general recommendations for future, further research on the topic.

9.1.1 Conclusions

Returning to the main research questions of this thesis, the following conclusions can be drawn:

Can hybridization of the energy storage system result in battery oversizing be avoided for shipboard high-power applications with significant fluctuations without compromising battery lifetime?

In this thesis, it has been demonstrated that by hybridizing a typical battery energy storage system with a supercapacitor device, it is feasible to:

- Avoid oversizing and achieve lighter installations in terms of total installation weight. Due to the improvements in the overall specific power, weight reductions of 33-43% for C-rate of 3 and 29-34% for a C-rate of 4 were reported.
- Control battery cycling aging and extend battery lifetime. According to the simulations presented in this thesis, for the same period of time and for the same load profile, the battery degradation rate was reduced between 5.7%-17.4% in compare to the battery only configuration. For Load Following, an improvement rate of 10% was demonstrated.
- While maintaining same level of performance reliability for the power system. Specifically, for a very fluctuating profile a power availability of 95+% was achieved without operating the engine in emergency mode.
- Expand analysis to include reduction in capital cost of the system. The smaller overall power rating in combination with the higher supercapacitor proportions, can lead into cost effective hybridized installations. Cost savings of 30% and 23% have been demonstrated for load levelling and load following respectively. Another benefit of hybridization is that design space is expanded to include many 'intermediate' cost-options that are not available for battery only configurations.

What are the key design aspects of a Battery-Supercapacitor Hybrid Energy Storage System for a typical shipboard application?

By reviewing the performance characteristics of each energy storage device, controllability was identified as a key functional requirement of the hybridized energy storage system. The degree of controllability depends on the selected topology of the hybrid energy storage system as this will define the system capabilities and restrictions with an application in mind. In the proposed design, high degree of controllability was achieved by selecting a full-active topology, where bidirectional DC-DC converters are directly connected to the energy storage devices through independent power lines. Following, this configuration was integrated to a generic diesel-electric DC propulsion layout.

Another key-design aspect of battery-supercapacitor energy storage system is the sizing and dimensioning of the energy storage devices. As mentioned in Chapters 3 and 5, dimensioning of a hybrid energy storage system is a more complex process than battery alone systems. This is because next to total system's outputs, proportions between each storage device need also to be considered. Power and capacity split ratios between the two sources need to be introduced as additional problem parameters.

Finally, the third key design aspect of a battery supercapacitor storage is related to its energy management system. This ensures proper energy flow from and to the DC-bus. The energy management strategy should determine the power split between the diesel generator, the battery and the supercapacitor while satisfying the load requirements with respect to dynamic constraints of the power system.

What are the trade-offs between design variables and desired outputs?

Summarizing, it has been demonstrated that there are hybridized combinations for which all key performance metrics are improved in compare to the battery-only case. Indicatively in load levelling and for $psr = 45\%$ substantial improvements have been observed in terms of cost (-37.6%), weight (-42%) and rate of battery aging (-11.4%). Lesser advances have been achieved with respect to system's energy consumption (-0.05%) and loss of load probability (-5%).

In addition, considerable trade-offs between desired performance metrics are noted when optimizing for a single metric. By selecting a solution of $psr = 40\%$, battery aging can be optimized meaning that it can further be slowed down by another 5.7%. For the same combination, weight and capital cost can be further reduced by 6.4% and 8.6% respectively. On the other hand, optimizing for battery lifetime will cause higher energy consumption in compare to the baseline case.

Another trade-off has been observed with respect to weight/cost optimization and battery degradation. The global minimum for these two parameters is achieved for a C-rate of 4. At the same time, improvements on aging and energy consumption start to compromise.

How do we size a Hybrid Energy Storage System? What is the ideal power and capacity split balance between the battery and the supercapacitor?

For the purposes of this thesis, a methodology was developed and proposed for the construction of a valid design space. The two energy storage devices were treated initially as an integrated homogeneous system to determine the overall power to meet application requirements. For each device, this was used as an input together with a secondary constraint to obtain maximum capacity. Following, for each feasible sizing combination the two devices where dimensioned based on their characteristics, for a series of power split ratios. A series of static parameters such as energy capacity, power and capacity split ratios, number of supercapacitor and battery cells were estimated and exported in the form of design exploration maps and arrays. The developed sizing methodology is considered successful as size convergence patterns can be detected and avoided. The detailed methodology was outlined in Chapter 5.

Ideal power and capacity split balance depend on selected optimization metric and the energy management approach followed but generally lie outside corner values. Combinations that were satisfying all desired criteria were found for a power split ratio ranging between 25% and 55%. It was derived that the split of power rating between battery and supercapacitor components of the HESS, is relatively balanced with a slight bias in favour of the supercapacitor. Practically, this means that neither battery nor supercapacitor devices should be sized to stand-alone serve most of overall power rating. Another conclusion that can be derived is that the effect of supercapacitor's larger power electronics in overall system's weight is limited. This is because the high specific power of the supercapacitor outweighs the necessity for heavier converters resulting in a net reduction in system's weight for $psr > 40\%$.

Moreover, it has been demonstrated that all preferred solutions (after filtering) are given for csr values between 97.5% and 99.5%. For lower csr, the battery damage is smaller. As the supercapacitor energy capacity increases, the battery can be utilized less and thus extend its lifetime. This means, that battery needs to be dimensioned close to the hybrid system's overall

energy capacity while the supercapacitor should only account for a small fraction of it. In other words, batteries are necessary to provide the bulk amount of energy and to ensure operating range.

How do these systems have to be managed to get the best of them?

- *What are the operation aspects of a Hybrid Energy Storage System?*
- *How do we decide when and for how long to utilize each source (i.e. battery and supercapacitor) ?*

Due to its simplicity and practicality, a rule-based energy management strategy was developed to realize real-time control of the power system. In this approach, the decision on power split between the engine, the battery and the supercapacitor, was pre-defined in a set of logical rules that describe the operational conditions under which a power allocation mode is employed. The power allocation is decided in two stages. In the first stage, the required load ,subjected to constraints, is split between the diesel generator and the hybrid energy storage system as a whole. In the second stage, decision is being made for the power allocation between the HESS components i.e. the battery and the supercapacitor. The three decision variables were namely identified as the State of Charge of the Supercapacitor, the State of Charge of the Battery, and the rate of change of the difference between required load and –preferred set point- engine load

Based on the obtained simulation results, the proposed rule-based energy management system was shown to control the HESS to follow required power well for both Load Levelling and Load following approaches. While the proposed rule-based EMS, overachieved the targets for less battery degradation and high system availability, more research is required to ensure consistent benefits in the overall energy performance.

What is the impact of hybridization on system's overall efficiency and performance?

Energy consumption represents the most significant challenge with both battery-only and battery-supercapacitor configurations performing about 2-7% worse than the diesel engine stand-alone operation for emergency curve. With further tuning of the energy management system parameters, it was shown that additional consumption of only 0.8% is possible. It should be reminded that the selected Wartsila 31 DG is already very efficient with a minimum specific fuel consumption of 171.4 g/kWh. Therefore, if the engine is allowed to operate in emergency load mode (at the expense of engine stress) a satisfactory consumption can already be achieved.

The additional losses can be explained by the fact that the introduced conversion losses are exceeding any savings from operation in higher SFC. Under certain operating conditions (e.g. heavy seas) additional fuel consumption might be accepted given that vessel responsiveness and reliability are number one priority.

For the proposed battery-supercapacitor energy storage system, the acceptable energy consumption varies depending the performance metric we wish to optimize for. With respect to battery only case, marginal differentiations between -0.5% and +0.25% of the battery-only energy consumption are observed. Positive variations can be explained by the developed energy management strategy that is preferentially operating battery and supercapacitor near their maximum power output (high efficiency region) and by the higher absorption of engine excess power by HESS.

9.1.2 Recommendations for further Work

The present thesis proposed a combination of battery and supercapacitor as a practical approach to overcome challenges related to size, cost, reliability and degradation of shipboard battery systems. Having established that the preliminary results of the present thesis are promising several recommendations for future work can be given:

- The first set of recommendations is related to actions that can further improve the accuracy of the simulation results.
    - Experimental data and real-life measurements have been used where possible (i.e. load profile, battery aging curves, efficiency models, engine shop trial curves). Nevertheless, no model is ever 100% accurate, therefore experimental validation of the simulation results is required to ensure that the model is sufficiently accurate for the purpose at hand. Keys issues are the requirements for removing initialization bias and replications[87].
    - Expand models of the batteries/supercapacitor to reproduce the voltage response more accurately and to capture phenomena such as self-discharge.
    - Expand models of DC/DC converters to estimate nonlinear switching dynamics of the MOSFET and calculate more accurately the dissipative power losses.
    - Expand battery aging model to capture calendar aging and effect of temperature aging on cycling aging. Temperature effect has been excluded from modelling to keep computational time and model complexity reasonable. By further developing the proposed model it is possible reduce uncertainty related to battery damage. It is expected though that a model that is also including the temperature phenomena will be more favourable for the proposed approach as high rate operations contribute to an increase in heat generated internal to the cell. The heat is generated because of joule heating which is proportional to the square of the current passing through the cell. This means that even a high-power lithium-ion battery with small internal resistance can generate a significant amount of heat when large quantities of charge flow through them[19].
    - Integrate a dynamic diesel generator component model to the developed hybrid energy storage system to increase prediction accuracy of the engine's operational limits under heavy conditions such as those discussed in the examined load profile.

- The second set of recommendations is related to the expansion of the scope of work to include more functions.
    - The energy analysis could be expanded to include available work (exergy) analysis. This way the type of energy (e.g. electrical in supercapacitor, chemical in MDO) can be considered in the evaluation of the results together with the quantity that is now only considered.
    - Another recommendation is related to the ability of the model to simulate power plant's emissions and specially NOx, PM and CO2. Ideally, this should be further investigated together with the dynamic model of the engine. It would be of interest to see if the reduced stress of the diesel generator as resulted by the high quick dynamic response of the proposed battery-supercapacitor hybrid energy storage system could lead into emission reduction.
    - Another recommendation for future work is to expand the system architecture of HESS to include multiple diesel generators as shown in Fig. 19. By adding additional generators, a more realistic propulsion configuration can be

examined. In terms of simulation, the challenge is to add another level of power allocation decision in the developed energy management system.

- Finally, the third set of recommendations is concerned applications and case studies that the undersigned considers of interest.
    - It has been shown that hybridization is meaningful in high power applications of high fluctuations on the demand side (e.g. manoeuvering) and/or applications where the prime mover has slower dynamic response than typical marine diesel engines (e.g. dual fuel engines, fuel cells). In the instances, a battery-alone system experiences high C-rates that deteriorates its lifetime. By over-sizing the system, it is only possible to partially control this degradation. It would be extremely insightful if a detailed case study could be conducted for one of these cases.
    - It is the author's personal opinion that the marginal improvements in overall energy consumption in compare to battery-only systems do not justify the development of the proposed system, if energy savings is the primary objective. This aside, there is still plenty of improvement room with regards to energy consumption as the proposed system is not optimized for this metric. A more elaborate energy management strategy as proposed by Kalikatzarakis [88] could be of interest.
    - More research should be conducted to evaluate the energy consumption for further operating load profiles and for different engine types.

10 Appendix

10.1 Battery Applications

10.1.1 Early battery applications

Ships incorporating electric energy storage systems, is often thought of as recent innovation, but as with many technological developments, it has a much longer history than might be expected. As early as 1831, an experiment was made to propel a paddle boat with battery power (primary) in St. Petersburg but with no successful outcome [89]. The first ever vessel to be powered by batteries successfully was built by Siemens back in 1886. ''Elektra'' was an 11m long passenger boat, that was propelled by a 4.5kW electric motor driven by accumulators that were regularly recharged from land based sources [90].

Figure 73: Elektra (1886) was the first battery powered vessel [Ref: siemens.com].

The development of reversible diesel engines and reversing gearboxes in the early 20th century, resulted in the demise of battery electric propulsion on ships. The main motivation up until then for electric propulsion had been reversibility. In addition, practical problems related to the high space and weight requirements of the accumulators, in combination with the limited operating range prevented extensive shipboard installations. However, batteries found other uses in ships and boats of all sizes. These included ships lighting, simple applications on ignition circuits for Internal Combustion Engines (ICEs), and propulsion of submarines.

10.1.2 Vessel Type Breakdown

Almost 1 out of 2 existing marine battery systems has been installed to power passenger ships. This can partially be explained by the favourable operational profile of these vessels for ES applications. In principle, they operate in coastal areas, and thus these vessels spend relatively little time in sailing between consecutive ports. In addition, passenger ships can be classified as medium powered vessels meaning that the total energy requirements per voyage are relatively low compared to other vessel types. Indicatively, passenger ferries of 2000+GT have an average installed power of 6,600kW, while Ro-Pax ferries of the same size category have an average installed power of 15,500kW[1].

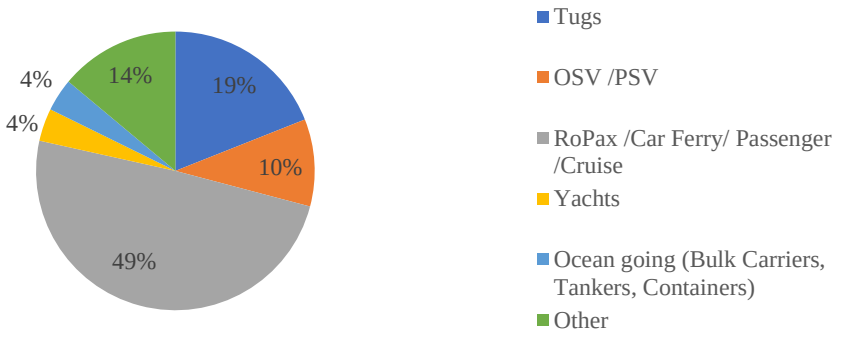

Figure 74 Ship Battery Installations per ship type

Ro-Ro/Ro-Pax ferries have an average of 156 calls at the same port per year and an average port stay of 6 hours. Comparatively, Container ships have an equivalent of 52 calls and 9 hours while Tankers 20 and 24 [91] . Frequent port visits are of utmost importance for ES technology implementation as they can facilitate charging schedules and justify the high cost of infrastructure upgrades in ports. Similarly, short port stays are favourable for zero-emission operation mode at ports as less energy is required per vessel.

According to the technology company of ABB,[91] vessels that combine frequent port visits and short stays such as Ro-Ro and passenger, tend to be more efficient in terms of cost of infrastructure per avoided ton of emission (g SOx or gCO2/$).

The second most common vessel type for ES applications, is a tugboat with 19% of total marine battery installations. One reason is related to their close to port operation. Secondly, the main engine of tugboats is designed for high-power propulsion during towing, but most of their operation time is spent in transit mode with low loads. Typical operational profile of tugboats can be seen in Fig.8.

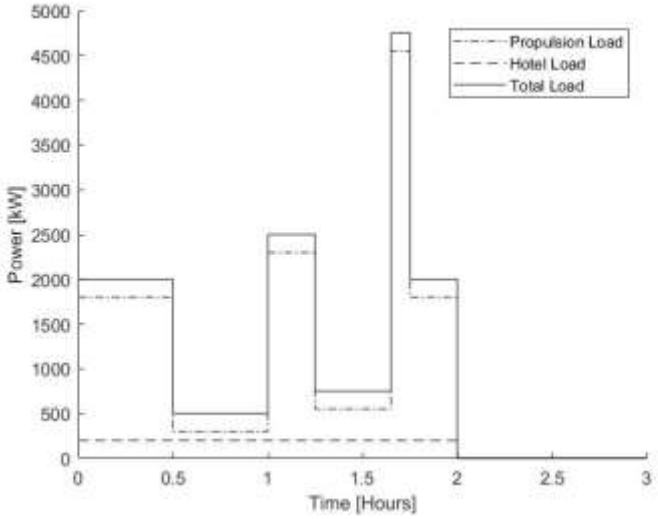

Figure 75 General operating data of harbour tugboats [92]

Finally, OSVs are the 3rd most popular option for marine battery installations. The first new-built offshore supply vessel with a battery system installed was the Østensjø-owned Edda Ferd that was put into operation in the autumn of 2013. Since then, at least 7 more OSVs that are powered by batteries have been deployed. The primary function of ES on-board OSVs is to ensure redundancy in special operational modes such as DP.

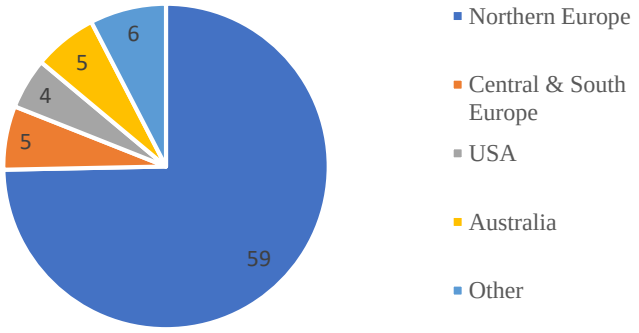

Figure 76 Geographical distribution of marine ESS.

By analysing the database of marine ES systems, a geographical concentration in Northern European countries. This can be explained by EU's strategy for more sustainable waterborne transportation; and other governmental initiatives, have encouraged the development of hybrid or full-electric ships in Northern Europe. In a total of 79 electric or hybrid ships, 59 are currently operating in the broader area of Northern Europe while 42 of these are concentrated in Norway [93-96].

10.1.3 Milestone Applications

At this paragraph, some of the most characteristic marine applications in in terms of technical characteristics and design philosophy are discussed.

‘’Viking Lady’’ is the world’s first (2009) hybrid OSV developed by Wärtsilä, DNV GL and Eidesvik Shipping. The Viking Lady is the first merchant ship to use fuel cells. The hybrid power system, consists of four LNG-powered Wärtsilä32DF dual-fuel engines, 5 driven generator sets of which each has a capacity of 1950 kW, an energy storage system in the form of a 442 kWh battery package and a 330 kW high temperature LNG fuel cell energy source specially adapted for marine use.

According to measurements, by introducing a hybrid energy system on-board Viking Lady, the fuel consumption was reduced by 15%. Finally, class rules for Battery Power and updated rules to cover Hybrid Energy System were developed by DNV GL specially for this project [97].

Figure 77 Viking Lady is the world's first hybrid OSV and also the world’s first merchant vessel using FCs.

Ampere is the world’s first (2015) large all-electric (100% battery) driven aluminium catamaran ferry in Norway. The double-ended ferry serves a 5.6 km single route 34 times daily at an average speed of 10 knots, with a crossing time of 20 minutes. In average, this crossing requires 150 kWh energy. Pausing time at quay is 10 minutes, which is used to charge the on-board, 1-MWh lithium-polymer battery pack (two modules mounted on each end of the ferry). Once the ferry has left, the shore-side battery slowly recoups energy from the local medium voltage grid (powered by hydroelectric plant) at a rate permitted by the grid infrastructure based on other demands, which reduce the need for expensive upgrades to electrical grid infrastructure at the ports [9].

MF Folgefonn is the first ferry in the world (2017) with inductive (wireless) charging, rather than conductive (a physical cable). The ship was originally built as diesel powered ferry but has been retrofitted into a hybrid diesel electric vessel. The inductive power system has been developed by Wartsila and Cavotec, can transfer 1MW of power within a range of 15-50cm, enabling the ship to start charging its batteries immediately after it arrives in port [98].

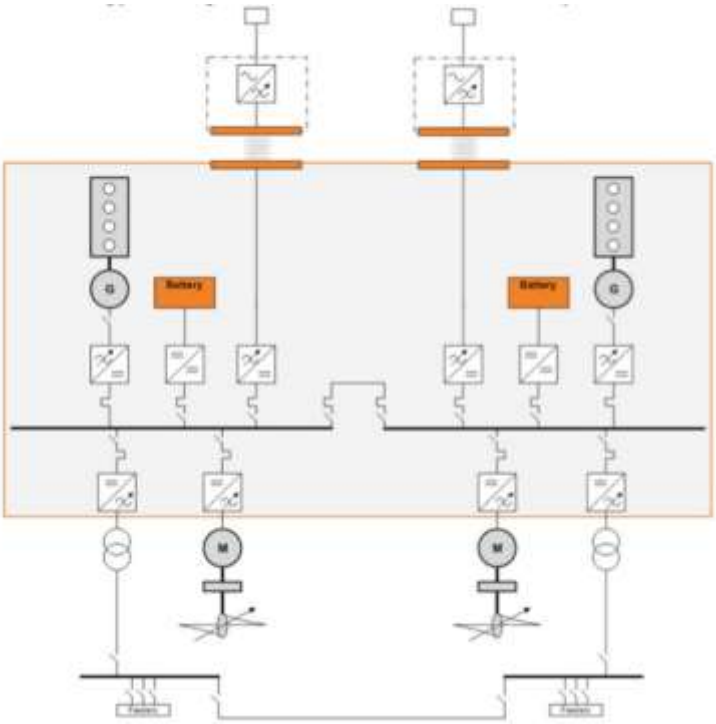

Figure 78 Typical plug-in hybrid solution with induction charging [Property: Wartsila]

MS Roald Amundsen is the world's first hybrid cruise ship. Operated by the Norwegian explorer cruise line Hurtigruten, it was built by Kleven shipyard and it was commissioned in 2019. The MS Roald Amundsen is powered by a hybrid solution including four Bergen B33:45 engines and 1.2 MWh of Corvus supplied batteries. The engines are also equipped with a selective catalytic reduction (SCR) system to meet the IMO Tier III nitrogen-oxide (NOx) emission limits [99]. As the ship operates in polar regions, there is a foresight for future expansion of the battery system up to 6 MWh to enable zero emission operation in these sensitive waters.

Figure 79 MS Roald Amundsen [Property: G Karras

10.1.4 Shipboard Battery Applications

	Owner	Name	Type	Type of Installation	Completion Date	Battery Type	Installed Capacity [MWh]	Shipyard	Country/ Route
1	Foss	Carolyn Dorothy	Tug	Hybrid DE with Battery	2009	Lead Acid	N/A		USA
2	Alster-Touristik GmbH	FCS Alsterwasser	Canal Boat	Hydrogen FC / Battery Back Up	2009	Lead-Gel	0.20		Germany
3	PlanetSolar SA	MS Tûranor PlanetSolar	Solar Boat	Renewables Integration	2010	Li-Ion	1.30	Knierim Yachtbau	Switzerland
4	University of Victoria	Tsekola II	Research Vessel	Hybrid	2011	Li-Ion	0.23		Canada
5	Kotug	RT Adriaan	Tug	Hybrid	2012	N/A	0.08		Netherlands
6	Island Offshore LNG KS	Island Crusader	PSV	Hybrid	2012	N/A	N/A		Norway
7	Foss	Campbell Foss	Tug	Hybrid	2012	Li-Ion	0.1		USA
8	Mitsui O.S.K Lines LTD	Emerald Ace	Car Carrier	Hybrid	2012	Li-Ion	2.2		Japan
9	Norled AS	M/F Finnoy	Car Ferry	Hybrid	2013	Li-Ion NMC	0.3		Norway
10	Nippon Kaiyosha Ltd	Tsubasa	Tug	Hybrid	2013	Li-Ion (LFP)	0.3	Universal SB Keihin	Japan
11	Caledonian MacBrayne	MV Hallaig	Ro-pax	Hybrid	2013	Li-Ion	0.8		UK
12	Caledonian MacBrayne	MV Lochinvar	Ro-pax	Hybrid	2013	N/A	0.8		UK
13	Lorient Agglomeration	Ar Vag Trendan	Ferry	Full Battery	2013	Superacapacitors	0.0	STX France Lorient	France
14	Kotug	RT Emotion	Tug	Hybrid	2014	Li-Ion NMC	0.1		Netherlands
15	Bhagwan Marine	Bhagwan Dryden	Diving Support	Hybrid	2014	N/A	0.1	Keppel Singmarine	Australia
16	Ballerina AB	Sjovagen	Passenger (Inland)	Full Electric	2014	N/A	0.5	Faaborg Vaerft	Sweden
17	Kotug	RT Evolution	Tug	Hybrid	2014	Li-Ion NMC	0.1		Netherlands

	Owner	Name	Type	Type of Installation	Completion Date	Battery Type	Installed Capacity [MWh]	Shipyard	Country/ Route
18	Sleepdienst B. Iskes & ZN B.V	Damen ASD Tug 2810 Hybrid	Tug	Hybrid	2014	N/A	0.2		Netherlands
19	Johannes Østensjø Dy AS	Edda Ferd	PSV	Hybrid	2014	Li-Ion	0.3		Norway
20	Eidesvik Shipping AS	OSV Viking Lady	PSV	Hybrid	2014	Li-Ion ; FCs	0.4		Norway
21	Scandlines	M/V Deutschland	Ro-pax	Hybrid	2014	Li-Ion NMC	1.6		Germany-Denmark
22	Scandlines	Schleswig-Holstein	Ro-pax	Hybrid	2014	Li-Ion NMC	1.6		Germany-Denmark
23	Scandlines	M/V Prins Richard	Ro-pax	Hybrid	2014	Li-Ion NMC	2.6		Germany-Denmark
24	Fafnir Offshore	N/A	PSV	Hybrid	2015	N/A	0.5	Havyard Ship Technology	Norway
25	Ora AS	El-max (Karoline)	Fishing Vessel	Full Electric (DE as a back-up)	2015	Li-Ion NMC	0.2	Selfa Arctic	Norway
26	Norwalk Maritime Aquarium	Spirit of the Sound	Research Vessel	Hybrid	2015	N/A	0.1		USA
27	Svitzer	Euro	Tug	Hybrid DE with Battery	2015	N/A	0.5	ASL Shipyard	Australia
28	Svitzer	Perentie	Tug	Hybrid DE with Battery	2015	N/A	0.5	ASL Shipyard	Australia
29	Svitzer	Boodie	Tug	Hybrid DE with Battery	2015	N/A	0.5	ASL Shipyard	Australia
30	Svitzer	Dugong	Tug	Hybrid DE with Battery	2015	N/A	0.5	ASL Shipyard	Australia
31	Johannes Østensjø Dy AS	Edda Freya	PSV	Hybrid DE with Battery	2015	Li-Ion polymer	0.5		Norway
32	Eidesvik Shipping AS	Viking Queen	PSV	Hybrid DE with Battery	2015	N/A	0.7		Norway

	Owner	Name	Type	Type of Installation	Completion Date	Battery Type	Installed Capacity [MWh]	Shipyard	Country/ Route
33	Caledonian MacBrayne	MV Catriona	Ro-pax	Hybrid DE with Battery	2015	Li-Ion	0.8		UK
34	N/A	M/Y Savannah	Megayacht	Hybrid DE with Battery	2015	N/A	1.0		Netherlands
35	Norled AS	Ampere	Ro-pax	Full Electric	2015	Li-Ion	1.0	Fjellstrad Shipyard	Norway
36	Norled AS	MF FOLGEFONN	Car Ferry	Hybrid	2015	N/A	1.4		Norway
37	TESO N.V.	Texelstroom	Ro-pax	Hybrid; Renewables Integration	2015	N/A	1.6		Netherlands
38	Fjord1 AS	Fannefjord	Ro-pax	Hybrid	2016	N/A	0.4		Norway
39	Royal Netherlands Navy	HNLMS Noordzee	Tug	Hybrid DE with Battery	2016	N/A	0.2	Damen Galati	Netherlands
40	Royal Netherlands Navy	HNLMS Waddenzee	Tug	Hybrid DE with Battery	2016	N/A	0.2	Damen Galati	Netherlands
41	Royal Netherlands Navy	HNLMS Zuiderzee	Tug	Hybrid DE with Battery	2016	N/A	0.2	Damen Galati	Netherlands
42	Kystverket	OV Bokfjord	Anti-Pollution Vessel	Hybrid	2016	N/A	0.9	Hvide Sande Shipyard	Norway
43	Maritime Mng AS	Vision of the Fjords	Ferry	Hybrid	2016	N/A	0.6	Brødrene Aa	Norway
44	Seaspan Ferries Corporation	Seaspan Swift	Ro-pax	Hybrid	2016	Li-Ion NMC	0.5	Sedef Gemi (Tuzla)	Canada
45	Scandlines	M/V Berlin	Ro-pax	Hybrid	2016	Li-Ion NMC	1.5		Germany-Denmark
46	Scandlines	M/V Copenhagen	Ro-pax	Hybrid	2016	Li-Ion NMC	1.5		Germany-Denmark
47	Nave VA	Chjara Stella	Excursion Boat	Hybrid	2016		0.1		France

	Owner	Name	Type	Type of Installation	Completion Date	Battery Type	Installed Capacity [MWh]	Shipyard	Country/ Route
48	N/A	San Lorenzo	Superyacht	Hybrid	2016	N/A	0.1	San Lorenzo Yachts	Italy
49	Scandlines	M/S Tycho Brahe	Car Ferry	Full Electric	2017	N/A	4.2	Öresund Dry Docks	Germany-Denmark
50	Rederiet Stenersen AS	N/A	Chemical Tanker	Hybrid	2017	Li-Ion polymer NMC	N/A		Norway
51	Rederiet Stenersen AS	N/A	Chemical Tanker	Hybrid	2017	Lithium-Ion	N/A		Norway
52	Scandlines	MF Aurora	Car Ferry	Full Electric	2017	N/A	4.2	Öresund Dry Docks	Germany-Denmark
53	N/A	E-ferry electric ferryboat	Ro-pax	Full Electric	2017	Li-Ion	4.2	Soby Vaerft A/S	Denmark
54	FinFerries	Elektra	Car Ferry	Full Electric (DE as a back-up)	2017	N/A	1.1	CRIST	Finland
55	Torghatten Trafikkeslskap	N/A	Car Ferry	Hybrid DE with Battery	2017	N/A	0.5	Fiskerstrand Verft	Norway
56	Torghatten Trafikkeslskap	MF Melshorn	Car Ferry	Hybrid DE with Battery	2017	N/A	0.5	Havyard Ship Technology	Norway
57	Torghatten Trafikkeslskap	MF Vard Horn	Car Ferry	Hybrid DE with Battery	2017	N/A	0.5	Havyard Ship Technology	Norway
58	Fori Municipality	Föri ferry	Ferry	Full Electric	2017	N/A	N/A		Finland
59	Salmar Farming	Elfrida	Aquaculture Support Vessel	Full Electric	2017	N/A	0.2	Ornli Slipp	Norway
60		Ferry Happiness	Ferry	Hybrid DE with Battery	2017	Lithium Iron Phosphate	0.1		Taiwan
61	Seaspan Ferries Corporation	Seaspan Reliant	Ro-pax	Hybrid	2017	Li-Ion polymer NMC	0.5	Sedef Gemi (Tuzla)	Canada

	Owner	Name	Type	Type of Installation	Completion Date	Battery Type	Installed Capacity [MWh]	Shipyard	Country/ Route
62	Eidesvik Shipping AS	Viking Princess	PSV	Spinning Reserve	2017	Li-Ion	0.5		Norway
63	Farstad Shipping	Far Sun	PSV	Spinning Reserve	2017	Li-Ion polymer NMC			Norway
64	Hav Line AS	N/A	Fishing Vessel	Hybrid DE with Battery	2018	N/A	N/A	Balenciaga	Norway
65	Fjord1 AS	TB1	Car Ferry	Full Electric	2018	Lithium-Ion	1	Tersan Shipyard	Norway
66	Fjord1 AS	TB2	Car Ferry	Full Electric	2018	Lithium-Ion	1	Tersan Shipyard	Norway
67	Fjord1 AS	N/A	Ferry	Full Electric	2018	Lithium-Ion	2	Havyard Ship Technology	Norway
68	Fjord1 AS	N/A	Ferry	Full Electric	2018	Lithium-Ion	2	Havyard Ship Technology	Norway
69	Fjord1 AS	N/A	Ferry	Full Electric	2018	Lithium-Ion	2	Havyard Ship Technology	Norway
70	N/A	Guangzhou Ruihua New Energy Electric Boat Co., Ltd.	Bulk Carrier	Full Electric	2018	Lithium-Ion / Supercapacitor	2.4		China
71	All American Marine	Enhydra	Ferry	N/A	2018	N/A	0.16		USA
72	Wightlink	Victoria of Wight	Ro-pax	N/A	2018	N/A	N/A		UK
73	N/A	AMELS 188	Superyacht	Hybrid (Peak Shaving)	2018	N/A	0.055	DAMEN	Netherlands
74	Rimorchiatori Riuniti	N/A	Tug	Hybrid DE+ battery	2018	N/A	N/A		Italy
75	YARA	Yara Birkeland	Container Ship	Full Electric	2018	N/A	4		Norway
76	Norwegian Coastal Administration	OV Ryvingen	Multipurpose Vessel	Full Electric	2018	N/A	2	Fitjar Mekaniske Verft	Norway

	Owner	Name	Type	Type of Installation	Completion Date	Battery Type	Installed Capacity [MWh]	Shipyard	Country/ Route
77	Hurtigruten	MS Ronald Amundsen	Cruise Ship	Hybrid	2019	Li-Ion	1.3	Kleven Maritime	Norway
78	Hurtigruten	MS Fridtjof Nansen	Cruise Ship	Hybrid	2019	Li-Ion	6	Kleven Maritime	Norway
79	Natural Environment Research Council	RRS Sir David Attenborough	Research Vessel	Hybrid	2019	Li-ion Super-Phosphate	1.45		UK
80	Color Line	Color Hybrid	Ferry	Hybrid	2019	N/A	5	Ulstein Verft	Norway
81	Grimaldi Group	Cruise Barcelona	Ro-pax	Hybrid	2019	Li-Ion	5.5	Fincantieri	
82	Grimaldi Group	Cruise Roma	Ro-pax	Hybrid	2019	Li-Ion	5.5	Fincantieri	

10.2 Energy Storage

10.2.1 Energy Storage Classification

In general, energy storage systems, can be categorized either based on form or function[100]. The most found classification in literature, is based on the form of converted energy and it consists of five major categories namely electrical, mechanical, chemical, electrochemical and Thermal energy storage. A more analytical classification of energy storage based on the form of converted energy, is shown in Fig.11. The storage technologies that stand outside the scope of the research are highlighted in red colour.

Electrical storage systems include capacitors, electric-double layer capacitors (EDLC) and super magnetic energy storage (SMES). The electric double layer capacitors are also known as supercapacitors and ultracapacitors. The supercapacitor differs from a regular capacitor in that it has very high capacitance. Contrary to electrochemical storage, supercapacitors store energy in the means of a static charge resulting to low heating losses and high lifetime.

In *mechanical storage systems*, the energy can be stored as potential, kinetic or internal mechanical. The most common mechanical storage systems of each type are pumped hydroelectric power plants (PHES), compressed air energy storage (CAES) and flywheel energy storage (FW).

Chemical storage systems are distinguished in conventional and alternative fuels. Conventional naturally formed fossil fuels are carbon sources and thus do not represent a sustainable storage solution. Alternative fuels such as hydrogen and biofuels represent more friendly options to the environment but as stated in the introduction, they lie outside the scope of the present thesis and have only been included in some of the comparisons as a reference measure of weight and spacing that is currently used in marine applications. Besides this, one should be particularly careful when directly comparing alternative fuels to electrical or electrochemical energy storage options. Specifically, the irreversibility of the energy throughput (in this case the conversion of energy from one type to another for the production and/or burning of hydrogen) should also be considered. Moreover, chemical storage media cannot be studied independently as they require external power conversion mechanisms to produce work.

Electrochemical storage devices or batteries are electrical energy source which can convert the chemical energy of its reacting substances directly into useful electrical energy that can be drawn from it at a certain voltage. A battery essentially comprises of two electrodes: an anode (negative electrode) and a cathode (positive electrode) and an electrolyte between them [101]. Batteries can be distinguished in secondary and flow batteries. Secondary batteries and more specifically lead-acid and li-ion represent the most widespread electricity storage option in marine applications. Batteries have stand-alone characteristics (similar to flywheels and supercapacitors) meaning that they can be considered both prime mover and energy storage medium and therefore power and capacity can directly be compared.

In *Thermal Energy Storage* (TES) available heat (i.e. waste heat) is stored by different means in the form of heat for later use in applications, such as air conditioning, hot water production or electricity generation. In compare to other energy storage types, TES systems have low roundtrip efficiency, high self-discharge rate but most importantly limited ability to produce mechanical work. In other words, if a TES is directly compared to an electrical or electrochemical (i.e. battery) storage device of the same efficiency and capacity, it will have the same amount of energy stored but this will be of lower quality (available work) due to the effect of energy conversions. Following this fact, TES are not recommended for applications where stored energy needs to be retrieved in the form of electricity. For this reason, the TES systems will not be further considered in this analysis.

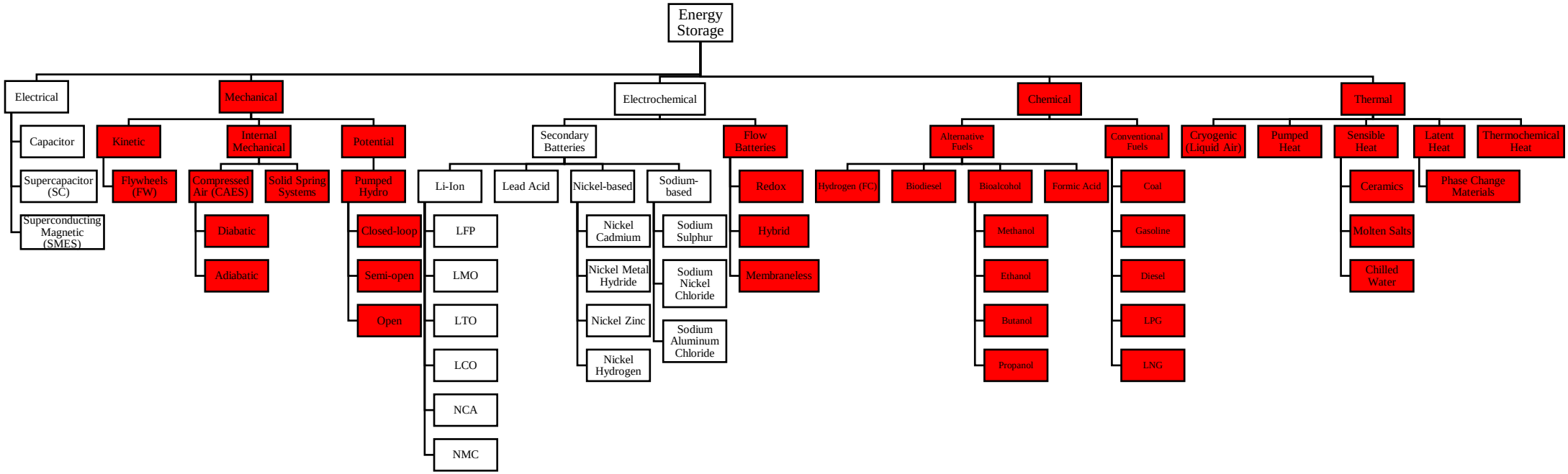

Figure 80 Classification of Energy Storage Systems based on the form of converted energy. ESDs outside the scope of this thesis are highlighted in red colour

10.2.2 Comparison and Selection

Energy storage devices are reviewed in terms of performance characteristics, limitations and improvement potential. The ESDs are compared to each other to identify the most suitable technology or combination of technologies for high power shipboard applications.

Criteria

When trying to directly compare energy storage devices of diverse types, simplifications need to be made. For the purposes of a top-level comparison, most popular energy storage devices have been compared to each other based on 5 primary comparison criteria namely Specific Energy/Energy Density, Specific Power/Power Density, Cycle Life/Longevity, Roundtrip Efficiency and Specific Capital Cost.

Specific Energy & Energy Density: Specific Energy is a measure of the energy storage device's ability to store energy per unit of mass [Wh/kg], while energy density is a measure of the system's ability to store energy per unit of volume [Wh/l]. They are both fundamental comparison criteria, as in ship applications space and weight tolerance are often limited. If the added weight of the energy storage is comparable to the ship's mass of displacement, then the ship power requirements will have to increase to retain vessel's service speed. Ideally, the energy storage device should have high specific energy and energy density that are comparable to those of fossil fuels. When referring to specific energy of energy storage device, the system level of detail (i.e. cell, module or stack) should always be clear. For electrochemical storage, the specific energy is given in cell level while for chemical storage both the fuel and the containment equipment have been considered.

Specific Power & Power Density: Similarly, to the previous criterion, specific power and power density refer to the system's discharge rate ability per unit of mass and unit of volume respectively. Quick and controllable discharge of stored energy is a desirable characteristic for ship applications where high peak powers are required. To compare the specific power of different ESDs, it is required to consider the full energy conversion chain as some of these media act solely for storage (i.e. fuel) while some other like the batteries are storing and deliver the power themselves.

Cycle Life or longevity is a measure of the system's resistance in aging and it is expressed in full charge/discharge cycles till the end of lifetime (EoL). It is an important criterion that directly affects the lifetime cost and thus the return on investment. The cycle life should be as high as possible to cover most of the ship's expected lifetime (about 20 to 30 years) or at least to lead to a minimum number of replacements over this period.

Roundtrip Efficiency is the ratio of energy put into energy retrieved from storage (in Wh) expressed in percentage (%). It is a critical factor in the usefulness of a storage technology as the higher it is, the less energy we lose due to storage and thus the more efficient the system as whole.

Cost represent the most trivia criterion as it highly depends on the type, the scale and the time of the application. For this reason, specific capital cost expressed in $/kWh has been used as it is more application insensitive than cost expressed in $/kW. When estimating the lifetime cost of the energy storage medium, specific cost is an insufficient indication as cycle life, roundtrip efficiency and maintenance cost also need to be considered.

Other points of interest when selecting an energy storage device for a certain application are safety, self-discharge rate, charging time, scalability, maintainability and environmental impact.

First Level Comparison

At first, energy density and specific energy characteristics of all storage technologies were plotted against each other. As can be seen in Fig. fossil fuels are located on the top right part of the graph meaning that they are the lightest and most compact among all storage media. Close to that, one can find alternative fuels such as liquid hydrogen and biofuels However, when comparing different Energy Storage Devices (ESDs) in terms of specific energy expressed in [Wh/kg] or energy density expressed in [Wh/L], there is the necessity to determine the available part of the energy, or the equivalent amount of mechanical work that could be extracted from it, alternatively this could lead to erroneous conclusions.

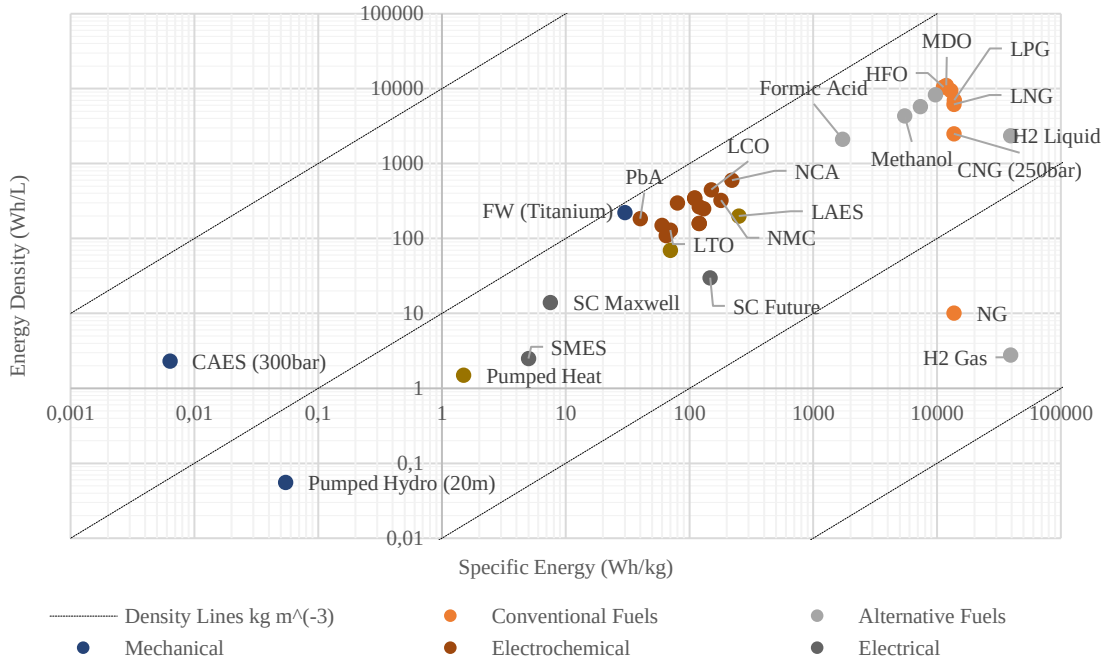

Figure 81 Specific Energy Map [102-104]

Indicatively, when considering fossil fuels for ship propulsion, the thermal efficiency of the ICE is approximately at 40-50%. In other words, only the 40-50% of the fuel's thermal energy is turned into useful mechanical work with the rest of it being released to the environment. If this analysis is expanded to the entire energy conversion chain on-board the ship (GBs, shaft liens, propeller etc.), this number will be further reduced. Respectively, when considering electrical energy storage systems such as batteries for ship propulsion, the energy conversions from electrical to mechanical (motors) must also be considered. Therefore, an appropriate normalization of the values should be made.

Excluding the chemical storage, li-ion battery technologies such as Nickel-Cobalt Aluminium (NCA) and Nickel Metal Hydride (NMH) have by far the highest specific energy and density. This is of no surprise as it represents the main reason for their high utilization in ship applications. Following Li-Ion batteries and in a logarithmic decline, flywheels, supercapacitors and SMES can be found. Finally, at the lower left corner of the specific energy map, the other mechanical and thermal options can be found. Their extremely low specific energy and energy density can be translated in major space and weight requirements that are not available on-board ships and therefore excludes them from realistic alternatives.

Following the specific energy analysis, the storage technologies have been plotted in terms of power rating vs discharge time at rated power. Similarly, marine ES applications have been

mapped for the same measures. The main ambition is to identify the most appropriate couplings of application and technology. A power range graph per vessel type can be found attached in the appendix.

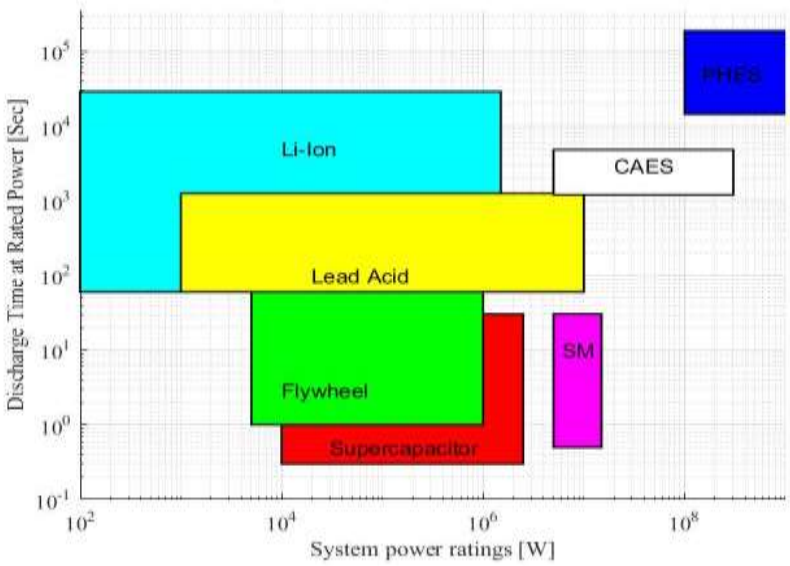

Figure 82 ES System Power Rating vs Discharge Time at Rated Power[105-107]

From the two graphs, it can be derived that based on function, ESD's can also be distinguished into those that are intended firstly for high power ratings with a relatively small energy content making them suitable for power quality (load fluctuations) or uninterruptible power supply (UPS) such as supercapacitors, SMES and flywheels; and those designed for energy management (peak shaving/spinning reserve) such as batteries. Zero emission mode is now borderline to Li-Ion batteries and therefore it is not fully available to a large scale. PHS and CAES are more appropriate for bulk energy management and thus they lie outside this function map.

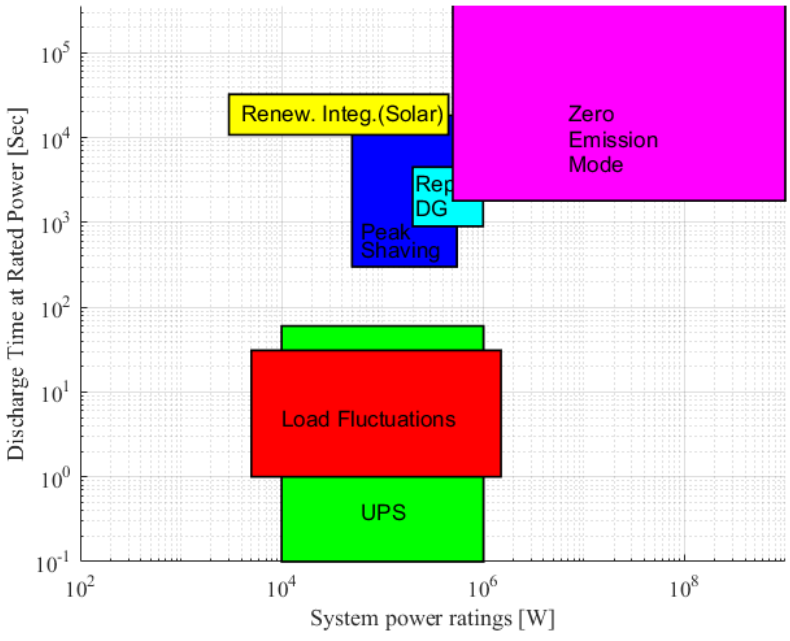

Figure 83 Marine ES Application Mapping Power Rating vs Discharge Time at Rated Power [105-107]

Expanding the analysis for other criteria as well, the following spider plot was obtained.

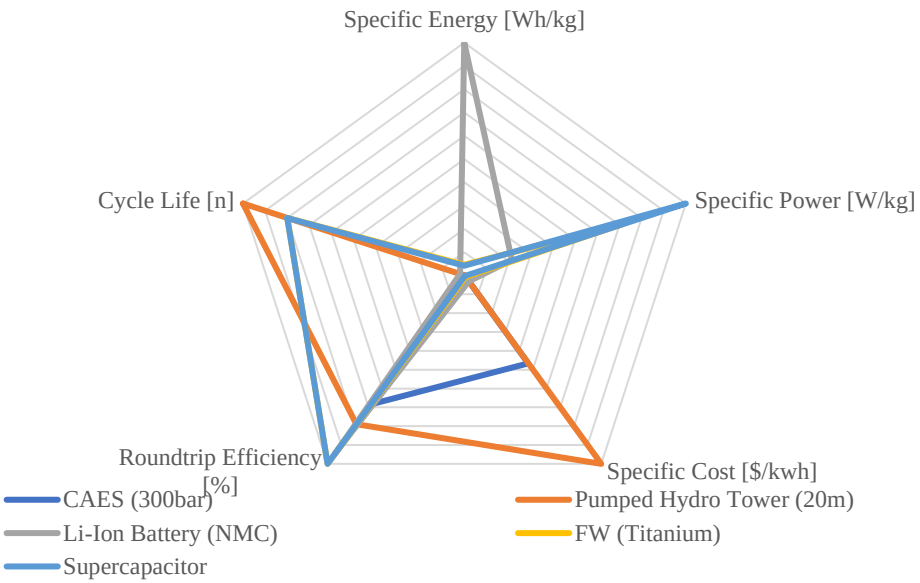

Figure 84 Top-layer comparison of ESDs Overview [107-109]

In summary, Li-Ion batteries have high specific energy, high efficiency but expensive specific cost and low life cycles. On the other hand, supercapacitors have high specific power and high life cycle but low specific energy and expensive cost per unit of energy. Flywheels have similar characteristics to the supercapacitor, but with more moderate values while it has also a very low standby efficiency. Compressed Air Energy Storage (CAES) and Pumped hydro represent very low-cost alternatives with high life cycle but as already stated they must be excluded from further analysis because of their extremely low sizing factors.

10.2.3 Ongoing Development in Battery Technologies

For batteries there are fundamental trade-offs associated with the electrochemical properties of their active materials and electrolytes, that set a barrier in development expectations and that make a one-fit-all solution an extremely challenging task. Given this, there is significant ongoing research in identifying and developing alternative battery chemistries and hybrid manufacturing approaches that will result in energy storage technologies with better performance or reduced cost. The most significant of which are advanced li-ion batteries, all solid-state batteries, li-air, li-sulphur and sodium-ion chemistries, liquid metal batteries and graphene enhanced supercapacitors.

2.3.1.1. Sodium-Ion (Na-Ion) Batteries

The widespread use of li-ion batteries has resulted in an increasing demand for lithium mineral. The concentration of the material in certain geographical regions in combination with the relatively limited stocks and the expected rise in energy storage demand, have driven lithium mineral prices to more than $16,500 per metric ton [110].

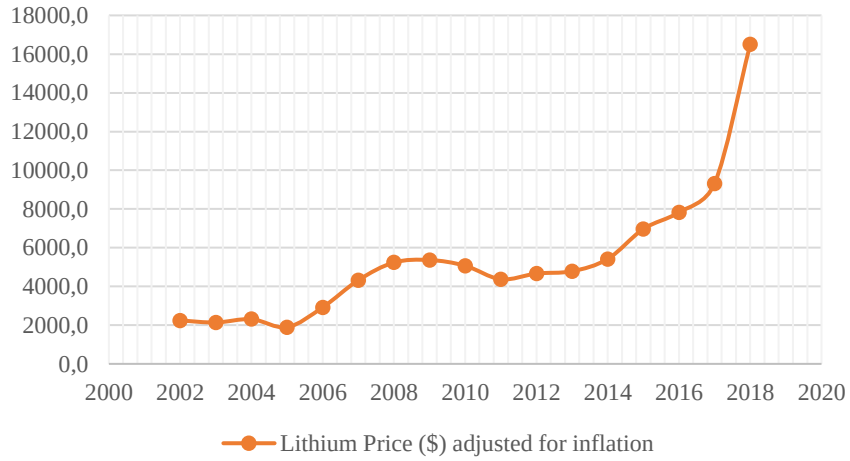

Figure 85 Lithium Price [$/ton] adapted by [110]

Driven by limited sources of Lithium, many researchers are considering more abundant cathode materials as an alternative. Sodium's abundance[4], makes sodium-based batteries a compelling chemistry as the cost of sodium carbonate is only about $135–165/ton [111]. Practical applications of sodium-ion full batteries have been hindered by many limitations, such as low working potential, short cycle life, and low safety. Moreover, their low specific energy and energy density, makes Na-Ion batteries less appealing to Electric Vehicle (EV) applications.

2.3.1.2. All Solid-State Battery

One of the most interesting technologies in development is the solid-state battery. The absence of liquid flammable electrolyte between the electrodes solves the safety concern of traditional lithium-ion batteries [112]. By simplifying the safety mechanism of the battery, it is also possible to increase the effective energy density of the battery[113]. On the other hand, the biggest disadvantage of solid-state batteries historically has been their low current and power output. Solid-state lithium-ion batteries of first generation, are still in an early commercialization phase [114], and it will take years before they are successfully employed in large ship applications.

2.3.1.3. Hybrid Supercapacitors

Current research is also working to increase the energy density of supercapacitors, thereby making them more competitive with traditional batteries. Zhang et al. [115] have designed and test a hybrid supercapacitor that consists of graphene-enhanced supercapacitor positive electrode and li-ion battery negative electrode. In lab conditions, high specific energies of 147 Wh/kg and 86 Wh/kg have been reported but at the expense of significant compromises in specific power of 150 W/kg and 2587 W/kg respectively.

2.3.1.4. Liquid Metal Batteries

Another interesting technology is liquid metal battery. Developed by scientists in MIT, liquid metal battery comprises two liquid metal electrodes separated by a molten salt electrolyte that self-segregate into three layers based upon density and immiscibility [116] .

[4] Sodium Carbonate has approximately one thousand times larger natural reserves than lithium

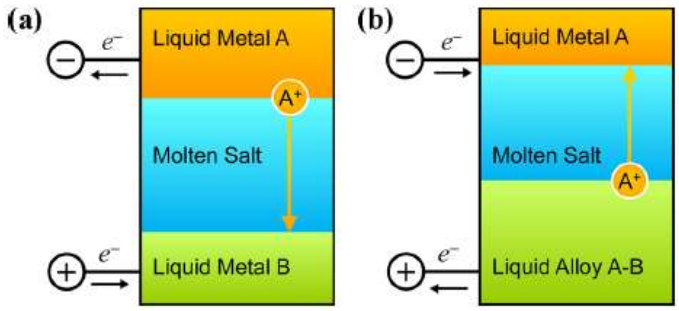

Figure 86 Schematic diagram of a liquid metal battery upon discharging and charging [116] .

It has low production cost potential as it uses earth-abundant electrode materials. In technical terms, liquid metal batteries are immune to microstructural electrode degradation mechanisms that limit the cycle life of a conventional battery, while they are capable of handling high discharge rates at high voltage efficiencies. Unfortunately, despite these advantages, liquid metal batteries possess forbidding disadvantages, which make them unsuitable for use in shipboard applications. The three liquid layers make battery operation sensitive to motion and potentially hazardous in case the liquid electrodes touch, leading to a short-circuited cell and rapid heat generation.

2.3.1.5. Li-Sulphur (Li-S)

In recent years, there has been growing interest in Lithium-Sulphur battery as an alternative to lithium-ion batteries. This can be explained by the high maximum theoretical capacity of sulphur (1675 mAh/g) that results in a subsequent maximum theoretical specific energy of 2600 Wh/kg [117]. This technology is also known for its potentially very high mechanical robustness and safety, for being maintenance free and for its very high depth of discharge[118]. Li-S has the potential to be financially competitive to lithium-ion battery due to lower raw material cost (i.e. Sulphur) and higher specific energy (less material required for same energy). However, there are key issues that need to be addressed before it becomes a commercial product. The primary issue of the Li-S battery is rapid capacity fade resulting in poor cycle life and continuous self-discharge of the cell upon storage.

2.3.1.6. Lithium-air (Li-air)

Another battery technology that is also receiving a lot of research attention today is the lithium air battery. The lithium-air battery (Li-air) is a metal–air electrochemical cell or battery chemistry that uses oxidation of lithium at the anode and reduction of oxygen at the cathode to induce a current flow [119]. Depending on materials used, Li-air will produce voltages in between 1.7 and 3.2V/cell. For a voltage of about 3V, the theoretical specific energy of Li_2O_2 battery is about 3500 Wh/kg, making this technology the one with the highest capacity potential overall.

It is expected that it will take at least two decades before the technology can be commercialized, due to substantial challenges that still need to be addressed. No one has yet demonstrated a li-air cell that is reversible and can be cycled over a significant fraction of its theoretical capacity [120]. TU Delft is conducting research on improving the reversibility of li-air batteries, with current cells demonstrating poor cycle life of 20-40 cycles at a specific energy of about 800 Wh/kg [33].The only short-term commercially viable applications for primary li-air cells could be those designed for high specific energy but not rechargeability. In addition, they have low power density and problems with overpotential leading to low energy storage efficiency.

10.2.4 Battery Supercapacitor HESS Application Overview in shipboard applications

Primary Source	High Capacity device	Application	EMS	Architecture /Topologies	Benefits	References
Diesel Electric Generator	Lithium-Ion Battery	Naval Ship	Fuzzy Logic	N/A	N/A	[121]
	Lithium-Ion Battery	Buck-up source for propulsion systems and pulse power loads in all-electric naval ships (Destroyer)	N/A	Dual Active full bridge DC/DC converter with IGBTs	DC bus voltage stability in step loads and stability of output power.	[54] [55]
	N/A	Handling of load fluctuations	Power Control	Bidirectional buck-boost DC/DC converter	Improve system stability and fuel-efficient operation of DGs	[122]
	NiMH Batteries	Handling of intermittent power demand of on-board loads for excursion ship	N/A	Passive parallel topology using bidirectional DC/DC converter	Reduction of generators maximum power, stabilization of DC link voltage, smoothing battery current effectively increasing battery lifetime and lower using cost of batteries	[58]
Fuel Cell / PEMFC	Lithium-Ion Battery	Emergency system of electric aircraft	Rule-Based Fuzzy Logic, Classical PI control strategy, State machine control strategy, frequency decoupling and FL strategy, Energy Consumption Minimization Strategy (ECMS)	N/A	N/A	[123]
	Lead-Acid Battery	High Pulse power management at passenger boat	Rule-Based Fuzzy Logic	N/A	Overall System Efficiency, Fuel consumption and Improved dynamic performance of fuel cell system	[57]
Gas Turbine Electric Generators	Battery (Not specified)	Support of MVDC (Peak demand and pulse power management) for Warship	Rule Based Fuzzy Logic	Bidirectional DC/DC converters with Dual Active Bridge	Full support of transient load	[53]
N/A	Lead Acid Battery	Experimental platform for ships	PI Control	Half Bridge bidirectional DC/DC controller	Better utilization rate and increased service life of battery	[56]

10.3 Datasheets

10.3.1 LFP – Seanergy

Seanergy® modules

High energy and high power Li-ion Super-Iron Phosphate

Saft's Seanergy® modules are the ideal choice for local energy management, particularly in conjunction with hybrid propulsion, photovoltaic and other renewable energy generators.

Built with proven Saft Li-ion Super-Iron Phosphate® ($LiFePO_4$) technology, the Seanergy® module provides maintenance-free energy storage in a reduced volume, combining high operational reliability over thousands of cycles with outstanding energy efficiency. Its modular design allows adaptation of the battery configuration to various energy and voltage levels.

Saft always supplies Li-ion 3U module with an associated Battery Management System (BMS).

Applications

- Hybrid-electric and/or full electric propulsion
- Auxiliary systems, hotel load
- Emergency back-up
- Actuators

Benefits of the Li-ion technology

- Reduced mass and volume
- Very long calendar, storage and cycling life
- Faster charging time
- Maintenance-free
- Operates in any orientation
- No memory effect
- High power (continuous and pulses)

Operational benefits

- Enable full electric propulsion with a compact volume (entering and exiting harbours and restricted areas)
- Load-levelling function to keep high level of fuel efficiency and reduced number of generating sets
- Standby power at shore
- Design flexibility (improved scalability and modularity)

Nominal characteristics	Seanergy® 48P (Power)	Seanergy® 48M (Energy)
Nominal voltage (V)	46.2	46.2
Minimum capacity (C/5) (Ah)	56	78
Nominal capacity (C/5) (Ah)	60	82
Minimum energy (C/5) (Wh)	2500	3600
Nominal energy (C/5) (Wh)	2600	3800
Nominal energy density (Wh/l)	76	106
Nominal specific energy (Wh/kg)	69	96
Mechanical characteristics		
Standard	19" - 3U - Double depth	
Width (mm)	448	
Height (mm)	133	
Depth (mm)	602.5	
Weight (kg)	39.5	
Electrical characteristics at + 25°C / + 77°F		
Voltage window (V)	37.8 to 53.2	
Maximum discharge current (A)	240	240
Peak discharge current (10 s) (A)	300	300
Maximum charge current (A)	240	80
Peak charge current (10 s) (A)	300	300
Recharge time (h) at nominal current (95% State of Charge)	0.5	2
Operating and storage conditions		
Lifetime at + 20°C perm (+ 68°F)	>20	
Lifetime at + 30°C (+ 86°F)	>10	
Cycle life (+ 20°C / + 68°F)	from 6000 cycles to 1 million	
Operating temperature - discharge - charge	 - 25°C / + 55°C (- 13°F / + 131°F) 0°C / + 55°C (+ 32°F / + 131°F)	
Storage temperature	- 40°C / + 55°C (- 40°F / + 131°F)	
Storage time	1 year	

saft

Features

- Compact modules integrating VLM Fe Li-ion cells, module supervision and cell balancing
- Advanced industrial design offering highest reliability and robustness
- 20 years design life with high daily energy throughput
- Multiple cycling patterns from daily deep discharge to dynamic multiple charge/discharge profiles from any state of charge
- Best energy efficiency of all available energy storage systems
- State of charge and state of health indication (through BMM)
- 2-level redundant safety

System capability

- Series connection of up to 1000 V
- Battery string management and interfacing through separate BMM module
- Multi-string paralleling through MBMM to upscale battery energy

Functional characteristics

Saft Seanergy® module technology contains VLM Fe cells with advanced nickel-based lithium-ion Super-Iron Phosphate® technology:

- Best safety among Li-ion chemistries
- Outstanding calendar and cycle life and reliability
- Stable internal resistance over entire life
- High capacity cell

Mechanical & electrical interface

- Vertical or horizontal implementation
- Systems for 19" rack-mount in 3U height
- Stackable
- Optional 3U rack-mount brackets
- 2 screw terminals

Safety

Redundant safety design to cope with component failure or abusive conditions:

- At cell level: no reaction in an abuse event with inert iron phosphate positive material, shutdown-effect separator, mechanical vent
- At module level: electronic board, individual cell voltage monitoring, module temperature monitoring, balancing, fuse
- At battery system level: electronic board, power switch, current sensor

Compliance to standards	
Module safety	EN 50178, cCSAus 60950, IEC 60950
United Nation Class	UN 3480
Hazard classification	Class 9
Transport regulation compliance	UN recommendations for dangerous goods transportation, model regulations and manual tests and criteria 38.3
EMC	EN 61000-4-2 Class B / EN 61000-4-3 Class A / EN 614000-4-4 Class B / EN 614000-4-6 Class A / EN 55022 Class B
Protection class	IP 20

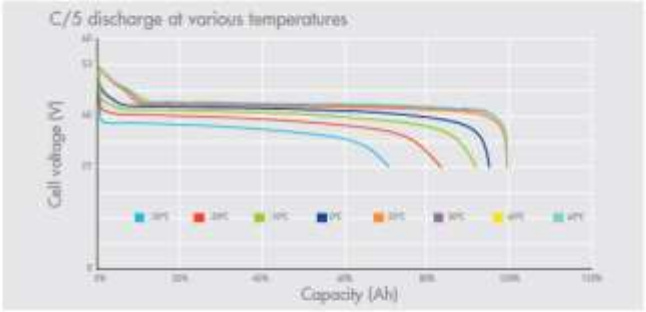

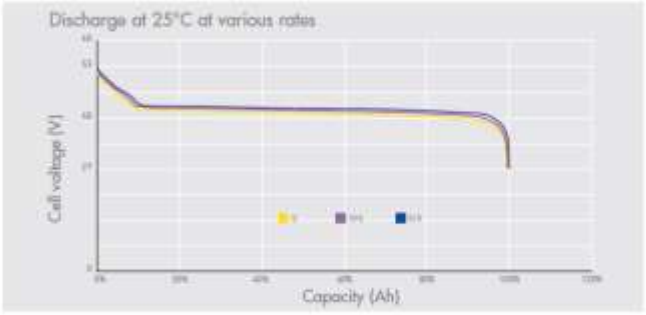

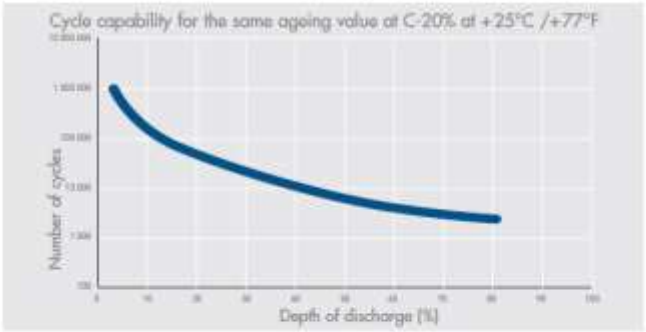

Saft
Specialty Battery Group
26 quai Charles Pasqua
92300 Levallois-Perret
France
www.saftbatteries.com

Saft Poitiers
Rue Georges Leclanché
86060 Poitiers - France
Tel. : +33 (0)5 49 55 48 48
Fax : +33 (0)5 49 55 48 50
www.saftbatteries.com

Doc No.: 3016-2-0617
Edition: June 2017

10.3.2 Supercapacitor - Maxwell Tech

DATASHEET K2 ULTRACAPACITORS - 2.7V SERIES

FEATURES AND BENEFITS*

- Up to 1,000,000 duty cycles or 10 year DC life
- High power density
- 650F to 3,000F capacitance range
- Threaded terminals or laser-weldable posts

TYPICAL APPLICATIONS

- Automotive subsystems
- Wind turbine pitch control
- Hybrid vehicles
- Rail
- Heavy industrial equipment
- UPS & telecom systems

PRODUCT SPECIFICATIONS

ELECTRICAL	BCAP0650	BCAP1200	BCAP1500	BCAP2000	BCAP3000
Rated Capacitance[1]	650 F	1,200 F	1,500 F	2,000 F	3,000 F
Minimum Capacitance, initial[1]	650 F	1,200 F	1,500 F	2,000 F	3,000 F
Maximum Capacitance, initial[1]	780 F	1,440 F	1,800 F	2,400 F	3,600 F
Maximum ESR_{DC}, initial[1]	0.8 mΩ	0.58 mΩ	0.47 mΩ	0.35 mΩ	0.29 mΩ
Test Current for Capacitance and ESR_{DC}[1]	65 A	75 A	100 A	100 A	100 A
Rated Voltage	2.70 V	2.70 V	2.70 V	2.70 V	2.70 V
Absolute Maximum Voltage[2]	2.85 V	2.85 V	2.85 V	2.85 V	2.85 V
Absolute Maximum Current	680 A	930 A	1150 A	1500 A	1900 A
Leakage Current at 25°C, maximum[3]	1.5 mA	2.7 mA	3.0 mA	4.2 mA	5.2 mA
TEMPERATURE					
Operating temperature (Cell case temperature)					
Minimum	-40°C	-40°C	-40°C	-40°C	-40°C
Maximum	65°C	65°C	65°C	65°C	65°C
Storage temperature (Stored uncharged)					
Minimum	-40°C	-40°C	-40°C	-40°C	-40°C
Maximum	70°C	70°C	70°C	70°C	70°C
PHYSICAL					
Mass, typical	160 g	260 g	280 g	360 g	510 g
Terminals	Threaded or Weldable	Threaded or Weldable	Threaded or Weldable	Threaded or Weldable	Threaded or Weldable
Maximum Terminal Torque (KD4)	14 Nm	14 Nm	14 Nm	14 Nm	14 Nm
Vibration Specification	ISO 16750, Table 14	ISO 16750, Table 14	ISO 16750, Table 14	ISO 16750, Table 14	ISO 16750, Table 14
Shock Specification	SAE J2464	SAE J2464	SAE J2464	SAE J2464	SAE J2464

*Results may vary. Additional terms and conditions, including the limited warranty, apply at the time of purchase. See the warranty details and enclosed information for applicable operating and use requirements.

Page 1 > Document number: 1015370.4 > maxwell.com

Maxwell TECHNOLOGIES Enabling Energy's Future

DATASHEET K2 ULTRACAPACITORS - 2.7V SERIES

PRODUCT SPECIFICATIONS (Cont'd)

POWER & ENERGY	BCAP0650	BCAP1200	BCAP1500	BCAP2000	BCAP3000
Usable Specific Power, P_u [4]	6,800 W/kg	5,800 W/kg	6,600 W/kg	6,900 W/kg	5,900 W/kg
Impedance Match Specific Power, P_{max} [5]	14,000 W/kg	12,000 W/kg	14,000 W/kg	14,000 W/kg	12,000 W/kg
Specific Energy, E_{max} [6]	4.1 Wh/kg	4.7 Wh/kg	5.4 Wh/kg	5.6 Wh/kg	6.0 Wh/kg
Stored Energy, E_{stored} [7,11]	0.66 Wh	1.22 Wh	1.52 Wh	2.03 Wh	3.04 Wh
SAFETY					
Short Circuit Current, typical (Current possible with short circuit from rated voltage. Do not use as an operating current.)	3,400 A	4,700 A	5,700 A	7,700 A	9,300 A
Certifications	UL810a, RoHS	UL810a, RoHS	UL810a, RoHS	UL810a, RoHS	UL810a, RoHS

TYPICAL CHARACTERISTICS

THERMAL CHARACTERISTICS					
Thermal Resistance (R_{cs}, Case to Ambient), typical[8]	6.5°C/W	5.3°C/W	4.5°C/W	3.8°C/W	3.2°C/W
Thermal Capacitance (C_{th}), typical[8]	190 J/°C	300 J/°C	320 J/°C	410 J/°C	600 J/°C
Maximum Continuous Current ($\Delta T = 15°C$)[8]	54 A_{rms}	70 A_{rms}	84 A_{rms}	110 A_{rms}	130 A_{rms}
Maximum Continuous Current ($\Delta T = 40°C$)[8]	88 A_{rms}	110 A_{rms}	140 A_{rms}	170 A_{rms}	210 A_{rms}
LIFE					
DC Life at High Temperature[2] (held continuously at Rated Voltage and Maximum Operating Temperature)	1,500 hours	1,500 hours	1,500 hours	1,500 hours	1,500 hours
Capacitance Change (% decrease from minimum initial value)	20%	20%	20%	20%	20%
ESR Change (% increase from maximum initial value)	100%	100%	100%	100%	100%
Projected DC Life at 25°C[3] (held continuously at Rated Voltage)	10 years	10 years	10 years	10 years	10 years
Capacitance Change (% decrease from minimum initial value)	20%	20%	20%	20%	20%
ESR Change (% increase from maximum initial value)	100%	100%	100%	100%	100%
Projected Cycle Life at 25°C[1,9,10]	1,000,000 cycles	1,000,000 cycles	1,000,000 cycles	1,000,000 cycles	1,000,000 cycles
Capacitance Change (% decrease from minimum initial value)	20%	20%	20%	20%	20%

Maxwell TECHNOLOGIES Enabling Energy's Future

10.4 Sizing Flow Charts

10.4.1 Battery Sizing

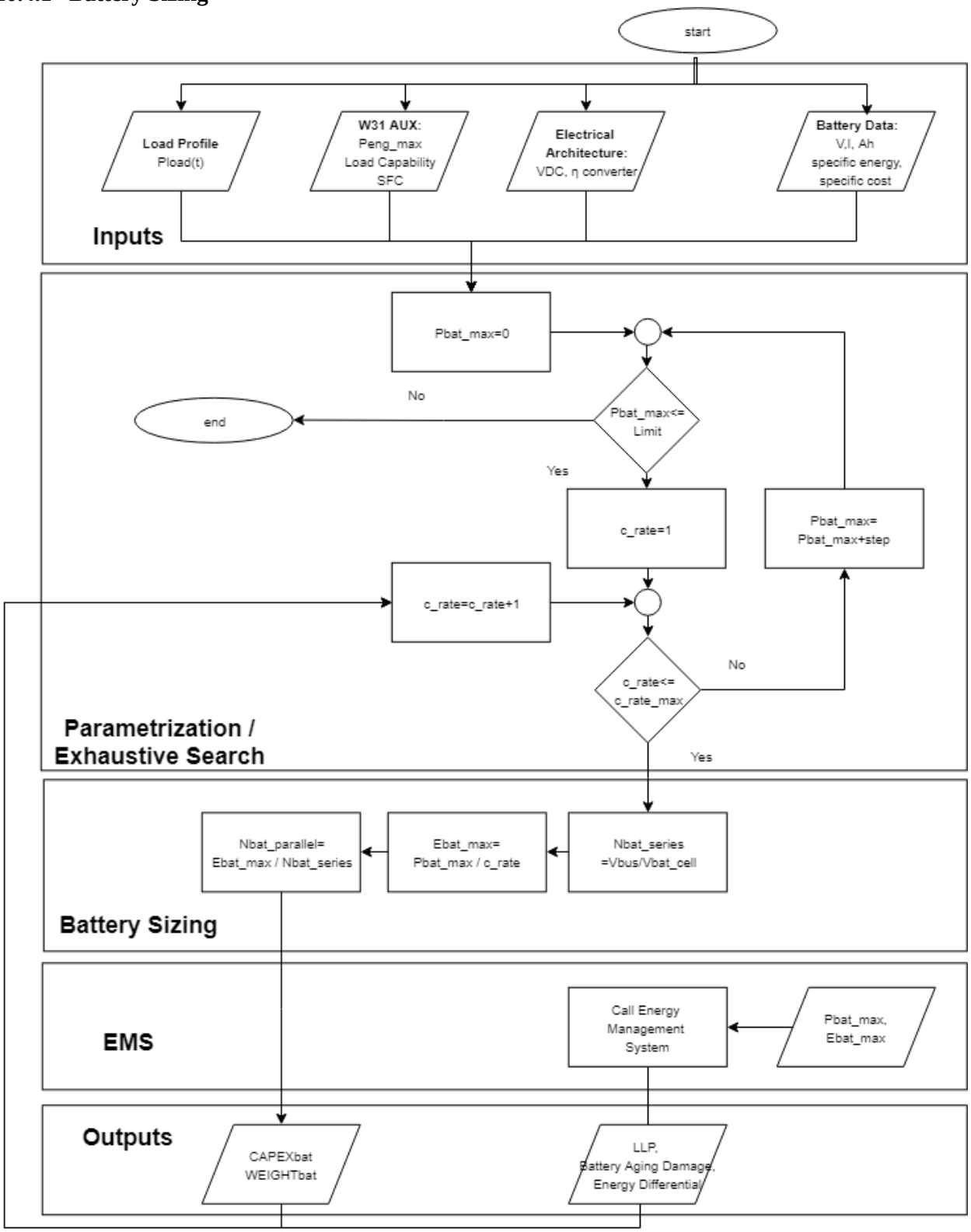

10.4.2 HESS Sizing

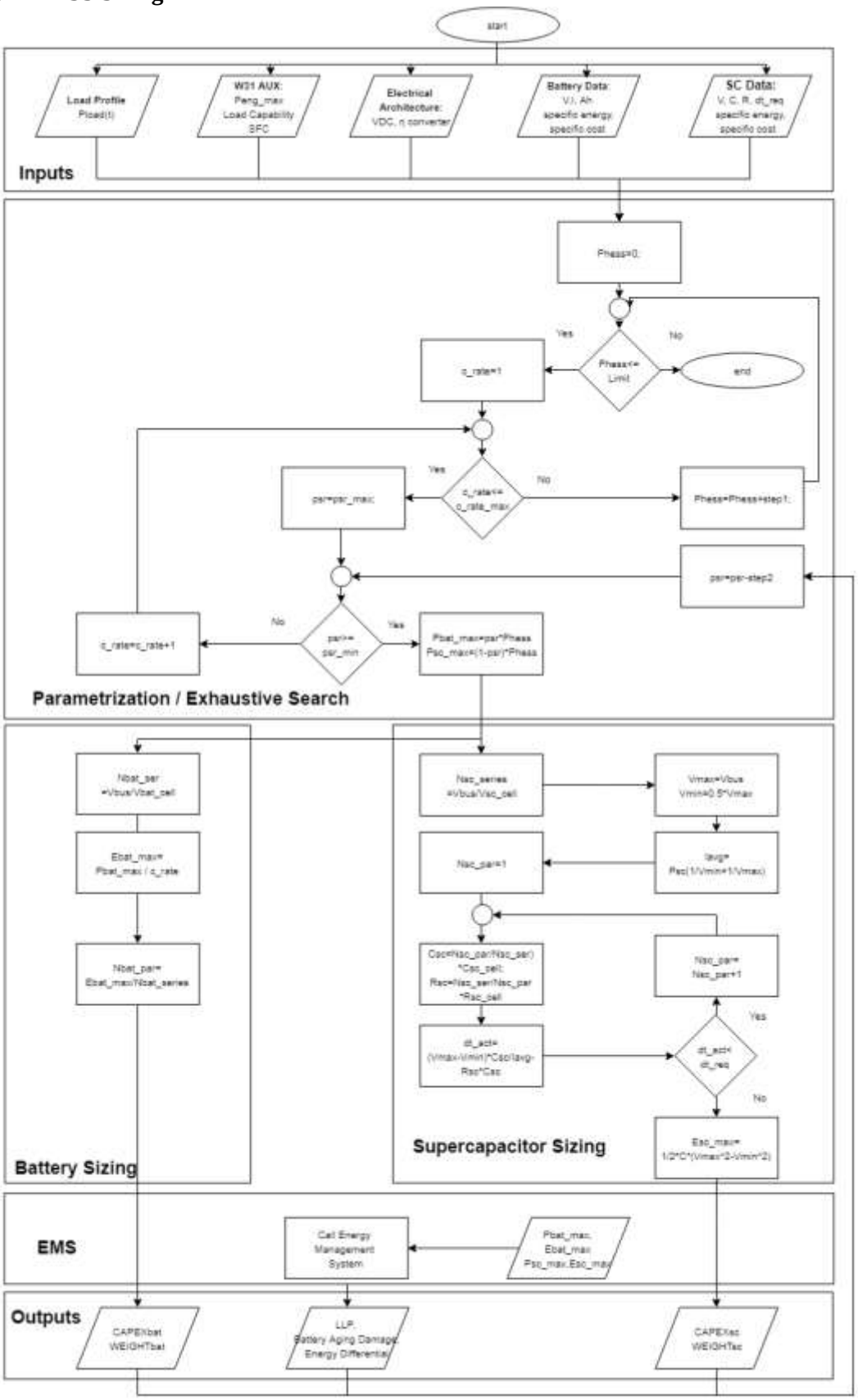

10.5 Simulation Flow Charts

10.5.1 Battery Only EMS Load Levelling

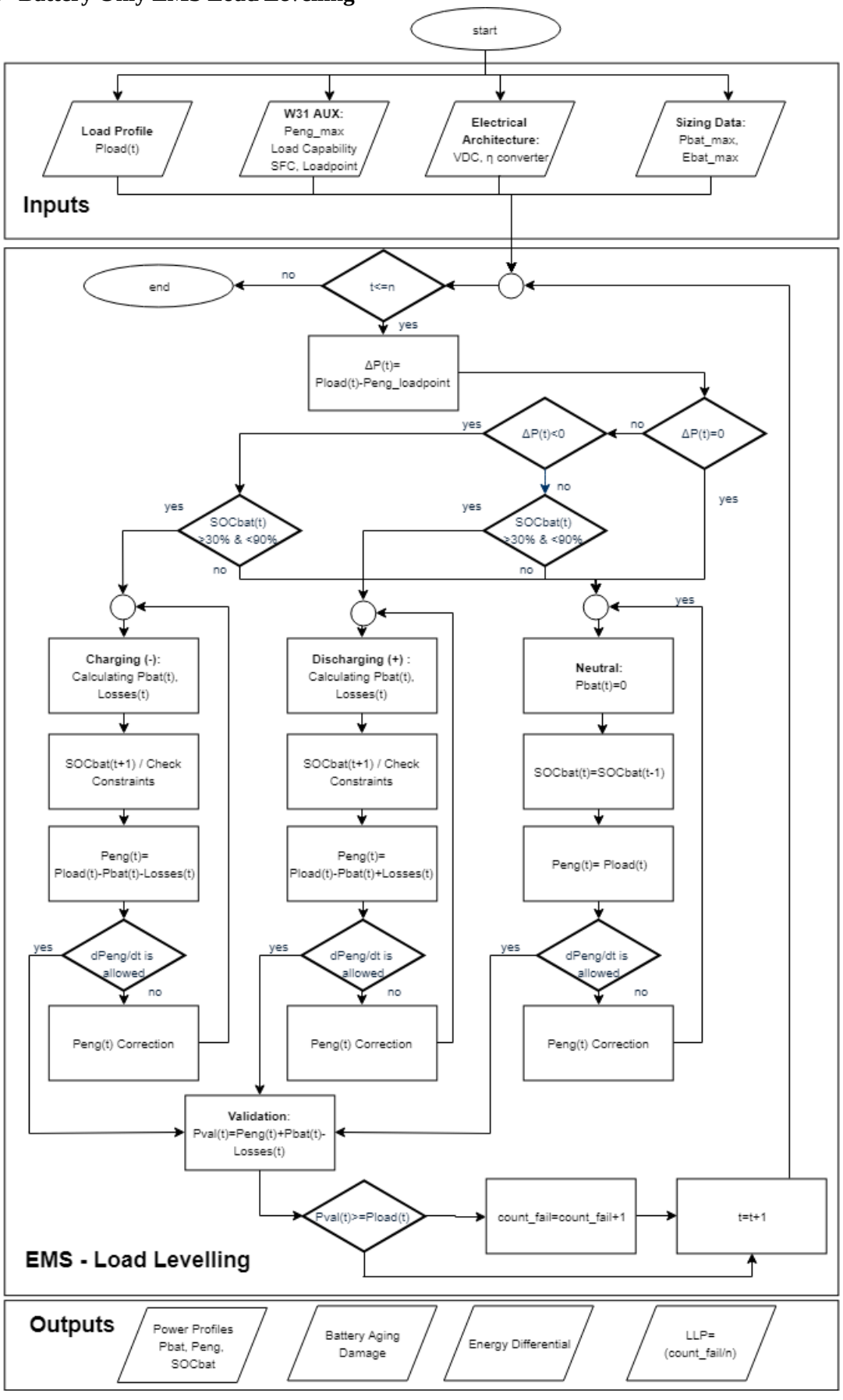

10.5.2 Battery Only EMS Load Following

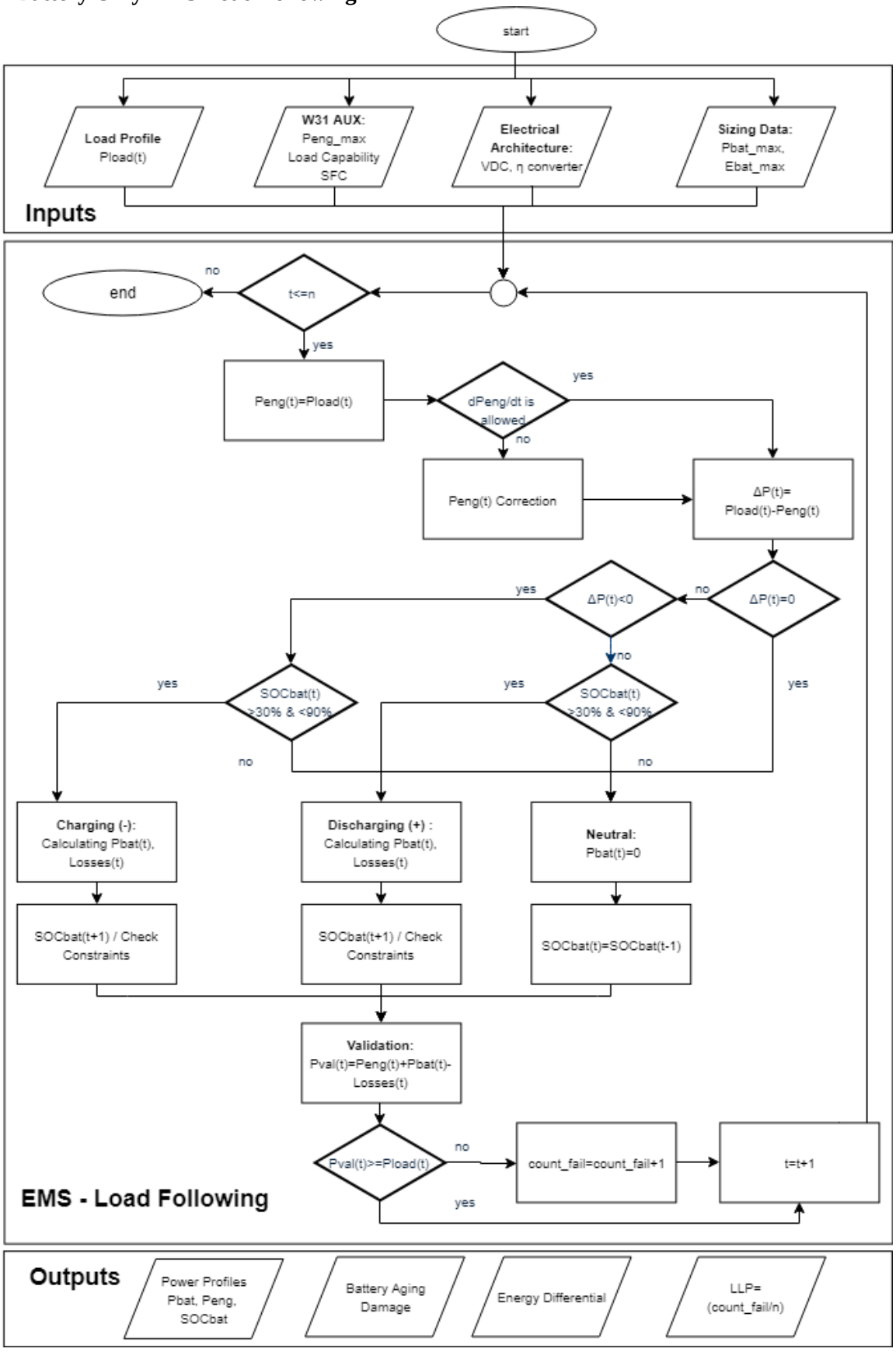

HESS EMS Load Levelling

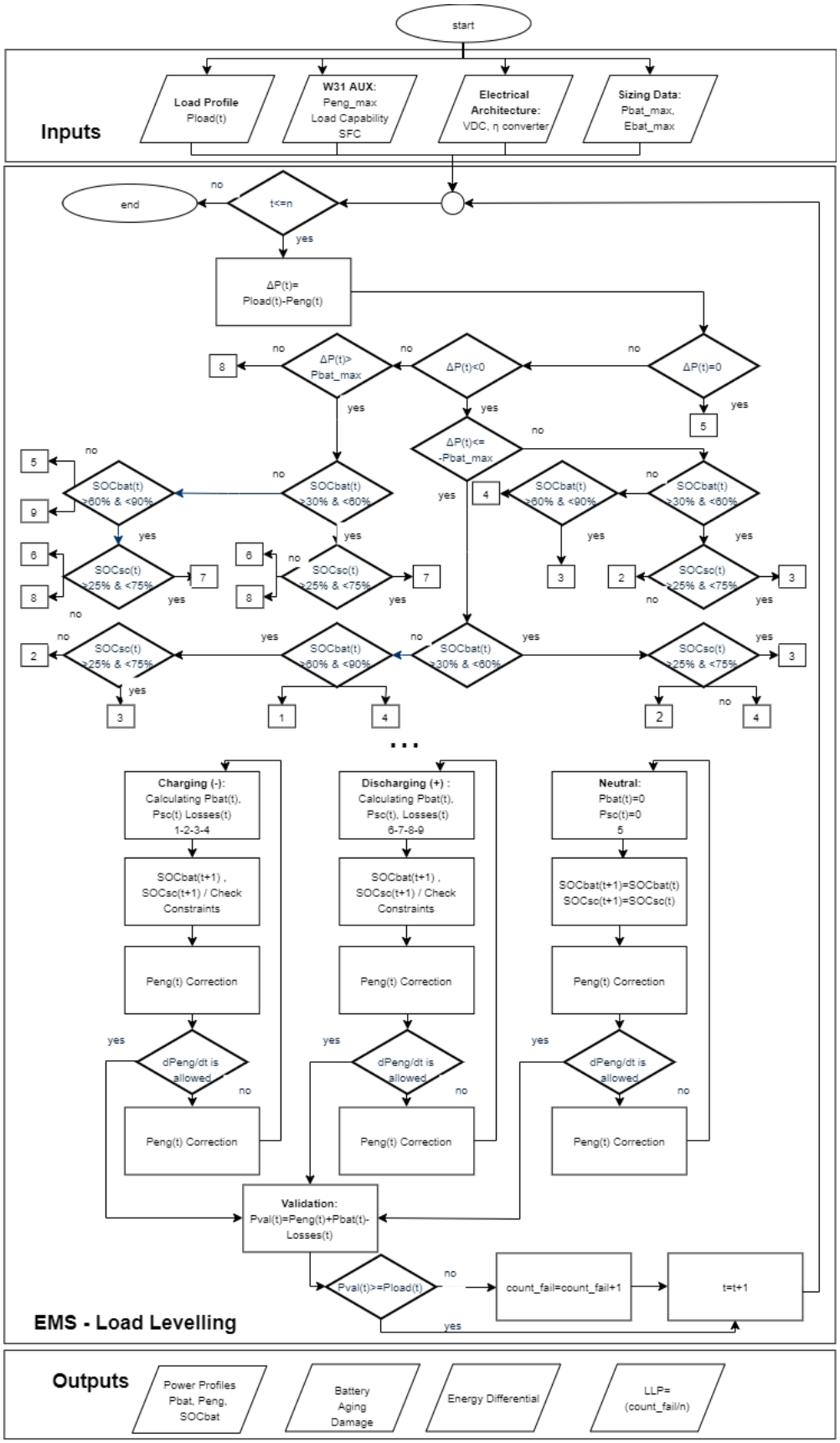

HESS EMS Load Following

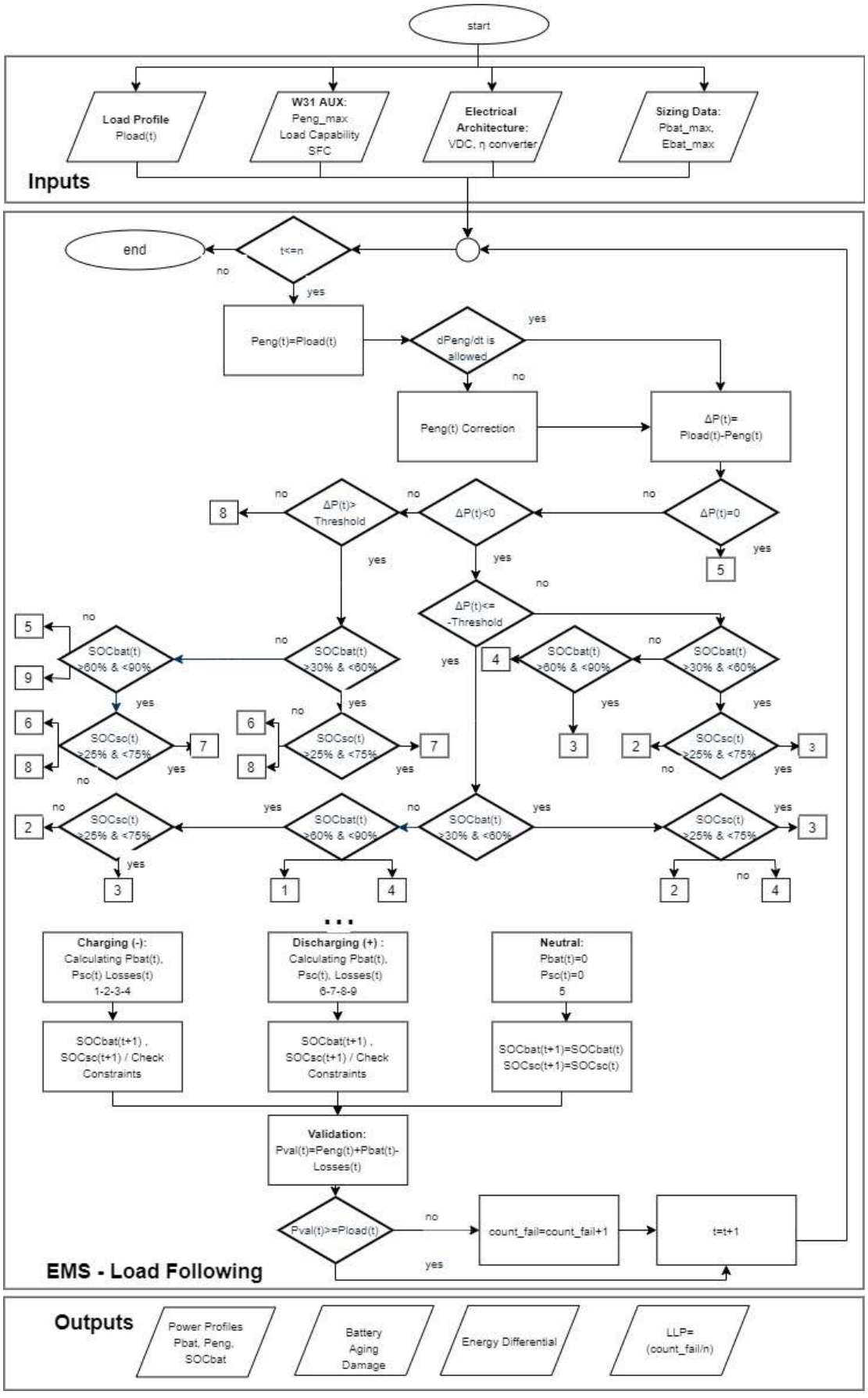

10.6 Pseudo-code (Matlab)

1. Power Allocation - Mode 3

```
function [ Pbat,Psc,Delta_P,Pbat_losses,Psc_losses] = ...
    power_alloc_three( Pbat_max,Psc_max,Delta_P,E_pos,E_neg,Ebat,Ebat_max,Esc,Esc_max)
```

Power Allocation Mode 3 :

Priority 1: Charge Supercapacitor

Priority 2: Charge Battery

Input: Pbat_max,Psc_max, Delta_P,E_pos,E_neg,.... Ebat,Ebat_max,Esc,Esc_max

Output: Pbat,Psc,... Delta_P, Pbat_losses,Psc_losses

SC Charge Priority 1

```
% Call SC Efficiency Function
[etta_sc] = efficiency_sc(E_pos,E_neg,Psc_max,Psc_max );
% Check that available power is less than SC rating
if -Delta_P>=Psc_max/etta_sc
    Psc=-Psc_max;
    % Check that SC capacity is not exceeding max.
    if -Psc+Esc>Esc_max
        Psc=-(Esc_max-Esc);
        % Call SC Efficiency Function
        [etta_sc] = efficiency_sc(E_pos,E_neg,Psc,Psc_max);
    end
    % Subtracting Psc from Available Power
    Delta_P=min(Delta_P+Psc_max/etta_sc,0);
    % Calculating Losses to charge SC
    Psc_losses=((1/etta_sc)-1)*Psc;
else
    % Call SC Efficiency Function
    [etta_sc] = efficiency_sc(E_pos,E_neg,Delta_P,Psc_max );
    Psc=Delta_P*etta_sc;
    % Check that SC capacity is not exceeding max.
    if -Psc+Esc>Esc_max
        Psc=-(Esc_max-Esc);
        % Call SC Efficiency Function
        [etta_sc] = efficiency_sc(E_pos,E_neg,Psc,Psc_max);
    end
    % All Available Power used
    Delta_P=0;
    % Calculating Losses to charge SC
    Psc_losses=Delta_P*(1-etta_sc);
end
```

Battery Charge Priority 2

```
% Call Battery Efficiency Function
[etta_bat] = efficiency_bat(E_pos,E_neg,Pbat_max,Pbat_max);
% Check that available power is less than battery rating
if -Delta_P>=Pbat_max/etta_bat
    Pbat=-Pbat_max;
    % Check that SOCbat is not exceeding 90%
    if -Pbat+Ebat>0.9*Ebat_max
        Pbat=-(0.9*Ebat_max-Ebat);
        % Call Battery Efficiency Function
        [etta_bat] = efficiency_bat(E_pos,E_neg,Pbat,Pbat_max);
    end
    % Subtracting Pbat from Available Power
    Delta_P=Delta_P+Pbat_max/etta_bat;
    % Calculating Losses to charge Battery
    Pbat_losses=((1/etta_bat)-1)*Pbat;
else                              %Max. available engine can give
    % Call Battery Efficiency Function
    [etta_bat] = efficiency_bat(E_pos,E_neg,Delta_P,Pbat_max);
    Pbat=Delta_P*etta_bat;
    % Check that SOCbat is not exceeding 90%
    if -Pbat+Ebat>0.9*Ebat_max
        Pbat=-(0.9*Ebat_max-Ebat);
        [etta_bat] = efficiency_bat(E_pos,E_neg,Pbat,Pbat_max);
    end
    % All Available Power used
    Delta_P=0;
    % Calculating Losses to charge Battery
    Pbat_losses=Delta_P*(1-etta_bat);
end
```

```
end
```

2. Power Allocation - Mode 7

```
function [ Pbat,Psc,Delta_P,Pbat_losses,Psc_losses]
= power_alloc_seven( Pbat_max,Psc_max,Delta_P,E_pos,E_neg,Ebat,Ebat_max,Esc,Esc_max)
```

Power Allocation Mode 7 :

Priority 1: Discharge Battery
Priority 2: Discharge Supercapacitor
Input: Pbat_max,Psc_max, Delta_P,E_pos,E_neg,.... Ebat,Ebat_max,Esc,Esc_max
Output: Pbat,Psc,... Delta_P, Pbat_losses,Psc_losses

Battery Discharge Priority 1

Call Battery Efficiency Function

```
[etta_bat] = efficiency_bat(E_pos,E_neg,Pbat_max,Pbat_max);
if Delta_P>Pbat_max*etta_bat
        Pbat=Pbat_max;                      %What battery gives
    % Check that Battery capacity is not below min
    if Ebat-Pbat<0.30*Ebat_max
        Pbat=Ebat-0.30*Ebat_max;
        [etta_bat] = efficiency_bat(E_pos,E_neg,Pbat,Pbat_max);
    end
    % Subtracting Pbat from Power Deficit
        Delta_P=Delta_P-Pbat*etta_bat;
    % Calculating Losses to discharge battery
    Pbat_losses=Pbat*(1-etta_bat);
else
    % Call Battery Efficiency Function
    [etta_bat] = efficiency_bat(E_pos,E_neg,Delta_P,Pbat_max);
        Pbat=min(Delta_P/etta_bat,Pbat_max);
    % Check that Battery capacity is not below min
    if Ebat-Pbat<0.30*Ebat_max %Not allowed to go below SOCmin=0.30;
        Pbat=Ebat-0.30*Ebat_max;
        [etta_bat] = efficiency_bat(E_pos,E_neg,Pbat,Pbat_max);
    end
    % Subtracting Pbat from Power Deficit
        Delta_P=max(Delta_P-Pbat*etta_bat,0);
    % Calculating Losses to discharge battery
    Pbat_losses=Pbat*(1-etta_bat);
end
```

SC Discharge Priority 2

Call SC Efficiency Function

```
[etta_sc] = efficiency_sc(E_pos,E_neg,Psc_max,Psc_max);
if Delta_P>Psc_max*etta_sc
        Psc=Psc_max;                        %What battery gives
    % Check that SC capacity is not below min
    if Esc-Psc<0.25*Esc_max
        Psc=Esc-0.25*Esc_max;
        % Call SC Efficiency Function
        [etta_sc] = efficiency_sc(E_pos,E_neg,Psc,Psc_max);
    end
    % Subtracting Psc from Power Deficit
        Delta_P=Delta_P-Psc*etta_sc;
    % Calculating Losses to discharge SC
    Psc_losses=Psc*(1-etta_sc);
else
    % Call SC Efficiency Function
    [etta_sc] = efficiency_sc(E_pos,E_neg,Delta_P,Psc_max);
        Psc=min(Delta_P/etta_sc,Psc_max);
    % Check that SC capacity is not below min
    if Esc-Psc<0.25*Esc_max
        Psc=Esc-0.25*Esc_max;
        % Call SC Efficiency Function
        [etta_sc] = efficiency_sc(E_pos,E_neg,Psc,Psc_max);
    end
    % Subtracting Psc from Power Deficit
        Delta_P=Delta_P-Psc*etta_sc;
    % Calculating Losses to discharge SC
    Psc_losses=Psc*(1-etta_sc);
end
```

```
end
```

10.7 Other Calculations

10.7.1 Cost Calculation

$$\text{cost}_{\text{total}}\,[\$] = \text{cost}_{\text{bat}} + \text{cost}_{\text{sc}} + \text{cost}_{\text{convert,bat}} + \text{cost}_{\text{convert,bat}}$$

where

$$\text{cost}_{\text{bat}} = \text{spec. cost battery} \cdot \text{E}_{\text{bat,max}}$$

$$\text{cost}_{\text{sc}} = \text{spec. cost battery} \cdot \text{C}_{\text{sc,cell}} \cdot \frac{\text{N}_{\text{sc,parallel}}}{\text{N}_{\text{sc,series}}}$$

$$\text{cost}_{\text{convert,bat}} = \frac{\text{P}_{\text{bat,max}}}{\text{Spec. Power Conv}}$$

$$\text{cost}_{\text{convert,bat}} = \frac{\text{P}_{\text{sc,max}}}{\text{Spec. Power Conv}}$$

10.7.2 Weight Calculation

$$\text{weight}_{\text{total}}\,[\text{tonnes}] = \text{weight}_{\text{bat}} + \text{weight}_{\text{sc}} + \text{weight}_{\text{convert,bat}} + \text{weight}_{\text{convert,sc}}$$

where

$$\text{weight}_{\text{bat}} = \left(\frac{1}{\text{spec. energy bat}}\right) \cdot \text{E}_{\text{bat,max}}$$

$$\text{weight}_{\text{sc}} = \left(\frac{1}{\text{spec. energy sc}}\right) \cdot \text{E}_{\text{sc,max}}$$

$$\text{weight}_{\text{convert,bat=}} \frac{\text{P}_{\text{bat,max}}}{\text{spec. power bat}}$$

$$\text{weight}_{\text{convert,sc}} = \frac{\text{P}_{\text{sc,max}}}{\text{spec. power sc}}$$

10.7.3 Engine Loading Capacity Calculations

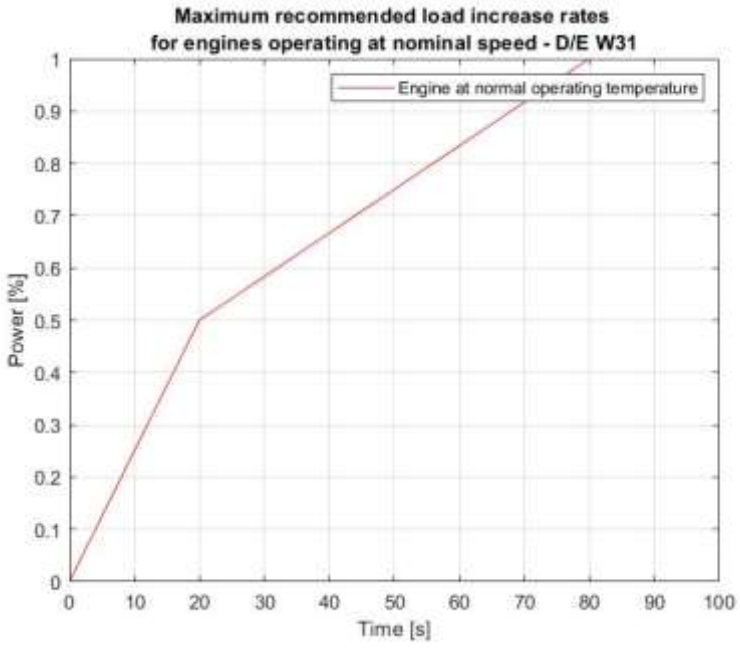

General line equation for normal operation:

$$P_{eng}(t) = \begin{cases} 2.5t & t < 20\ s \\ \frac{5}{6}t_1 + 33.3t & t \geq 20\ \ s \end{cases}$$

Power at t_O is given by:

$$P_{eng}(t_0) = \begin{cases} 2.5t_0 & t_0 < 20\ s \\ \frac{5}{6}t_0 + 33.3t_0 & t_0 \geq 20\ \ s \end{cases}$$

Solving for known $P_{eng}(t_0)$:

$$t_o = \begin{cases} 0.40\ P_{eng}(t_0) & P_{eng}(t_0) < 50\%\ MCR \\ \frac{6}{5}P_{eng}(t_0) - 40 & P_{eng}(t_0) \geq 50\%\ MCR \end{cases}$$

After a pre-defined simulation time step of 1sec, it is possible to reversely calculate engine power corresponding at this minimum dt.

$$t_1 = t_0 + 1$$

$$P_{eng}(t_1) = \begin{cases} 2.5t_1 & t_1 < 20 \\ \frac{5}{6}t_1 + 33.3t_1 & t_1 \geq 20 \end{cases}$$

Therefore max. permissible movement on the line for the pre-defined time step of 1 sec is given by:

$$\frac{\Delta P_{eng,permisible}}{dt} = P_{eng}(t_0) - P_{eng}(t_1)$$

$$P_{eng,permissible} = P_{eng}(t_1)$$

10.8 Simulation Runs

Baseline Runs

	Battery Only		HESS	
Run	EMS1	EMS2	EMS1	EMS2
dt_{req}	N/A	N/A	8	8
Engine Set Loadpoint [%MCR]	60%	N/A	60%	N/A
HESS Decisive Threshold [%MCR]	N/A	N/A	15	15%MCR
Battery Cost [$/kWh]	800	800	800	800
Simulation Duration	x3	x3	x3	x3

Min. requested duration of SC discharge pulse (dt_req)

	Battery Only		HESS	
Run	EMS1	EMS2	EMS1	EMS2
dt_req			4	4
Engine Set Loadpoint [%MCR]			60%	N/A
HESS Decisive Threshold [%MCR]			0.1	0.1
Battery Cost [$/kWh]	800	800	800	800
Simulation Duration			x3	x3

	Battery Only		HESS	
Run	EMS1	EMS2	EMS1	EMS2
dt_req			12	12
Engine Set Loadpoint [%MCR]			60%	N/A
HESS Decisive Threshold [%MCR]			0.1	0.1
Battery Cost [$/kWh]	800	800	800	800
Simulation Duration			x3	x3

HESS Decisive Threhold [%]

	Battery Only		HESS	
Run	EMS1	EMS2	EMS1	EMS2
dt_req			8	8
Engine Set Loadpoint [%MCR]			60%	N/A
HESS Decisive Threshold [% MCR]			0.1	0.1
Battery Cost [$/kWh]	800	800	800	800
Simulation Duration			x3	x3

	Battery Only		HESS	
Run	EMS1	EMS2	EMS1	EMS2
dt_req			8	8
Engine Set Loadpoint [%MCR]			60%	N/A
HESS Decisive Threshold [% MCR]			0.2	0.2
Battery Cost [$/kWh]			800	800
Simulation Duration			x3	x3

Engine Loadpoint [%] only for Load Levelling

	Battery Only		HESS	
Run	EMS1	EMS2	EMS1	EMS2
dt_req	N/A		8	
Engine Set Loadpoint [% MCR]	55%		55%	
HESS Decisive Threshold [%MCR]	N/A		0.1	
Battery Cost [$/kWh]	800		800	
Simulation Duration	x3		x3	

	Battery Only		HESS	
Run	EMS1	EMS2	EMS1	EMS2
dt_req	N/A		8	
Engine Set Loadpoint [% MCR]	65%		65%	
HESS Decisive Threshold [%MCR]	N/A		0.1	
Battery Cost [$/kWh]	800		800	
Simulation Duration	x3		x3	

Battery Cost

	Battery Only		HESS	
Run	EMS1	EMS2	EMS1	EMS2
dt_req	N/A	N/A	8	8
Engine Set Loadpoint [% MCR]	55%	N/A	55%	N/A
HESS Decisive Threshold [%MCR]	N/A	N/A	0.1	0.15
Battery Cost [$/kWh]	400	400	400	400
Simulation Duration	x3		x3	

	Battery Only		HESS	
Run	EMS1	EMS2	EMS1	EMS2
dt_req	N/A	N/A	8	8
Engine Set Loadpoint [% MCR]	65%	N/A	65%	N/A
HESS Decisive Threshold [%MCR]	N/A	N/A	0.1	0.15
Battery Cost [$/kWh]	1200	1200	1200	1200
Simulation Duration	x3		x3	

10.9 Load Levelling (EMS1) – Graphs

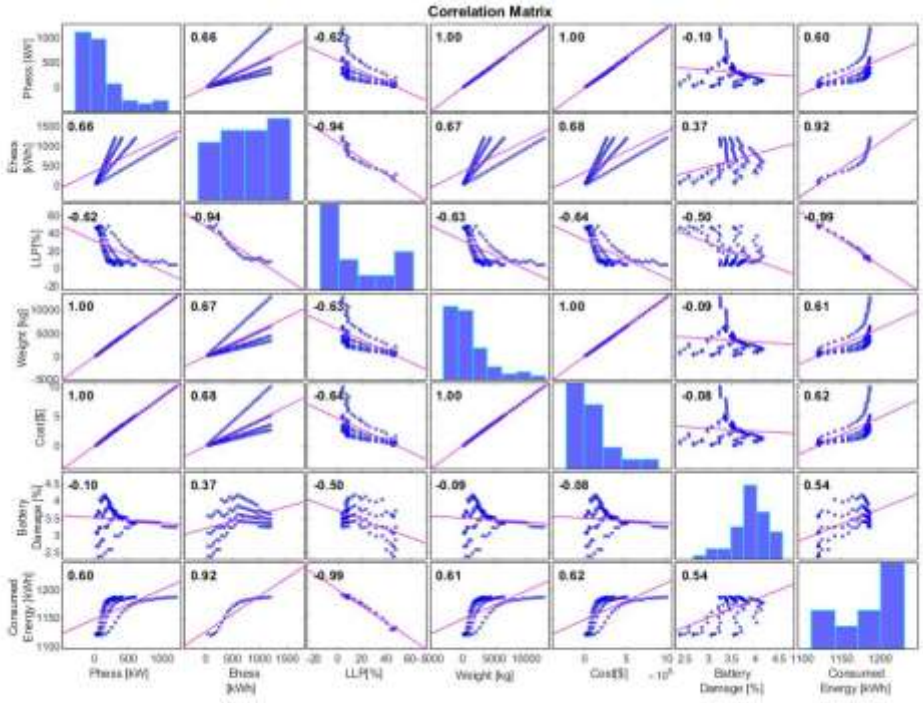

Figure 87 Correlation Matrix for Load Levelling EMS1 – Battery + Supercapacitor

10.10 Load Following (EMS2) – Graphs

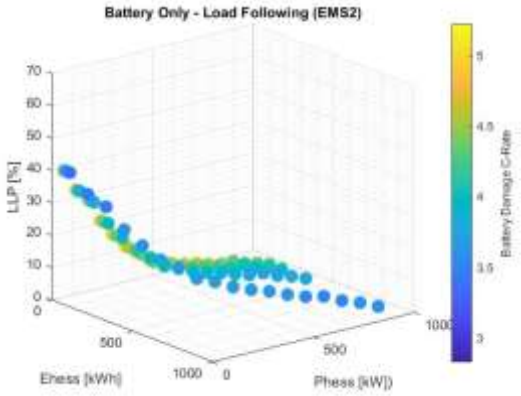

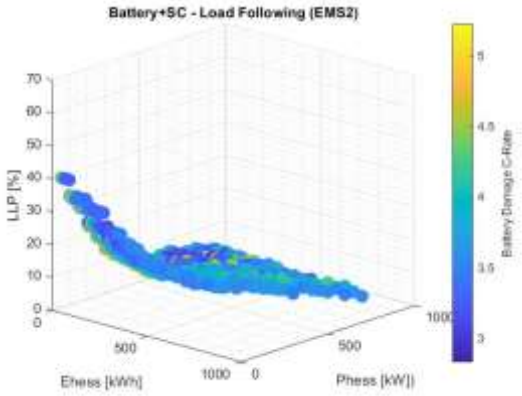

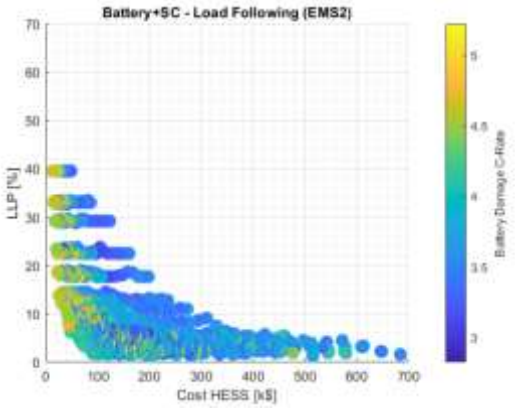

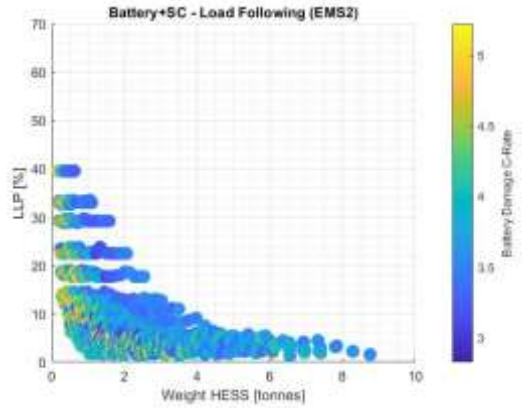

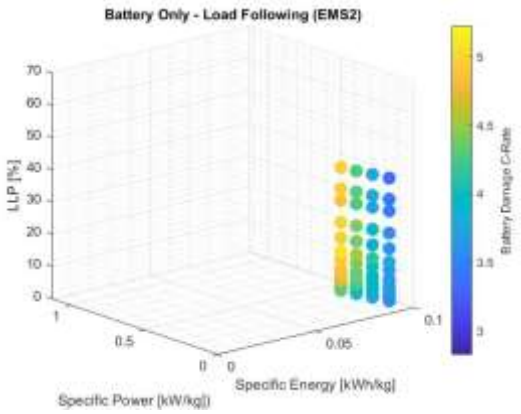

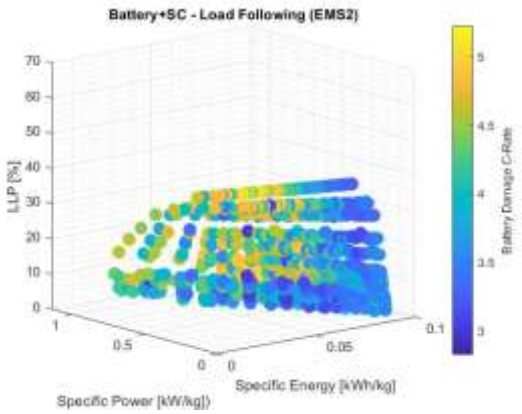

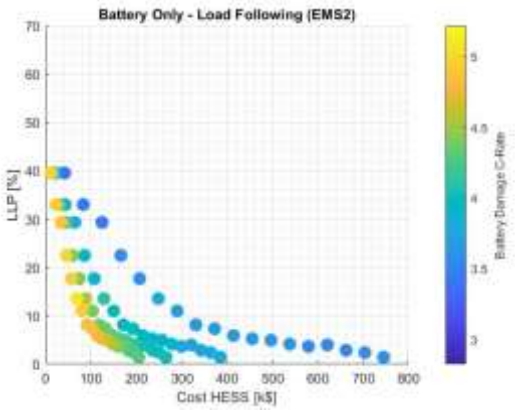

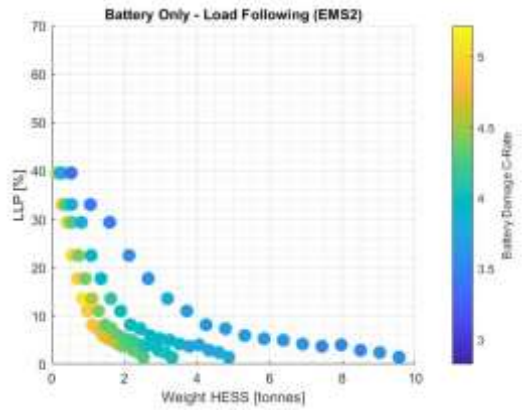

Bibliography

1. Smith, T., et al., *Third imo ghg study 2014*. International Maritime Organization (IMO), London, http://www. iadc. org/wp-content/uploads/2014/02/MEPC-67-6-INF3-2014-Final-Report-complete. pdf, 2014.
2. Kim, K., et al. *A study on applicability of Battery Energy Storage System (BESS) for electric propulsion ships*. in *2016 IEEE Transportation Electrification Conference and Expo, Asia-Pacific (ITEC Asia-Pacific)*. 2016. IEEE.
3. Stolper, A. *ZEM/SHIPS - Zero.Emission.Ships*. 2010; Available from: http://ec.europa.eu/environment/life/project/Projects/index.cfm?fuseaction=search.dspPage&n_proj_id=3081
4. *The boat - Fondation Planetsolar*. 2010; Available from: https://www.planetsolar.swiss/en/world-premiere/boat/.
5. Lines, M.M.O.S.K. *World's First Hybrid Car Carrier Emerald Ace Completed*. 2012; Available from: http://www.mol.co.jp/en/pr/2012/12035.html.
6. Moore, R., *HH Ferries world's-largest electric ferries to use PBES energy storage*, in *marine propulsion & auxiliary machinery*. 2016.
7. Gunton, P., *Hurtigruten newbuilds boost battery power*, in *Passenger Ship Technology*. 2017.
8. Geertsma, R.D., et al., *Design and control of hybrid power and propulsion systems for smart ships: A review of developments.* Applied Energy, 2017. **194**: p. 30-54.
9. *CASE STUDY: Norled AS, MF Ampere, Ferry*. 2014.
10. GL, D., *The Future is Hybrid: a guide to the use of batteries in shipping*, in *In Focus*. 2015, DNV GL Maritime Communications: Hamburg.
11. Valkeejärvi, K., *The ship's electrical network, engine control and automation.* Gallois magazine.[Online], 2006. **3**(1).
12. *Wärtsilä 31 Product Guide*. 2019, Wärtsilä Marine Solutions: Vaasa.
13. Woud, H.K. and D. Stapersma, *Design of propulsion and electric power generation systems*. Vol. 1902536479. 2002: IMarEST.
14. Zu, C.-X. and H. Li, *Thermodynamic analysis on energy densities of batteries.* Energy & Environmental Science, 2011. **4**(8): p. 2614-2624.
15. Lambert, F. *Tesla is now claiming 35% battery cost reduction at 'Gigafactory 1' – hinting at breakthrough cost below $125/kWh*. 2017; Available from: https://electrek.co/2017/02/18/tesla-battery-cost-gigafactory-model-3/.
16. Raadschelders, J., *Zonder energieopslag is transitie van fossiele - naar duurzame energie niet mogelijk (Seminar)*. 2016, DNV-GL Energy Storage Advisory Services: The Netherlands.
17. Nykvist, B. and M. Nilsson, *Rapidly falling costs of battery packs for electric vehicles.* Nature climate change, 2015. **5**(4): p. 329.
18. Xu, B., *Degradation-limiting optimization of battery energy storage systems operation.* 2013.
19. Omar, N., et al., *Lithium iron phosphate based battery – Assessment of the aging parameters and development of cycle life model.* Applied Energy, 2014. **113**: p. 1575-1585.
20. Team, M., *A guide to understanding battery specifications.* Academia. edu, 2008.
21. Barré, A., et al., *A review on lithium-ion battery ageing mechanisms and estimations for automotive applications.* Journal of Power Sources, 2013. **241**: p. 680-689.
22. ten Cate Hoedemaker, S., *An assessment of the relationship between battery size, charging strategy and battery lifetime*, in *TU Delft Mechanical, Maritime and Materials Engineering; TU Delft Marine and Transport Technology*. 2017, TU Delft: Delft.
23. Warner, J.T., *The handbook of lithium-ion battery pack design: chemistry, components, types and terminology*. 2015: Elsevier.

24. Sabri, M., K. Danapalasingam, and M. Rahmat, *A review on hybrid electric vehicles architecture and energy management strategies.* Renewable and Sustainable Energy Reviews, 2016. **53**: p. 1433-1442.
25. Soleymani, M., A. Yoosofi, and M. Kandi-D, *Sizing and energy management of a medium hybrid electric boat.* Journal of Marine Science and Technology, 2015. **20**(4): p. 739-751.
26. Ertan, H.B. and F.R. Arikan. *Sizing of Series Hybrid Electric Vehicle with Hybrid Energy Storage System*. in *2018 International Symposium on Power Electronics, Electrical Drives, Automation and Motion (SPEEDAM)*. 2018. IEEE.
27. H. Bulent Ertan, F.R.A., *Sizing of Series Hybrid Electric Vehicle with Hybrid Energy Storage System.* 2018.
28. Khaligh, A. and Z. Li, *Battery, ultracapacitor, fuel cell, and hybrid energy storage systems for electric, hybrid electric, fuel cell, and plug-in hybrid electric vehicles: State of the art.* IEEE transactions on Vehicular Technology, 2010. **59**(6): p. 2806-2814.
29. Kim, Y. and N. Chang, *Design and management of energy-efficient hybrid electrical energy storage systems*. 2014: Springer.
30. Cohen, I.J., et al., *Evaluation of a hybrid energy storage module for pulsed power applications.* IEEE Transactions on Plasma Science, 2014. **42**(10): p. 2948-2955.
31. Veeke, H.P., J.A. Ottjes, and G. Lodewijks, *The Delft systems approach: Analysis and design of industrial systems*. 2008: Springer Science & Business Media.
32. Limited, A.s., *Seanergy modules - High energy and high power Li-ion Super Iron Phosphate*. 2017, SAFT Batteries: Levallois-Perret.
33. Wagemaker, F.M.M.M., *Sustainable Hydrogen and Electrical Energy Storage: Lecture Notes - Batteries Vol. 5*. 2017, Delft University of Technology, Faculty of Electrical Engineering, Mathematics and Computer Science.
34. Zhao, R., J. Liu, and J. Gu, *The effects of electrode thickness on the electrochemical and thermal characteristics of lithium ion battery.* Applied Energy, 2015. **139**: p. 220-229.
35. Buchmann, I. *BU-209: How does a Supercapacitor Work?* 2017.
36. <*Maxwell Tech Application Note on Supercapacitor Aging.pdf*>.
37. Pedram, M., et al. *Hybrid electrical energy storage systems*. in *Proceedings of the 16th ACM/IEEE international symposium on Low power electronics and design*. 2010. ACM.
38. Hadjipaschalis, I., A. Poullikkas, and V. Efthimiou, *Overview of current and future energy storage technologies for electric power applications.* Renewable and sustainable energy reviews, 2009. **13**(6): p. 1513-1522.
39. Hu, S., Z. Liang, and X. He, *Ultracapacitor-battery hybrid energy storage system based on the asymmetric bidirectional Z-source topology for EV.* IEEE Transactions on Power Electronics, 2015. **31**(11): p. 7489-7498.
40. Xiang, C., et al., *A new topology and control strategy for a hybrid battery-ultracapacitor energy storage system.* Energies, 2014. **7**(5): p. 2874-2896.
41. Zimmermann, T., et al., *Review of system topologies for hybrid electrical energy storage systems.* Journal of Energy Storage, 2016. **8**: p. 78-90.
42. Hofmann, P., *Hybridfahrzeuge: ein alternatives Antriebssystem für die Zukunft*. 2014: Springer-Verlag.
43. Carpinelli, G., F. Mottola, and D. Proto, *Probabilistic sizing of battery energy storage when time-of-use pricing is applied.* Electric Power Systems Research, 2016. **141**: p. 73-83.
44. Hu, X., et al., *Integrated Optimization of Battery Sizing, Charging, and Power Management in Plug-In Hybrid Electric Vehicles.* IEEE Transactions on Control Systems Technology, 2016. **24**(3): p. 1036-1043.
45. Salman Mashayekh, Z.W., Lisa Qi, John Lindtjorn,Tor-Arne Myklebust, *Optimum Sizing of Energy Storage for an Electric Ferry Ship.*

46. Lopes, J., J. Pomilio, and P. Ferreira. *Optimal sizing of batteries and ultracapacitors for fuel cell electric vehicles*. in *IECON 2011-37th Annual Conference of the IEEE Industrial Electronics Society*. 2011. IEEE.
47. R. Sadoun, N.R., P. Bartholomeüs, B. Barbedette, P. Le Moigne, *Influence of the drive cycles on the sizing of hybrid storage system battery supercapacitor supplying an EV*.
48. Akli, C.R., et al. *Energy management and sizing of a hybrid locomotive*. in *2007 European conference on power electronics and applications*. 2007. IEEE.
49. Li, J., et al., *Design and test of a new droop control algorithm for a SMES/battery hybrid energy storage system.* Energy, 2017. **118**: p. 1110-1122.
50. Gan, L.K., J.K. Shek, and M.A. Mueller, *Hybrid wind–photovoltaic–diesel–battery system sizing tool development using empirical approach, life-cycle cost and performance analysis: A case study in Scotland.* Energy Conversion and Management, 2015. **106**: p. 479-494.
51. Sun, L., *An Analytical Optimal Sizing Method for Battery Supercapacitor Powertrain Interfaced with a Buck-boost Converter*, in *KINTEX*. 2015: Korea.
52. Sun, L., et al., *Multi-objective component sizing for a battery-supercapacitor power supply considering the use of a power converter.* Energy, 2018. **142**: p. 436-446.
53. Khan, M.M.S., M.O. Faruque, and A. Newaz, *Fuzzy Logic Based Energy Storage Management System for MVDC Power System of All Electric Ship.* IEEE Transactions on Energy Conversion, 2017.
54. Tang, Y. and A. Khaligh. *On the feasibility of hybrid battery/ultracapacitor energy storage systems for next generation shipboard power systems*. in *Vehicle Power and Propulsion Conference (VPPC), 2010 IEEE*. 2010. IEEE.
55. Tang, Y. and A. Khaligh. *Bidirectional hybrid Battery/Ultracapacitor Energy Storage Systems for next generation MVDC shipboard power systems*. in *Vehicle Power and Propulsion Conference (VPPC), 2011 IEEE*. 2011. IEEE.
56. Song, J.-Y., et al. *A hybrid energy storage system based on DSP for the ship*. in *Intelligent Control and Automation (WCICA), 2016 12th World Congress on*. 2016. IEEE.
57. Zhu, L., et al. *Fuzzy logic based energy management strategy for a fuel cell/battery/ultra-capacitor hybrid ship.* in *Green Energy, 2014 International Conference on*. 2014. IEEE.
58. Trovão, J.P., F. Machado, and P.G. Pereirinha, *Hybrid electric excursion ships power supply system based on a multiple energy storage system.* IET Electrical Systems in Transportation, 2016. **6**(3): p. 190-201.
59. *Supercapacitor electric boat : Ar Vag Tredan operates in France*. 2014; Available from: https://www.supercaptech.com/supercapacitor-electric-boat-ar-vag-tredan-operates-in-france.
60. Lambert, F. *A new all-electric cargo ship with a massive 2.4 MWh battery pack launches in China*. 2017; Available from: https://ww.electrek.co/2017/12/04/all-electric-cargo-ship-battery-china/.
61. ABS, *Guide for use of supercapacitors in the marine and offshore industries*, A.B.o. Shipping, Editor. 2017.
62. Schaltz, E., A. Khaligh, and P.O. Rasmussen, *Influence of battery/ultracapacitor energy-storage sizing on battery lifetime in a fuel cell hybrid electric vehicle.* IEEE Transactions on Vehicular Technology, 2009. **58**(8): p. 3882-3891.
63. AS, D.-G., *Recommended Practise - Safety, operation and performance of gridconnected energy storage systems*, DNV-GL, Editor. 2017. p. 21.
64. Butcher, M., R. Maltby, and P. Parvin. *Compact DC power and propulsion systems-the definitive solution?* in *2009 IEEE Electric Ship Technologies Symposium*. 2009. IEEE.
65. Åstrand, U., *The wärtsilä 31-the world's most efficient 4-stroke engine.* Marine Engineering, 2016. **51**(2): p. 203-207.

66. B. Shrestha, P.M.N., D.A. Wetz, A.F. Matasso, *Evaluation of High C Rate Cycle Induced Aging On Low Impedance Lithium-Ion Batteries Using In-Situ Electrochemical Impedance Spectroscopy (EIS) Analysis.*
67. Nishant Narayana, T.P., Victor Vega-Garitaa, Jelena Popovic-Gerbera, Pavol Bauera, and Miro Zemana, *A simple methodology for estimating battery lifetimes in Solar Home System design.*
68. Dedes, E.K., D.A. Hudson, and S.R. Turnock, *Assessing the potential of hybrid energy technology to reduce exhaust emissions from global shipping.* Energy policy, 2012. **40**: p. 204-218.
69. Buchmann, I., *Batteries in a portable world: a handbook on rechargeable batteries for non-engineers*. 2001: Cadex Electronics Richmond.
70. *Datasheet - K2 Ultracapacitors - 2.7V Series (BCAP3000)*. 2013, Maxwell Technologies: San Diego, USA.
71. *Application Note - Ultracapacitor Cell Sizing Rev 3*. 2009, Maxwell Technologies: San Diego.
72. Kuperman, A., et al., *Supercapacitor Sizing Based on Desired Power and Energy Performance.* IEEE Transactions on Power Electronics, 2014. **29**(10): p. 5399-5405.
73. *Technology Watch State of the Art Report update into Energy Storage, Conversion and Distribution*. 2015, Joint Operation for Ultra Low Emission Shipping (JOULES).
74. Bradbury, K., *Energy storage technology review.* Duke University, 2010: p. 1-34.
75. Nykvist, B. and M. Nilsson, *Rapidly falling costs of battery packs for electric vehicles.* Nature Climate Change, 2015. **5**(4): p. 329-332.
76. Michalczuk, M., B. Ufnalski, and L. Grzesiak. *Fuzzy logic control of a hybrid battery-ultracapacitor energy storage for an urban electric vehicle*. in *2013 eighth international conference and exhibition on ecological vehicles and renewable energies (EVER)*. 2013. IEEE.
77. Gao, C., et al. *Optimal fuzzy logic based energy management strategy of battery/supercapacitor hybrid energy storage system for electric vehicles*. in *2016 12th World Congress on Intelligent Control and Automation (WCICA)*. 2016. IEEE.
78. Martinez-Laserna, E., et al., *Li-Ion Battery Lifetime Model's Influence on the Economic Assessment of a Hybrid Electric Bus's Operation.* World Electric Vehicle Journal, 2018. **9**(2): p. 28.
79. Rossi, F., P. Van Beek, and T. Walsh, *Handbook of constraint programming*. 2006: Elsevier.
80. Shabbir, W., *Control strategies for series hybrid electric vehicles*. 2015, Imperial College London.
81. Tankari, M.A., et al., *Use of ultracapacitors and batteries for efficient energy management in wind–diesel hybrid system.* IEEE Transactions on Sustainable Energy, 2012. **4**(2): p. 414-424.
82. Nieslony, A., *Rainflow counting algorithm.* File Exchange-MATLAB Central, http://www. mathworks. com/matlabcentral/fileexchange/3026-rainflow-counting-algorithm, 2003.
83. Niesłony, A., *Determination of fragments of multiaxial service loading strongly influencing the fatigue of machine components.* Mechanical Systems and Signal Processing, 2009. **23**(8): p. 2712-2721.
84. *Resolution Mepc.281(70): Amendments to the 2014 Guidelines on the Method of Calculation of the Attained EEDI For New Ships* I.M. Organization, Editor. 2016: London. p. 8/12.
85. Ismail, M.S., et al., *Effective utilization of excess energy in standalone hybrid renewable energy systems for improving comfort ability and reducing cost of energy: A review and analysis.* Renewable and Sustainable Energy Reviews, 2015. **42**: p. 726-734.
86. Krstic, S., et al. *Circuit breaker technologies for advanced ship power systems*. in *2007 IEEE Electric Ship Technologies Symposium*. 2007. IEEE.

87. Robinson, S., *Simulation: the practice of model development and use*. Vol. 50. 2004: Wiley Chichester.
88. Kalikatzarakis, M., et al., *Ship energy management for hybrid propulsion and power supply with shore charging.* Control Engineering Practice, 2018. **76**: p. 133-154.
89. Bagshaw, N.E., *Batteries on ships*. Vol. 1. 1982: John Wiley & Sons.
90. Ray, K., *Electric propulsion at sea - Part 1*, in *Marine Engineers Review, MER*. February 2013, IMarEST
91. *Plugged in*, in *ABB review - corporate technical journal*. April 2014. p. 66.
92. Natali, M., *Introduction to Wartsila HY- Internal Webinar*. 2017, Wartsila Netherlands B.V.
93. Riisgaard, H., Hermann, Roberto Rivas. *Maritime Competence and Innovation Skagerrak and Kattegat (MARKIS)*. 2013; Available from: https://vbn.aau.dk/en/projects/maritime-competence-and-innovation-skagerrak-and-kattegat.
94. *E-ferry – prototype and full-scale demonstration of next generation 100% electrically powered ferry for passengers and vehicles*

2017; H2020-EU.3.4. - SOCIETAL CHALLENGES - Smart, Green And Integrated Transport]. Available from: https://cordis.europa.eu/project/rcn/193367/factsheet/en.
95. *Green Shipping Programme 2015-2030*. 2017; Norway establishes the world's most efficient and environmentally friendly shipping.]. Available from: https://www.dnvgl.com/maritime/green-shipping-programme/index.html.
96. *NCE Martime CleanTech*. 2018; Available from: https://maritimecleantech.no/projects/.
97. TÖRNKVIST, A. *Harvesting power for a fitful lady*. 2014; Available from: https://www.wartsila.com/twentyfour7/innovation/harvesting-power-for-a-fitful-lady.
98. SØRFONN, I. *Hybrid technology for new emerging markets – inductive charging*. 2016; Available from: https://www.wartsila.com/twentyfour7/in-detail/hybrid-technology-for-new-emerging-markets-inductive-charging.
99. *MS Roald Amundsen Polar Cruise Ship*. Ship Technology, 2017.
100. Chen, H., et al., *Progress in electrical energy storage system: A critical review.* Progress in Natural Science, 2009. **19**(3): p. 291-312.
101. Cheruvally, G., *Lithium iron phosphate: a promising cathode-active material for lithium secondary batteries*. 2008: Trans Tech Publications Limited.
102. *Heat Values of Various Fuels*. 2018; Available from: https://www.world-nuclear.org/information-library/facts-and-figures/heat-values-of-various-fuels.aspx.
103. *Fossil and Alternative Fuels - Energy Content [online]*. 2008; Available from: https://www.engineeringtoolbox.com/fossil-fuels-energy-content-d_1298.html.
104. *NIST Guide to the SI, Chapter 4: The Two Classes of SI Units and the SI Prefixes*. 2018; Available from: https://www.nist.gov/pml/special-publication-811/nist-guide-si-chapter-4-two-classes-si-units-and-si-prefixes.
105. Rahman, F., S. Rehman, and M.A. Abdul-Majeed, *Overview of energy storage systems for storing electricity from renewable energy sources in Saudi Arabia.* Renewable and Sustainable Energy Reviews, 2012. **16**(1): p. 274-283.
106. Kousksou, T., et al., *Energy storage: Applications and challenges.* Solar Energy Materials and Solar Cells, 2014. **120**: p. 59-80.
107. Whittingham, M.S., *History, evolution, and future status of energy storage.* Proceedings of the IEEE, 2012. **100**(Special Centennial Issue): p. 1518-1534.
108. Ribeiro, P.F., et al., *Energy storage systems for advanced power applications.* Proceedings of the IEEE, 2001. **89**(12): p. 1744-1756.
109. Thackeray, M.M., C. Wolverton, and E.D. Isaacs, *Electrical energy storage for transportation—approaching the limits of, and going beyond, lithium-ion batteries.* Energy & Environmental Science, 2012. **5**(7): p. 7854-7863.
110. *Historical Lithium price per metric ton*. 2018; Available from: https://www.metalary.com/lithium-price/

111. Slater, M.D., et al., *Sodium-ion batteries.* Advanced Functional Materials, 2013. **23**(8): p. 947-958.
112. Takada, K., *Progress and prospective of solid-state lithium batteries.* Acta Materialia, 2013. **61**(3): p. 759-770.
113. Kim, J.G., et al., *A review of lithium and non-lithium based solid state batteries.* Journal of Power Sources, 2015. **282**: p. 299-322.
114. Sun, C., et al., *Recent advances in all-solid-state rechargeable lithium batteries.* Nano Energy, 2017. **33**: p. 363-386.
115. Zhang, F., et al., *A high-performance supercapacitor-battery hybrid energy storage device based on graphene-enhanced electrode materials with ultrahigh energy density.* Energy & Environmental Science, 2013. **6**(5): p. 1623-1632.
116. Kim, H., et al., *Liquid metal batteries: past, present, and future.* Chemical reviews, 2012. **113**(3): p. 2075-2099.
117. Canas, N.A., et al., *Investigations of lithium–sulfur batteries using electrochemical impedance spectroscopy.* Electrochimica Acta, 2013. **97**: p. 42-51.
118. Patel, K., *Lithium-sulfur battery: Chemistry, challenges, cost, and future.* The Journal of Undergraduate Research at the University of Illinois at Chicago, 2016. **9**(2).
119. Badwal, S.P., et al., *Emerging electrochemical energy conversion and storage technologies.* Frontiers in chemistry, 2014. **2**: p. 79.
120. Christensen, J., et al., *A critical review of Li/air batteries.* Journal of the Electrochemical Society, 2011. **159**(2): p. R1-R30.
121. Cohen, I.J., *The Design and Control of a Battery-Supercapacitor Hybrid Energy Storage Module for Naval Applications*. 2016, UNIVERSITY OF TEXAS AT ARLINGTON.
122. Chen, J.W., *Dynamic Modeling of a Super-capacitor Hybrid Converter*. 2009, Universite de Nantes: Nantes.
123. Motapon, S.N., L.-A. Dessaint, and K. Al-Haddad, *A comparative study of energy management schemes for a fuel-cell hybrid emergency power system of more-electric aircraft.* IEEE transactions on industrial electronics, 2014. **61**(3): p. 1320-1334.